Graduate Mechatronics Engineering Program
School of Engineering
American University of Sharjah

NEXT GENERATION 10 Gb/s RZ OPTICAL TRANSMITTERS

Thesis for Master of Science in Mechatronics Engineering

Submitted by:
Amira Mohamed Al Houli
@00009487

Supervised by:
Dr. Aly Elrefaie

May 6, 2004

NEXT GENERATION 10 Gb/s RZ OPTICAL TRANSMITTERS

Approved by:

Dr. Aly Elrefaie Chair of Committee	Dr. Khaled Assaleh (Member)
	Dr. Mohamed El-Tarhuni (Member)
	Dr. Mohammad Ameen Al-Jarrah (Program Director)
	Prof. Leland T. Blank (Dean of School)
	Date Approved

ABSTRACT

We propose an alternate chirp RZ optical transmitter that provides telecommunication carriers with a cost effective solution for upgrading the existing 2.5 Gb/s fiber links to 10 Gb/s. The performance of the proposed alternate chirp RZ transmitter has been compared with the chirp-free RZ with 33% duty cycle, chirp-free RZ with 50% duty cycle, and NRZ transmitters. Two dispersion compensation schemes have been used in the evaluation. In the first scheme, the fiber dispersion is compensated at the transmitter and receiver sites (end-to-end compensation) for 1000 km and 2000 km links. In the second scheme, the fiber dispersion is compensated every 640 km where optical switches are normally located. Computer simulation results indicate that RZ transmitters are better than NRZ transmitter for both dispersion compensation schemes. They also indicate that alternate chirp RZ transmitter can tolerate nonlinear effects than other classical chirp-free RZ transmitters for transmission up to 2000 km using end-to-end compensation scheme. Transmission up to 4000 km using dispersion compensation every 640 km is also possible using alternate chirp RZ transmitter but not possible with chirp-free RZ transmitters nor NRZ transmitter.

AKNOWLEDGEMENT

I'd like to express my gratitude to my thesis advisor, Dr. Aly Elrefaie, for his guidance, support, good attitude, motivation, and patience that have led to the successful completion of this work. I gained a lot of beneficial knowledge in this thesis which will help me in my work.

I'd like to thank also the director of Mechatronics program, Dr. Mohammad Ameen Jarrah, for his help and guidance.

Special thanks to Engineer Ahmed Abdul Salam for allowing me to use the Communication Lab whenever I need.

And finally I'd like to thank undergraduate senior students, Mr. Eyad and Mr. Tariq, for verifying the results I achieved.

TABLE OF CONTENTS

LIST OF FIGURES

LIST OF TABLES

ACRONYMS

AM	Amplitude Modulator
APD	Avalanche Photodiode
ASE	Amplified Spontaneous Emission
BER	Bit Error Rate
BER ISI	Bit Error Rate Intersymbol Interference
CMEMS	Compliant Microelectromechanical Systems
CS-RZ	Carrier Suppressed - Return to Zero
CW	Continuous-Wave
DCF	Dispersion Compensating Fiber
DEMUX	Demultiplexer
DFB	Distributed Feedback
DWDM	Dense Wave Division Multiplexer
EDFA	Erbium-Doped Fiber Amplifier
FEC	Forward Error Correction
FFT	Fast Fourier Transform

FWHM	Full-Width-Half-Maximum
FWM	Four-Wave Mixing
GVD	Group-Velocity Delay
IFWM	Intrachannel Four-Wave Mixing
LED	Light Emitting Diode
LPCVD	Low-Pressure Chemical Vapor Deposition
MEMS	Microelectromechanical System
MUX	Multiplexer
NF	Noise Figure
NLS	Nonlinear Schrödinger
NRZ	Non-Return to Zero
OA	Optical Amplifier
OEO	Optical/Electrical/Optical
OI	Optical Isolator
OADM	Optical Add/Drop Multiplexer
PIN	Positive-Intrinsic-Negative
PM	Phase Modulator
PRBS	Pseudo Random Binary Sequence

RZ	Return to Zero
RZ-DPSK	Return to Zero Phase-Shift Keying
RZ-OOK	Return to Zero On-Off Keying
SSMF	Standard Single Mode Fiber
SNR	Signal-to-Noise Ratio
SOA	Semiconductor Optical Amplifier
SPM	Self-Phase Modulation
SSFM	Split-Step Fourier Method
WDM	Wave Division Multiplexer
WSC	Wavelength-Selective Coupler
XPM	Cross-Phase Modulation

CHAPTER 1

INTRODUCTION

A communication system, in general, is defined as a system that conveys signals from a source to a destination over a transmission medium [1]. So it basically consists of a transmitter, transmission link, and receiver. This definition applies to all types of communication systems including fiber optic communication system.

Any fiber optic communication system consists of an optical transmitter that converts the electrical input signals into modulated optical signals, fiber optic link that acts as a waveguide for the optical signal, and optical receiver that converts the modulated optical signals back into a replica of the original electrical signal.

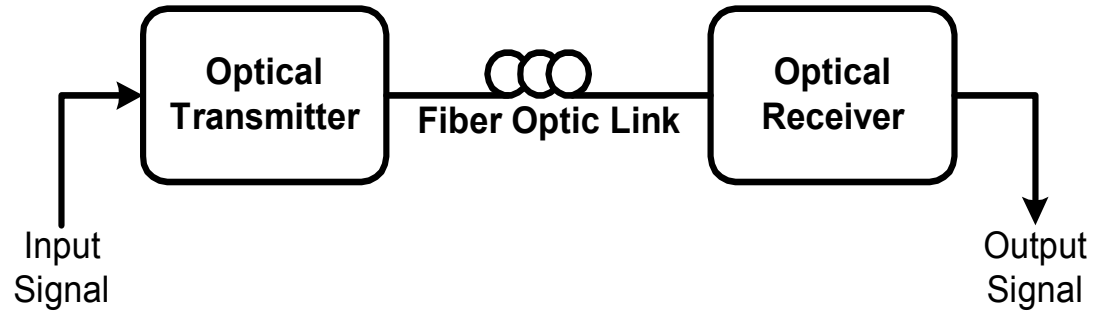

Figure 1-1 Fiber optic communication system components

Despite of the high cost and special skills required to handle fiber optics, it has some great advantages over the traditional copper-based transmission systems such as:

1. Fiber optics cables carry signals with lesser energy loss and higher bandwidth than copper cables and consequently they can carry more channels of information over longer distances.

2. Fiber optic cables are lighter and thinner than copper cables and this means that less space is required in underground cabling ducts.

3. Fiber optics are immune to electromagnetic interference from radio signals, car ignition systems, lightning etc. They can be routed safely through explosive or flammable atmospheres, for example, in the petrochemical industries or munitions sites, without any risk of ignition.

It is very important in a long-haul[1] terrestrial fiber optic communication system to transmit the maximum number of bits per seconds over the maximum possible distance with the minimum bit error rate.

1.1 NRZ versus RZ Coding

NRZ (non-return to zero) coding uses 0 volts for a data bit of '0' and +V volts for a data bit of '1' as shown in Figure 1-2 (a). With RZ (return to zero) coding, a '0' bit is also represented by 0 volts whereas a '1' data bit is represented by +V volts for part of the cycle and 0 volts for the remaining part of the cycle as shown in Figure 1-2 (b) [2].

[1] Long-haul optics refers to the transmission of visible light signals over optical fiber cable for great distances especially without the use of repeaters.

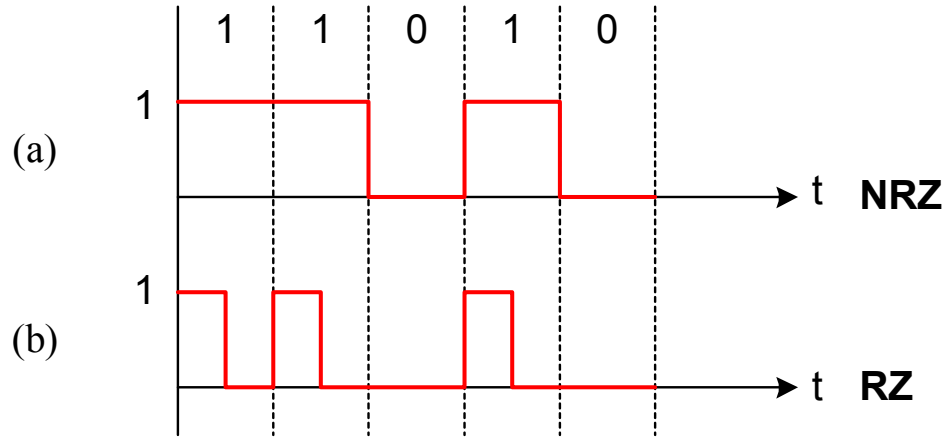

Figure 1-2 (a) NRZ versus (b) RZ encoding

The RZ pulses return to the 0 state before reaching the end of the bit interval, therefore they are not as wide as NRZ pulses and this requires wider transmission bandwidth. However, with using suitable bandwidth, RZ coding has proven that it is better, in optical fiber transmission, than NRZ especially with higher transmission bit rates and longer distances. It has been experimentally proven that at higher data rates RZ encoding is superior to NRZ for several reasons such as:

1. RZ signal performs better than NRZ signal because of the interaction between self-phase modulation (SPM) and chromatic dispersion [3].

2. RZ is better than NRZ in tolerating fiber nonlinearity. This is because long strings of "1's" in NRZ as compared to RZ have much longer cross-wavelength interaction time, thereby producing more severe penalty from nonlinearity [4].

3. Some RZ systems reduce the effect of the intrachannel four-wave mixing (IFWM) [4]-[5] such as RZ-OOK (return to zero on-off keying) and RZ-DPSK (return to zero phase-shift keying). As a result RZ signal can operate at higher

channel power, which translates longer fiber span or longer transmission distance [3].

1.2 Chromatic Dispersion

In long-haul systems, it is possible for pulses to spread out after traveling for several kilometers. It will then become difficult, sometimes impossible, to distinguish between two adjacent bits. This spreading of pulses is known as dispersion [6]. Therefore, dispersion can limit the transmission bit rate and transmission distance.

Chromatic dispersion, or group-velocity dispersion (GVD), is one type of dispersion which is severely experienced in SSMF (standard signal mode fiber). It represents the fact that different colors or wavelengths travel at different speeds in an optical fiber link. Chromatic dispersion is expressed as:

$$D(\lambda) = \frac{1}{L}\frac{d\tau(\lambda)}{d\lambda} \qquad \textbf{(1-1)}$$

where L is the total fiber length, τ is the delay, and λ is the wavelength [7]. Therefore, dispersion is measured in units of ps/nm/km.

SSMF has zero dispersion at wavelength of 1310 nm as shown in Figure 1-3, although it has higher optical loss than the 1550 nm wavelength [7]. The problem of the chromatic dispersion will appear with the 1550 nm wavelength. To overcome this problem, a special type of fiber called dispersion compensating fiber (DCF) is being used.

DCF consists simply of a single mode dispersion compensating fiber with a highly negative dispersion. The use of DCF allows conventional fiber to still be used even over long distances and at high bit rates [8].

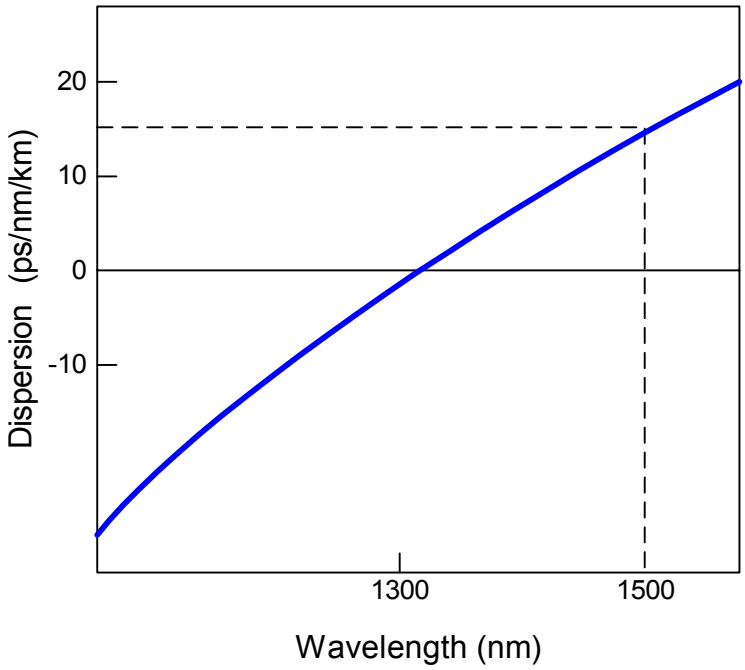

Figure 1-3 The relation between dispersion and wavelength for SSMF

1.3 DWDM System

DWDM stands for Dense Wave Division Multiplexer. It is an evolution of the WDM (Wave Division Multiplexer) which is, DWDM, capable of providing 16 to 40 channels with channel spacing of 100 to 200 GHz or 64 to 128 channels with channel spacing of 50 or even 25 GHz [9].

A typical DWDM system compromises the function of transmitting and separating multiple optical channels as shown in Figure 1-4. The input optical signals will be generated by the optical transmitters, each signal has its own wavelength (λ) which should differ from other signals wavelengths. A DWDM multiplexer (MUX) combines all signals in order to be transmitted over common optical fiber link. Normally there are optical amplifiers located at fixed distances to amplify the transmitted signals especially in the case of the long spans. The most commonly used optical amplifiers is called the Erbium-Doped Fiber Amplifiers (EDFAs). Then finally a DWDM demultiplexer will separate the received signals and send each one to its desired destination [9].

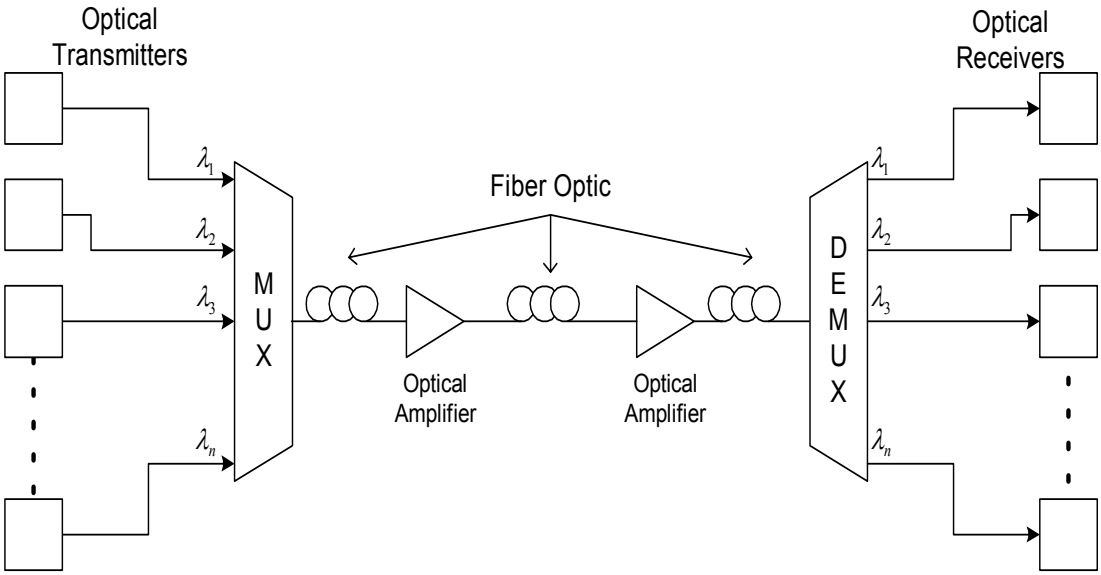

Figure 1-4 DWDM functional schematic diagram

DWDM system requires the following essential components:

1. Very precise light source with stable wavelengths.

2. Fiber optic link that exhibits low loss, in addition to optical amplifiers to boost the signal on longer spans.

3. Photodetectors on the receiving side.

4. Optical add/drop multiplexers (OADMs) and optical switches.

1.3.1 Light Sources

Light sources, or light emitters, are transmitter side devices. Two general types of light sources devices are used in optical transmission: light emitting diodes (LEDs) and laser diodes [10]. LEDs are relatively slow devices and have wider spectrum, therefore they are suitable for use at low speeds and not for DWDM systems. On the other hand, laser diodes have better performance than LEDs and can produce single frequency, therefore they can be used in DWDM systems.

Laser diodes are semiconductor devices that produce light waves by emitting photons. Figure 1-5 illustrates the possible photon emission and absorption processes for a two-level atomic system. An electron can move from an energy level (E_1) to a higher energy level (E_2) by either being pumped externally or by absorbing the energy ($h\nu_{12}$) from a passing photon, this process is called "stimulated absorption". The excited electron can return to energy level (E_1) either spontaneously or by stimulation, as a result a photon will be emitted. Spontaneous emission occurs randomly and therefore the emitted photons have random phases and frequencies, this type of light has a broad spectral width and is called incoherent. On the other hand, stimulated emission occurs when some external stimulant, i.e. incident photon, causes an excited electron to drop to the ground state. The photon emitted in this process has the same energy or wavelength as the incident photon and in phase with it. This means that their, incident photon and

emitted photon, amplitudes add to produce a brighter light or coherent light. In order for stimulated emission to occur, there must be more electrons in the energy level (E_2) than in the energy level (E_1); this can be achieved by supplying additional external energy to pump electrons to a higher energy level [10].

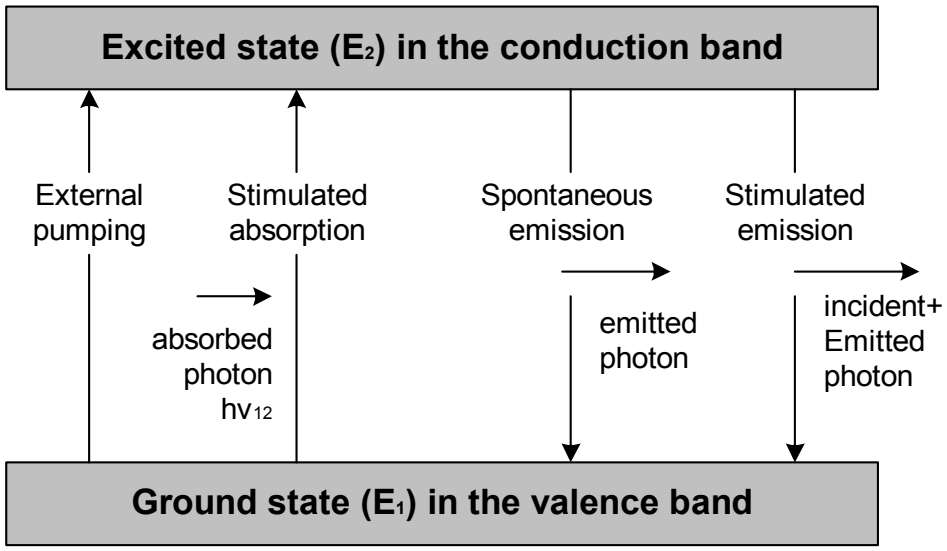

Figure 1-5 Possible photon emission and absorption processes for a two-level atomic system

Laser action takes place within a region called the gain medium or laser cavity. To achieve lasing action within this region, the photon density needs to be built up so that the stimulated emission rate becomes higher than the rate at which photons are absorbed by the semiconductor material. With each pass through the cavity, the photons stimulate more excited electrons to drop to the lower energy level and more photons of the same wavelength will be emitted. If the gain is sufficient to overcome the losses in the cavity, the device will start to oscillate at a particular optical frequency which is called lasing threshold. Beyond the lasing threshold the device behaves as a laser and the light output increases sharply with bias voltage [10].

In DWDM systems, where multiple wavelengths are sent at the same time using the same fiber optic link, any stray wavelengths can cause problems by interfering with other signals. Therefore, it is highly recommended to use a laser source that emits light at single frequency.

Distributed feedback (DFB) laser is a single frequency laser which is widely used in DWDM systems. In this type of laser, a series of closely spaced reflectors provide light feedback in a distributed fashion throughout the cavity as shown in Figure 1-6. Through a suitable design of these reflectors spacing during fabrication, the device can be made to oscillate in only a well-defined wavelength [10].

Light that is traveling in the active layer goes in all directions and it will eventually hit the corrugated structure of the grating reflectors. As consequences, the grating reflectors will reflect only a specific wavelength back into the cavity and allow other wavelengths to pass through. The grating reflectors are feeding back the desired wavelength into the cavity and this is taking place over the whole length of the laser, therefore the feedback is distributed. The only laser light that builds up within the active layer is the light of the specific wavelength which will be emitted accordingly [11].

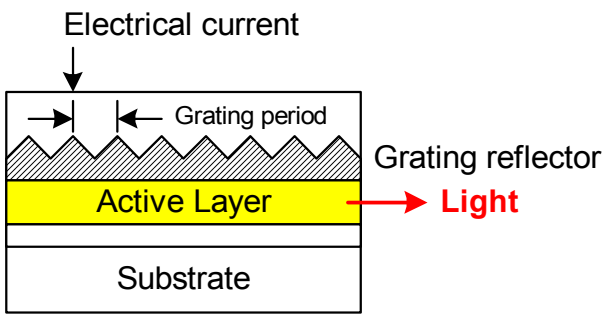

Figure 1-6 Schematic structure of a DFB laser

1.3.2 Erbium-Doped Fiber Amplifiers (EDFAs)

There are limits to how long a fiber segment can propagate a signal before it has to be amplified due to fiber attenuation or loss. Traditionally, optical signals used to be amplified by converting them to an electrical format, amplifying the electrical signals, and then reconverting the electrical signals into optical ones. With the invention of the optical amplifiers (OAs), the process of amplifying the optical signals becomes much easier and the performance of the optical communication links becomes better. There are three fundamental types of optical amplifiers: the semiconductor optical amplifiers (SOAs) that are based on the same operating principles as laser diode, the erbium-doped fiber amplifiers (EDFAs) that use specially constructed fiber for the amplification medium, and the Raman amplifiers that make use of the transmission fiber itself [10]. All optical amplifiers increase the power level of the light through the stimulation emission process that described in section 1.3.1.

EDFA consists of optical fibers of 10 to 30 meters length that has been lightly doped with a rare-earth element (erbium), one or more pump lasers, a wavelength-selective coupler (WSC), optical isolators (IOs), and tap couplers as shown in Figure 1-7 [10]. The WSC handles either 980/1550-nm or 1480/1550-nm wavelength combinations to couple both the pump and signal optical powers efficiently into the fiber amplifier. Tap couplers are used on both sides of the amplifier to compare the incoming signal with the amplified output. Optical isolators prevent the amplified signal from reflecting into the device, where it could increase the amplifier noise and decrease its efficiency [10].

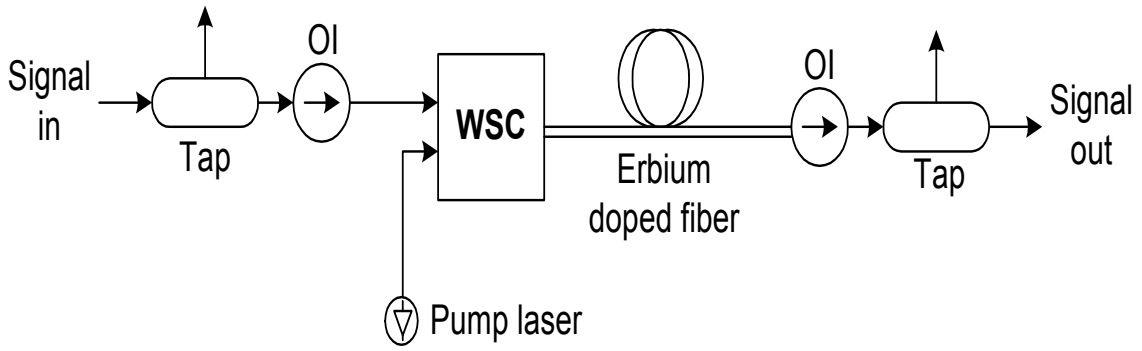

Figure 1-7 EDFA configuration

Amplifier gain is one of the most important parameter for any optical amplifier. The amplifier gain (G) is defined as:

$$G = \frac{P_{out}}{P_{in}} \qquad \textbf{(1-2)}$$

where P_{in} and P_{out} are the input and output signal powers. The gain is generally measured in decibel units as $G[dB] = P_{out}[dB] - P_{in}[dB]$ [10].

The dominant noise generated in an optical amplifier results from amplified spontaneous emission (ASE). When there are more electrons sitting in the higher energy level than the lower energy level, some of these electrons may spontaneously drop down to the lower energy level. This process generates unwanted photons which will be amplified by the EDFA to produce what is known as ASE, and this will definitely degrade the signal-to-noise ratio (SNR) of the amplified signal [10]. The noise figure (NF) is a measure of this degradations and it is generally equal to the electrical SNR at the

input divided by the electrical SNR at the output. The ASE noise power at the output of the amplifier is defined as [12]:

$$P_N = n_{sp} h f_c (G-1) B_o \qquad \textbf{(1-3)}$$

where n_{sp} is the spontaneous emission factor, h is the photon energy, f_c is the center frequency, G is the amplifier gain, and B_o is the optical bandwidth.

1.3.3 Photodetectors

It is necessary to recover the transmitted signals at different wavelengths at the receiving end. The demultiplexer will separate different wavelengths and then the photodetector will convert the optical power into a corresponding electrical current.

Two types of photodetectors are widely deployed, the positive-intrinsic-negative (PIN) photodiode and the avalanche photodiode (APD). PIN photodiodes have many advantages, including low cost and reliability, but APDs have higher receive sensitivity and accuracy. However, APDs are more expensive than PIN photodiodes, they can have very high current requirements, and they are temperature sensitive [9].

PIN photodiodes work on principles similar to, but in the reverse of, LEDs. That is, light is absorbed rather than emitted, and photons are converted to electrons. PIN photodiode consists of *p* and *n* semiconductor regions separated by an intrinsic (*i*) region

as shown in Figure 1-8. A reverse-bias voltage is applied across the photodiode so that no free electrons or holes exist in the intrinsic region.

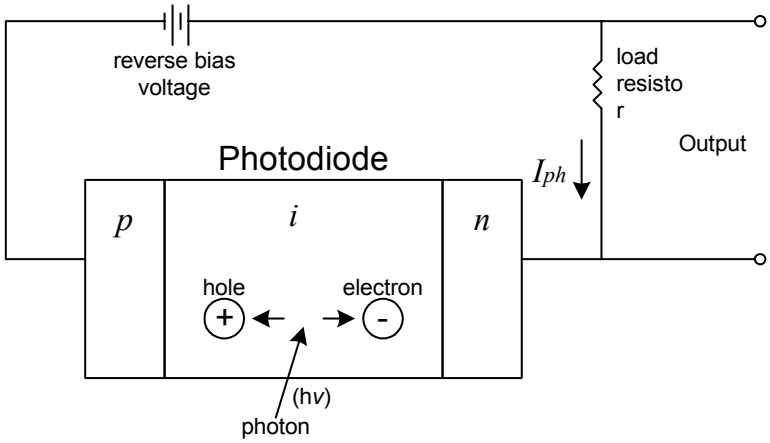

Figure 1-8 PIN photodiode circuit with an applied reverse bias

As explained earlier in section 1.3.1, electrons in semiconductor materials are allowed to reside in only two specific energy bands, (E_1) and (E_2) which are separated by an energy gap region, as shown in Figure 1-9, and the difference between E_2 and E_1 is called bandgap energy. If an incident photon has energy greater than or equal to the bandgap energy of the semiconductor material, then it will give up its energy and excite an electron from the valence band to the conduction band. This process which occurs in the intrinsic region generates free electron-hole pairs known as photocarriers. The electric field across the device causes the photocarriers to be swept out of the intrinsic regions which accordingly increases the current flow in the external circuit; this current flow is known as the photocurrent [10]. The photocurrent equal to [12]:

$$I_{ph} = \mathcal{R} P \qquad \textbf{(1-4)}$$

Where P is the received optical power, and $\mathcal{R}$ is the photodetector responsivity.

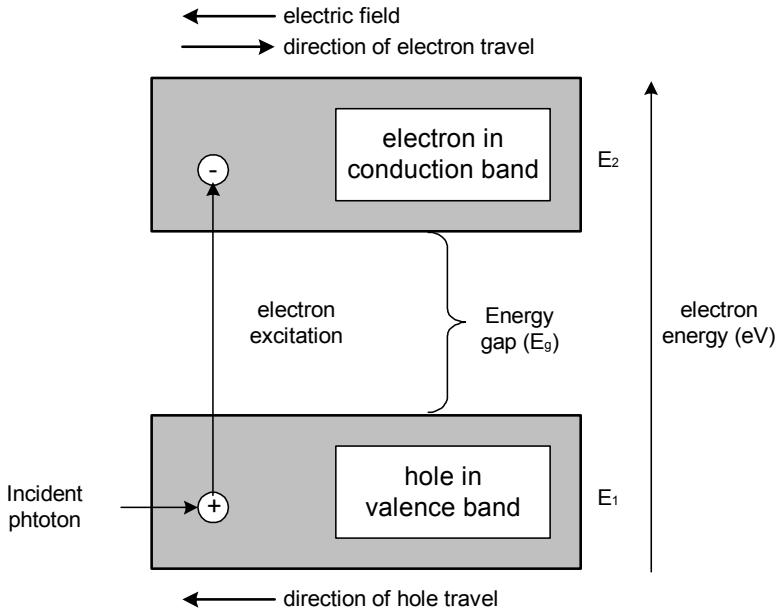

Figure 1-9 Electron excitation process

APDs are similar devices to PIN photodiodes, but provide gain through an amplification process: one photon acting on the device releases many electrons.

1.3.4 Optical Receiver

Optical receiver is the last optical component in an optical communication system. The function of an optical receiver is to convert the modulated optical pulses into a replica of the original signal. The photodiode is therefore in charge of this conversion. Typical optical receiver consists of a photodiode followed by an electrical low-pass filter as shown in Figure 1-10.

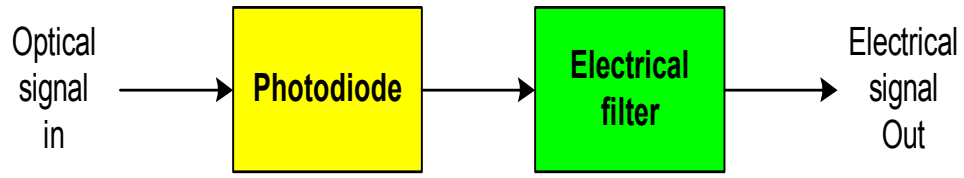

Figure 1-10 Optical receiver block diagram

1.4 MicroElectroMechanical Systems (MEMSs)

MEMS are miniature devices that combine mechanical, electrical, and optical components to provide sensing and actuation functions. MEMS devices are fabricated using integrated-circuit techniques and range in size from micrometers to millimetres. The control or actuation of a MEMS device is done through electrical, thermal, or magnetic means [10].

A simple example of a MEMS actuation method is shown in Figure 1-11. There is a thin suspended polysilicon beam at the top of the device, and at the bottom there is a silicon ground plane which is covered by an insulator material as shown in Figure 1-11 (a). When a voltage is applied between the silicon ground plane and the polysilicon beam, the electric force pulls the beam down so that it makes contact with the lower structure as shown in Figure 1-11 (b).

Initially MEMS devices were based on silicon technology which is very stiff material and therefore it will require higher voltages to produce mechanical motion or deflection. Highly compliant polymeric materials that are less stiff than silicon started to

take place from silicon in MEMS devices. This class of components is referred to as compliant MEMS or CMEMS. CMEMS devices require lower voltages to achieve a required mechanical motion or deflection [10].

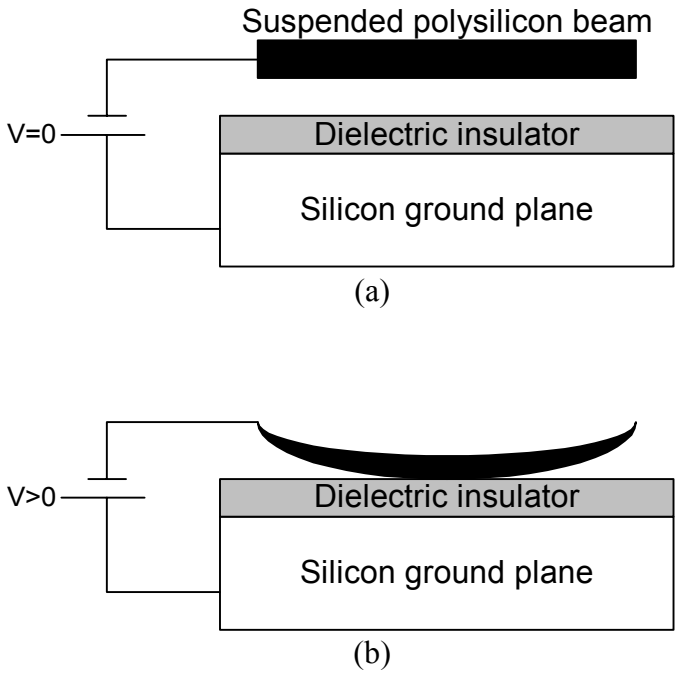

Figure 1-11 A simple example of a MEMS actuation method

MEMS devices have some reliability problems if the manufacturer does not follow strict fabrication procedures such as stiction, which is the tendency of two silicon surfaces to stick to each other permanently. A second issue is how to keep contaminants such as dust particles away from MEMS structures during singulation[2]. A third issue is related to the packaging of the devices so that no contaminants are present to cause mal functions in the moving parts of the MEMS device.

[2] Singulation is the process of cutting up a large fabricated wafer into individual MEMS devices [10].

1.4.1 MEMS in Optical Switches

Many types of optical components such as optical add/drop multiplexers (OADMs) and optical switches are fabricated using MEMS technology. The function of OADM is to insert (add) or extract (drop) one or more selected wavelengths at a designated point in an optical network, whereas the function of an optical switch is to switch wavelengths between different locations.

MEMS in context of optical switches refers to miniature movable mirrors fabricated in silicon with dimensions ranging from a few hundred micrometers to few millimetres [12]. Two types of mirror structures are being used: the 2D mirror and the 3D mirror. The 2D mirror, it is also called two-state pop-up mirror, is shown in Figure 1-12. In one state, the mirror is flat in line with the substrate and therefore the light beam will not be deflected. In the other state the mirror pops up to a vertical position and the light beam, if present, will be deflected [12].

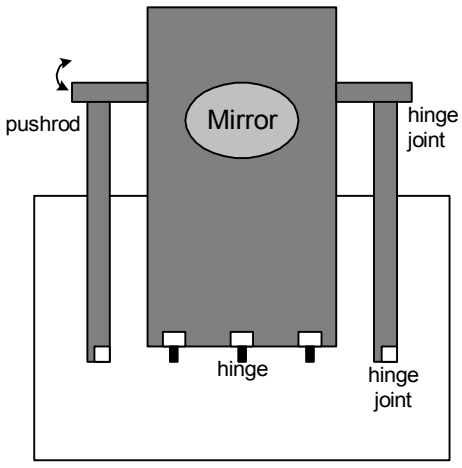

Figure 1-12 2D MEMS mirror

The second type of mirror structures is the 3D mirror shown in Figure 1-13. The mirror is connected through flexures to an inner frame, which in turn is connected through another set of flexures to an outer frame. The flexures allow the mirror to be rotated freely on two distinct axes [12]. The control of this mirror requires a fairly sophisticated servo control mechanism to deflect the mirror to its correct position [12].

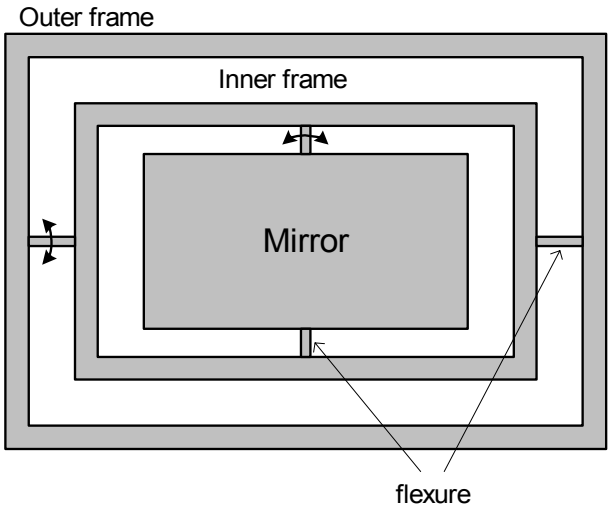

Figure 1-13 3D MEMS mirror

Figure 1-14 shows an $n \times n$ optical switch using two arrays of 3D mirrors. Each array has n mirrors, one associated with each switch port. An input signal is coupled to its associated mirror in the first array. The first mirror can be deflected to point the light beam to any of the mirrors in the second array. For example, to make a connection from port i to port j, the mirror i in the first array is pointed to mirror j in the second array and vice versa. Mirror j then allows the beam to be coupled out of port j.

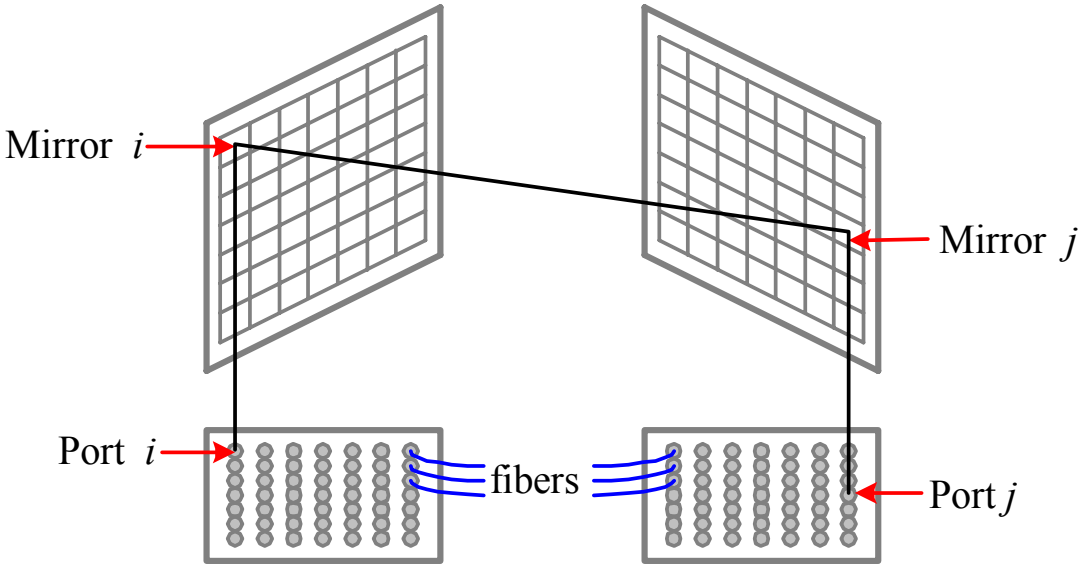

Figure 1-14 An *n*×*n* optical switch built using two arrays of 3D MEMS mirrors

MEMS can be fabricated either by using surface micromachining or bulk micromachining techniques. Surface micromachining technique is an additive process whereby layers are selectively deposited by low-pressure chemical vapour deposition (LPCVD), then patterned and removed to create the desired structures on top of the silicon substrate. The substrate in this case is only used as a support or anchor [13]. Bulk micromachining is the process whereby the pieces for the microstructure are formed in the bulk of the wafer by anisotropic etching [13]. 2D mirrors are fabricated using surface micromachining technique and 3D mirrors are fabricated using bulk micromachining technique [12].

1.5 BER, BER ISI, and Q-factor

With the high bit rates and long-haul transmission links, there is a need to measure the end-to-end performance of the system. Bit error rate (BER) is one performance measurement that is used at the receiver side. It is defined as the probability of incorrect identification of a bit by the decision circuit of the receiver [7] as expressed in equation (1-5). In another words, the probability of making an error is the average of the probability of calling a '1' a '0' given that a '1' was sent plus the probability of calling a '0' a '1' given that a 0 was sent [7].

$$BER = P(1)P(0/1) + P(0)P(1/0) \qquad \textbf{(1-5)}$$

where:

P(1) is the probability of sending bit 1.

P(0) is the probability of sending bit 0.

P(0/1) is the probability of deciding 0 when 1 is transmitted.

P(1/0) is the probability of deciding 1 when 0 is transmitted.

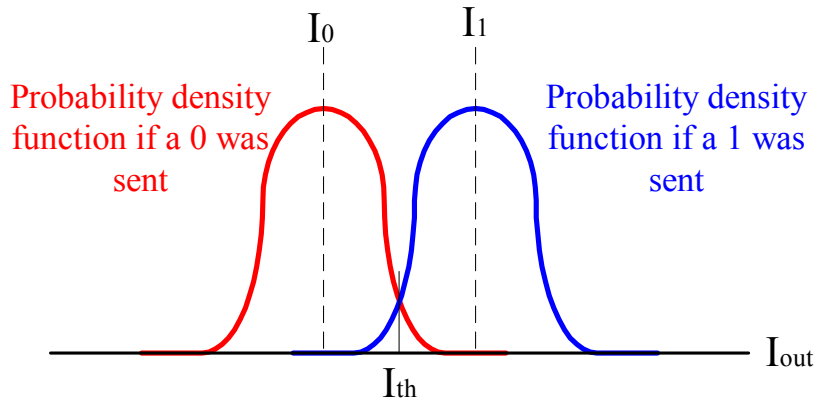

Figure 1-15 Probability density curves for a logical '1' and a logical '0'

Normally the receiver makes decision whether the received bit is 0 or 1 by sampling the photocurrent. The receiver could make a wrong decision due to the presence of noise which is assumed to be Gaussian. The photocurrent for a 1 bit is a sample of a Gaussian random variable with mean I_1 and variance σ_1. Similarly, the photocurrent for a 0 bit is a sample of a Gaussian random variable with mean I_0 and variance σ_0. σ_1 and σ_0 are not equal in our case because the optical amplifiers noise is included [12]. The receiver should check each sample and decide whether the transmitted bit is 1 or 0 by minimizing the bit error rate. One way to do that is by defining a threshold current value (I_{th}). If $I \geq I_{th}$, then a 1 bit was transmitted, and if $I < I_{th}$, then a 0 bit was transmitted. The threshold photocurrent is given approximately by equation (1-6) which minimizes the error [8]:

$$I_{th} = \frac{\sigma_0 I_1 + \sigma_1 I_0}{\sigma_0 + \sigma_1} \qquad \textbf{(1-6)}$$

Equation (1-6) satisfies the condition [8]:

$$\frac{I_1 - I_{th}}{\sigma_1} = \frac{I_{th} - I_0}{\sigma_0} \equiv Q \qquad \textbf{(1-7)}$$

The complementary error function (erfc) is expressed as [8]:

$$erfc(x) = \frac{2}{\sqrt{\pi}} \int_x^{\infty} e^{-y^2} dy \qquad \textbf{(1-8)}$$

This erfc can be used to calculate P(0/1) and P(1/0) [8]:

$$P(0/1) = \frac{1}{\sigma_1\sqrt{2\pi}} \int_{-\infty}^{I_{th}} \exp\left[-\frac{(I - I_1)^2}{2\sigma_1^2} \right] dI = \frac{1}{2} erfc\left(\frac{I_1 - I_{th}}{\sigma_1\sqrt{2}} \right) \quad \textbf{(1-9)}$$

$$P(1/0) = \frac{1}{\sigma_0\sqrt{2\pi}} \int_{I_{th}}^{\infty} \exp\left[-\frac{(I - I_0)^2}{2\sigma_0^2} \right] dI = \frac{1}{2} erfc\left(\frac{I_{th} - I_0}{\sigma_0\sqrt{2}} \right) \quad \textbf{(1-10)}$$

Since P(0) = P(1) = ½ , then from (1-5), (1-9), and (1-10), the BER can be shown to equal:

$$BER = \frac{1}{4}\left[erfc\left(\frac{I_1 - I_{th}}{\sigma_1\sqrt{2}} \right) + erfc\left(\frac{I_{th} - I_0}{\sigma_0\sqrt{2}} \right) \right] \quad \textbf{(1-11)}$$

By using the relation in equation (1-7), the BER can be expressed as:

$$BER = \frac{1}{4}\left[erfc\left(\frac{Q}{\sqrt{2}} \right) + erfc\left(\frac{Q}{\sqrt{2}} \right) \right]$$

$$BER = \frac{1}{2} erfc\left(\frac{Q}{\sqrt{2}} \right) \approx \frac{\exp\left(-Q^2/2\right)}{Q\sqrt{2\pi}} \quad \textbf{(1-12)}$$

Equation (1-12) is valid for Q > 3 [8]. Figure 1-16 shows the relation between the BER and Q-factor.

The Q-factor can be easily evaluated using equations (1-6) & (1-7):

$$Q = \frac{I_{th} - I_0}{\sigma_0} = \frac{\frac{\sigma_0 I_1 + \sigma_1 I_0}{\sigma_0 + \sigma_1} - I_0}{\sigma_0}$$

$$Q = \frac{I_1 - I_0}{\sigma_1 + \sigma_0} \quad \textbf{(1-13)}$$

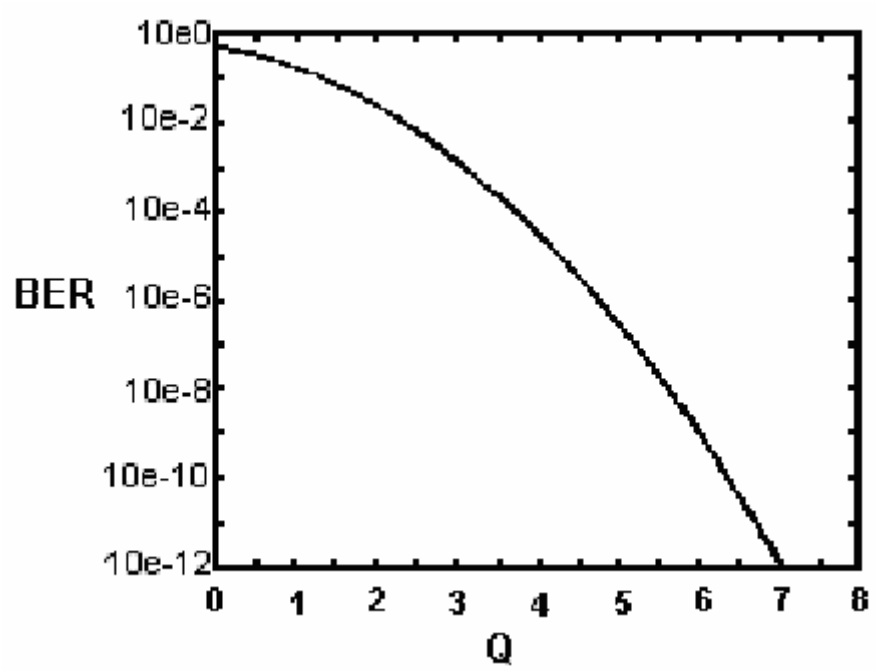

Figure 1-16 BER versus Q-factor

Normally BER will include the Gaussian noise as mentioned before, but it is not considering the intersymbol interfernce[3] effect. The pulse spreading in the received signal lead to a form of noise noted as intersymbol interference [8] as shown in Figure 1-17 which is neglected by the BER. Therefore, the BER ISI (bit error rate due to intersymbol interference) is considered to be better performance measurement than BER.

BER ISI is a better approach to estimate the error probability by viewing each bit in the context of its two adjacent bits [14]. Each bit triplet is referred to as a metasymbol. There are four possible metasymbols corresponding to a logical '1': 010, 011, 110, and

[3] In a digital transmission system, distortion of the received signal, manifested in the temporal spreading and consequent overlap of individual pulses to the degree that the receiver cannot reliably distinguish between changes of state, i.e., between individual signal elements [15].

111. Similarly, ther are four metasymbols corresponding to a logical '0: 000, 001, 100, and 101. In the ISI analysis methods, the statistics of the central bit in each of the eight different metasymbols are calculated rather than computing the statistical parameters for only two types of symbol (logical ‘1’ and logical ‘0’). In this way, the variations in mean levels caused by ISI are accounted for correctly, and are not erroneously included in the noise variance. Computer simulation tool "VPItransmissionMaker^{TM}WDM" that is used in this thesis has the ability to calculate the BER ISI [16].

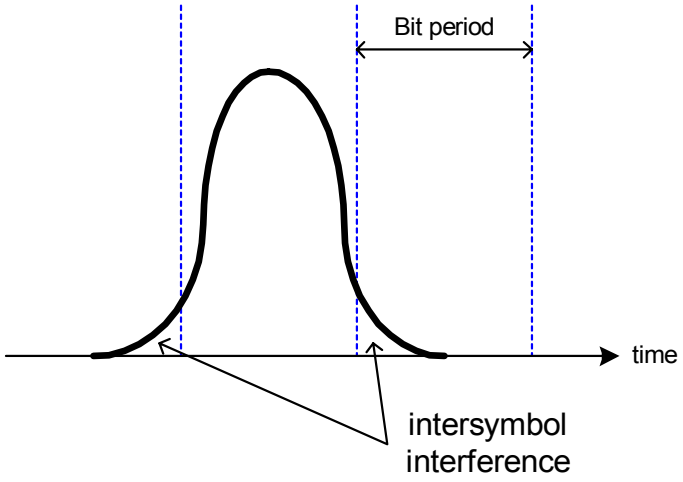

Figure 1-17 Example of intersymbol interference

1.6 Eye Diagram

Eye diagram, or eye pattern, is a way of evaluating the performance of an optical fiber data link [17], in other words, it is an indication of signal quality. It overcomes the limitations of a single-value display by superimposing all 1's and 0's [17]. If the eye is closed, then this is an indication of degradation in the receiver performance and accordingly this will increase the BER. An example of how to display a 3-bit long NRZ data by an eye diagram is shown in Figure 1-18.

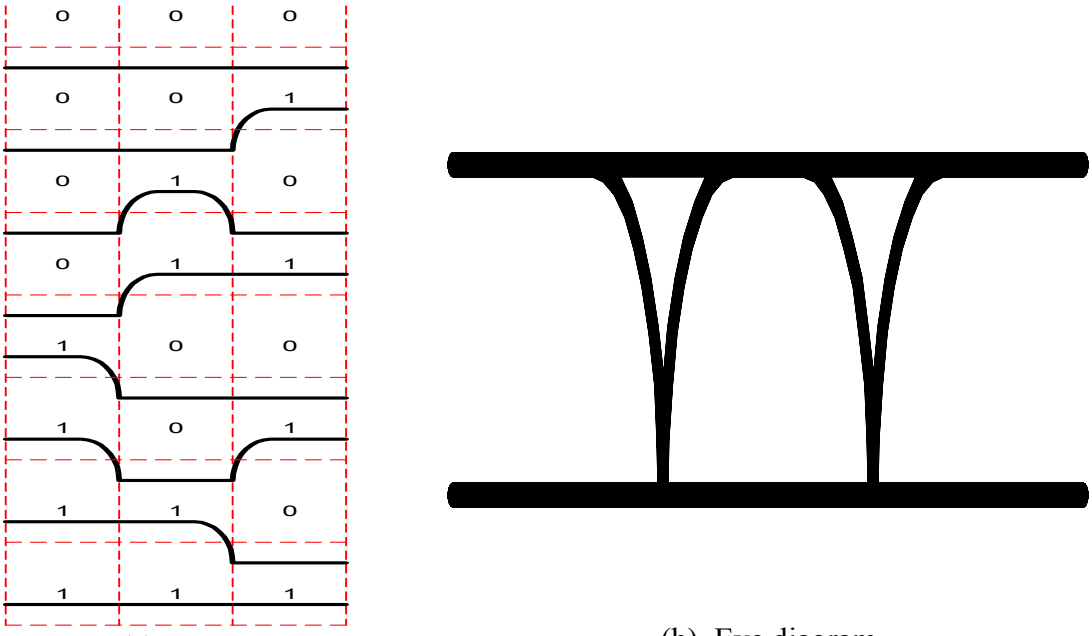

(a) Data (b) Eye diagram

Figure 1-18 Eye diagram of a 3-bit long NRZ data

1.7 Thesis Outline

In Chapter 2, Optical Transmitters Design, different types of optical transmitters will be described: NRZ, chirp-free RZ transmitters with 33% duty cycle and 50% duty cycle, and alternate chirp RZ transmitters using two modulators and one modulator.

In Chapter 3, System Model, the model of fiber optic link will be introduced, derivation of Nonlinear Schrödinger (NLS) equation and its numerical solution using the Split-Step Fourier Method, and how to upgrade existing 2.5 Gb/s fiber links to 10 Gb/s.

In Chapter 4 and Chapter 5, we will evaluate the performance of different optical transmitters described in Chapter 2 by using two different dispersion compensation schemes. In the first scheme, dispersion compensating modules will be inserted at the transmitter and the receiver sites (end-to-end compensation). Whereas in the second

scheme, dispersion compensating modules will be inserted at the transmitter, receiver, and optical switches sites that are normally located every 640 km (super span).

Finally Chapter 6, Conclusion, will be dedicated for summarizing the work, commenting on the results, and future work.

CHAPTER 2
OPTICAL TRANSMITTERS DESIGN

Optical transmitters are devices that convert electrical input signals into modulated optical signals. Normally an optical transmitter consists of a light source which is used to launch the optical power into the fiber, and its driver circuit. Three main types of optical transmitters are going to be explained in this chapter: NRZ, chirp[4]-free RZ, and alternate chirp RZ transmitters. Two types of chirp-free RZ transmitters will be covered: chirp-free RZ transmitter with 50% duty cycle (or RZ-50% duty cycle transmitter), and chirp-free RZ transmitter with 33% duty cycle (or RZ-33% duty cycle transmitter). Similarly, two types of alternate chirp RZ transmitters will be covered: alternate chirp RZ transmitter using two modulators and alternate chirp RZ transmitter using one modulator. First, we will introduce the amplitude modulator and then we will discuss the design of different optical transmitters mentioned above.

2.1 Mach-Zehnder Amplitude Modulator (Lithium Niobate)

Amplitude modulator (AM) is a key component which is being used in the design of all optical transmitters. Mach-Zehnder AM is widely used in the filed of optical communication. It is built using two phase modulators and two optical couplers as shown in Figure 2-1 where m(t) is either (1) or (0).

[4] An optical pulse is said to be chirped if its carrier frequency changes with time in a deterministic fashion [7].

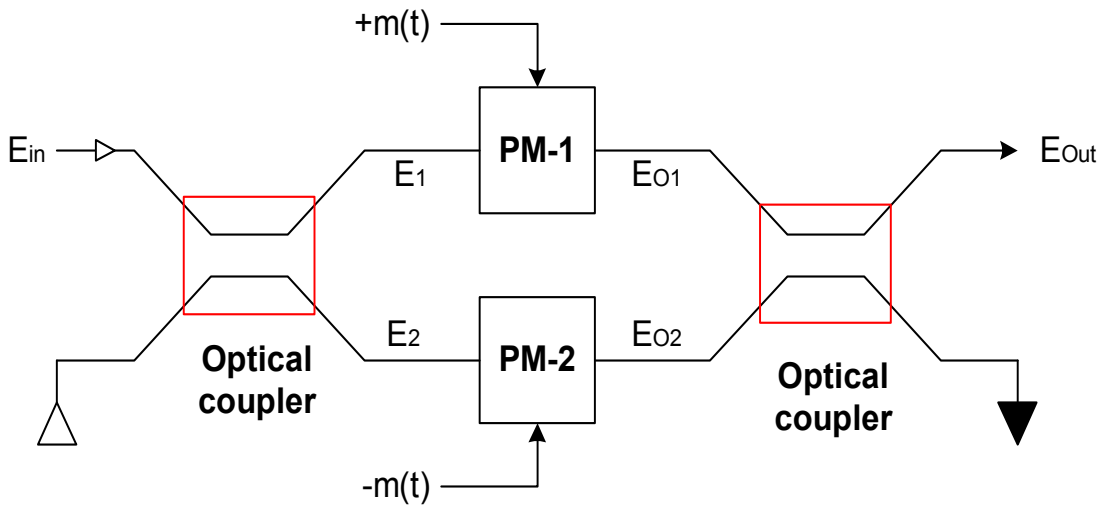

Figure 2-1 Mach-Zehnder amplitude modulator block diagram

In order to find the output electrical field (E_{out}), we have to find the quantities E_1, E_2, E_{o1}, and E_{o2}. It is necessary here to know the function of the optical coupler.

An optical coupler is used to combine or split optical signals. A 2×2 optical coupler shown in Figure 2-2 has two inputs and two outputs and therefore the input/output relation can be expressed as [18]:

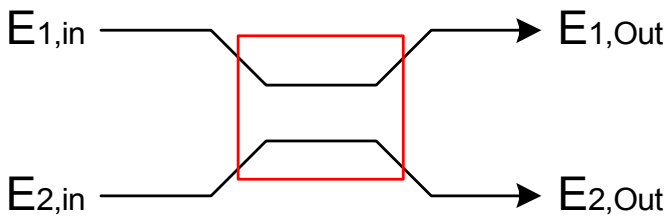

Figure 2-2 A 2×2 optical coupler

$$\begin{bmatrix} E_{1,out} \\ E_{2,out} \end{bmatrix} = \begin{bmatrix} \sqrt{1-\alpha} & j\sqrt{\alpha} \\ j\sqrt{\alpha} & \sqrt{1-\alpha} \end{bmatrix} \begin{bmatrix} E_{1,in} \\ E_{2,in} \end{bmatrix} \quad \textbf{(2-1)}$$

where α is the coupling factor. It can be inferred from Figure 2-2 that:

$E_1 = \sqrt{1-\alpha} E_{in} = \sqrt{\frac{P_{in}}{2}}$, where $E_{in} = \sqrt{P_{in}}$ is the input electrical field and $\alpha = ½$.

$E_2 = j\sqrt{\alpha} E_{in} = j\sqrt{\frac{P_{in}}{2}}$

$E_{o1} = E_1 e^{j\phi m(t)}$, where ϕ is the phase modulation index and is equal to 90°.

$E_{o2} = E_2 e^{-j\phi m(t)}$

$$E_{out} = \sqrt{1-\alpha} E_{o1} + j\sqrt{\alpha} E_{o2} = \frac{\sqrt{P_{in}}}{2}\left[e^{j\phi m(t)} - e^{-j\phi m(t)}\right] \quad \textbf{(2-2)}$$

Since $\sin(\phi m(t)) = \frac{e^{j\phi m(t)} - e^{-j\phi m(t)}}{j2}$, then equation (2-2) can be rewritten as:

$$E_{out} = j\sqrt{P_{in}} \sin(\phi m(t)) \quad \textbf{(2-3)}$$

E_{out} is a complex quantity which can be represented by a magnitude and phase:

$$\text{Magnitude} = \sqrt{P_{in}} \sin(\phi m(t)) \quad \textbf{(2-4)}$$

$$\text{Phase} = \phi_{out} = \arctan\left(\frac{\text{Im}}{\text{Re}}\right) = \arctan\left(\frac{\sqrt{P_{in}} \sin(\phi m(t))}{0}\right) = \frac{\pi}{2} \quad \textbf{(2-5)}$$

Output Power = $P_{out} = |E_{out}|^2 = P_{in} \sin^2(\phi m(t))$ **(2-6)**

From equation (2-6), if m(t) = 1, then the output power will equal to the input power ($P_{out} = P_{in}$) , and if m(t) = 0, then the output power will equal to zero.

2.2 NRZ Transmitter

NRZ transmitter is the most famous optical transmitters that exists in reality. The block diagram of this type of transmitters is shown in Figure 2-3. It consists of a data source that is supplied to an NRZ encoder, with a rise time of approximately 25% of the bit time. The light from a continuous-wave (CW) laser source is then modulated with the NRZ signal by a Lithium Niobate amplitude modulator which discussed in section 2.1. The power and chirp of the modulator output for 10 Gb/s system are shown Figure 2-4 where the peak power is equal to 1 mW, note that the output signal does not have chirp.

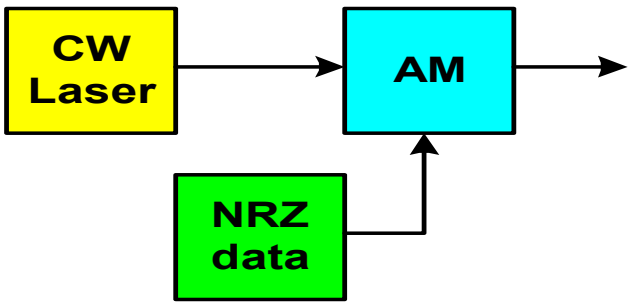

Figure 2-3 NRZ transmitter block diagram

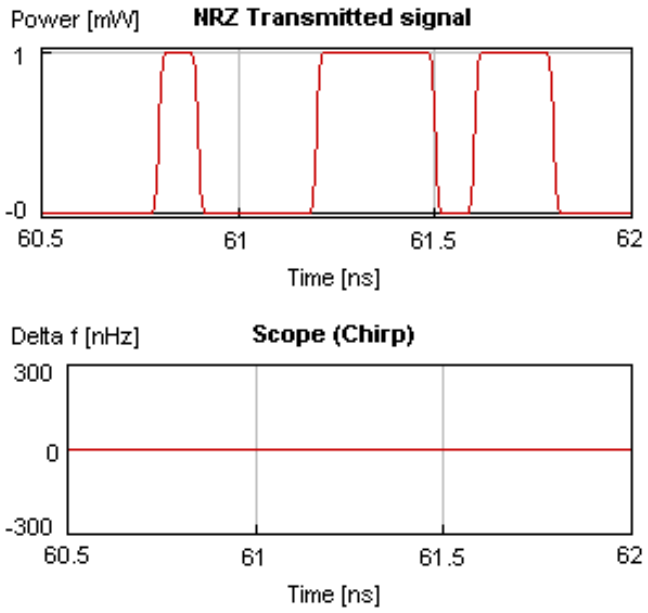

Figure 2-4 Sample of output power and chirp of an NRZ transmitter

2.3 Chirp-Free RZ Transmitters

Chirp-free RZ transmitters are comprised of three basic optical components: a CW laser as a light source, an LiNb amplitude modulator for RZ pulse generation, and another LiNb amplitude modulator to modulate the input data with the RZ pulses. Additional support circuitry may be required to maintain phase relationship between the pulse generation modulator and the data modulation [19]. Figure 2-5 shows the described scenario.

As mentioned in section 2.1, AM-1 can be represented by two phase modulators and two optical couplers where $E_{in} = \sqrt{P_{in}}$ is the input laser electrical field and P_{in} is the

input laser average power, $m(t) = \frac{1}{2}\left[1 + \cos(2\pi ft)\right]$ is a sinusoidal wave with a peak-to-peak value equal to 1 and frequency (f).

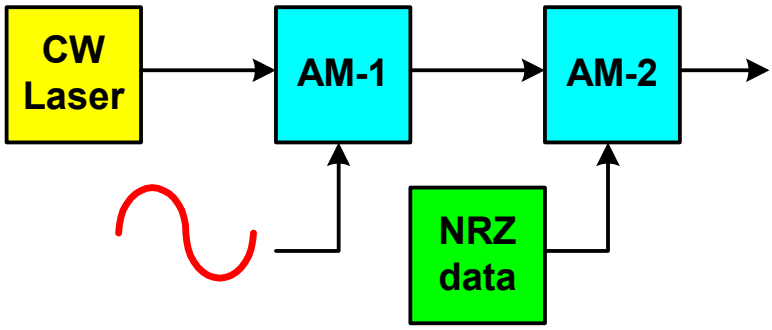

Figure 2-5 Chirp-free RZ transmitter block diagram

Conventional chirp-free RZ transmitters have duty cycle of 33% and 50% [20]. The precise choice of the frequency and the amplitude of the sine wave in addition to the phase modulators indices will result in providing the 50 ps full-width-half-maximum (FWHM[5]) RZ pulses or the 33 ps FWHM RZ pulses for the 10 Gb/s transmission system. There are other chirp-free RZ transmitters such as carrier-suppressed RZ (CS-RZ) which provides 66% duty cycle [21].

In order to generate an RZ pulses with full-width-half-maximum (FWHM) equal to 50 ps for 10 Gb/s system, the phase modulator indices of PM-1 and PM-2 that are inside the first AM should be -90^o and 90^o respectively. The Sinusoidal signal should have a peak-to-peak value of 1 and frequency of 10 GHz. The output power and chirp of

[5] The full width between half-maximum values of a function.

the first AM is shown in Figure 2-6 where the peak power is equal to 1 mW. The power and chirp of the transmitted signal (output of the second AM) are shown in Figure 2-7. The RZ pulses have 50 ps FWHM and the output signal is chirp-free.

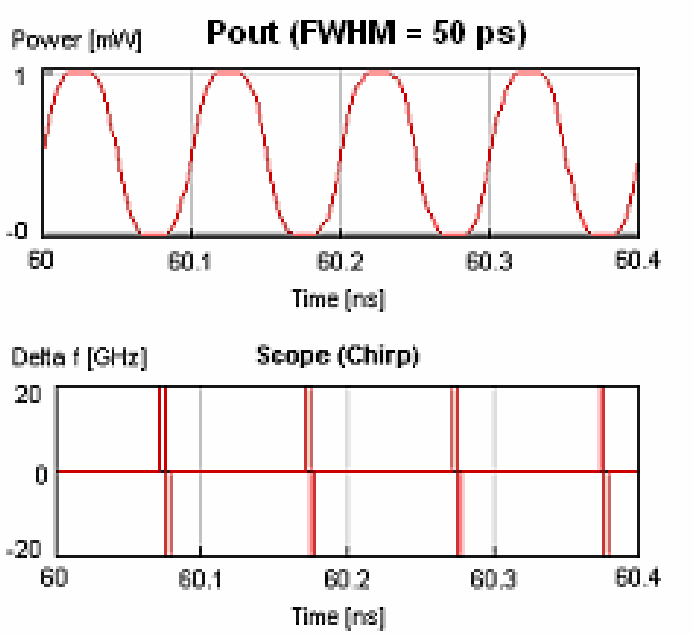

Figure 2-6 Sample of output power and chirp of AM-1 for 50% duty cycle

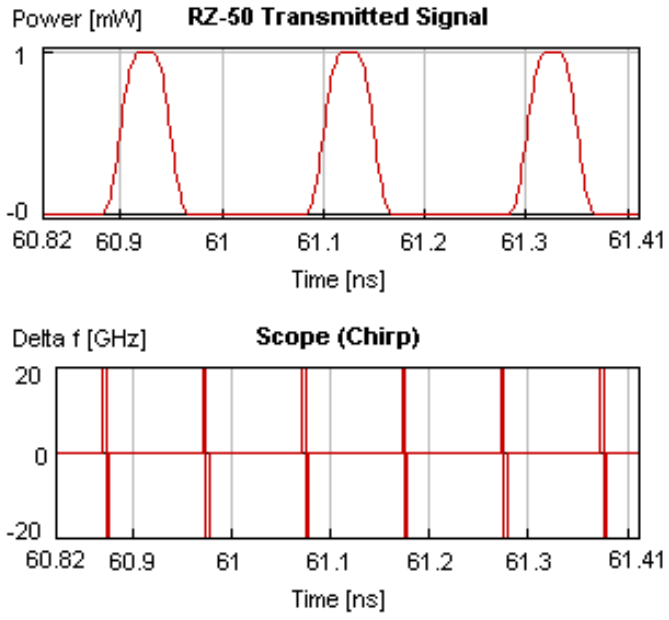

Figure 2-7 Sample of the output power and chirp of the RZ-50% transmitter

To generate a chirp-free RZ pulses with FWHM equal to 33 ps for 10 Gb/s system, the phase modulator indices of PM-1 and PM-2 which are inside the first AM should be -180^{o} and 180^{o} respectively. The Sinusoidal signal should have a peak-to-peak value of 1 and frequency of 5 GHz. The output power and chirp of the first AM is shown in Figure 2-8 where the peak power is equal to 1 mW.

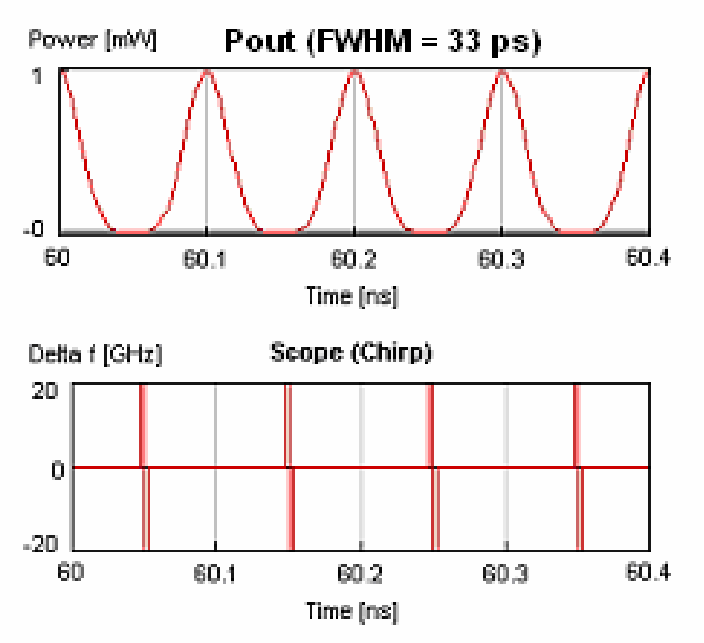

Figure 2-8 Sample of output power and chirp of AM-1 for 33% duty cycle

The power and chirp of the transmitted signal are shown in Figure 2-9. The RZ pulses have 33 ps FWHM and the output signal is chirp-free too. The 33 ps RZ pulses can also be generated by using a sine wave generator that generates sine wave signal of peak-to-peak value of 2 and frequency of 5 GHz, but the phase modulators indices should be set in this case to -90^{o} and 90^{o} for PM-1 and PM-2 respectively.

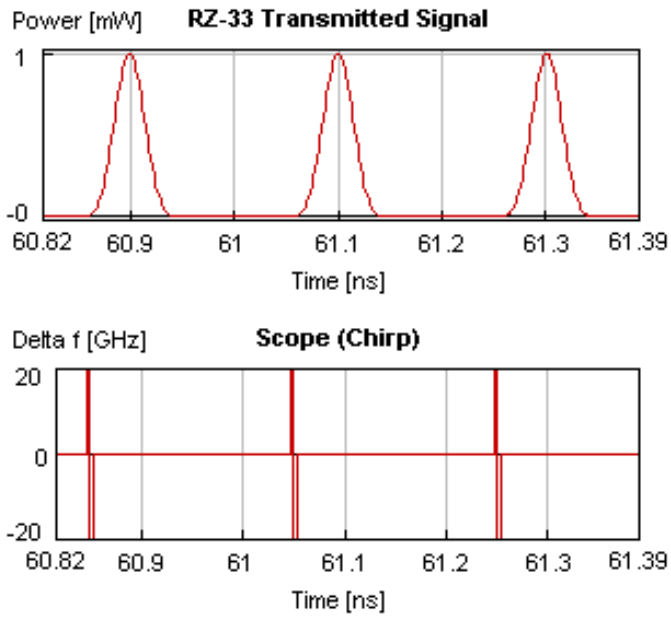

Figure 2-9 Sample of the output power and chirp of the RZ-33% transmitter

2.4 Alternate Chirp RZ Transmitters

The alternate chirp RZ transmitters can be designed using either two modulators, as the case with the chirp-free RZ transmitters, or one modulator as described in sections 2.4.12.4.2 and 2.4.2 as they are commercially available [22]-[23]. Another approach of designing an alternate chirp RZ transmitters is described in [24].

2.4.1 Alternate Chirp RZ Transmitter with Two Modulators

In this type of RZ transmitters, the light from a CW laser source is passed through single phase modulator that is driven by a square wave. A subsequent optical delay (interferometer) converts the phase modulated pulses into an RZ pulses with a width corresponding to the optical delay [22]. The phase modulated RZ pulses will be further modulated with the data source by an amplitude modulator to provide an output of an RZ

pulses. In our simulation, the optical delay is set to 20 ps and therefore the output power which is shown in Figure 2-12 has a FWHM of 20 ps for 10 Gb/s system. The alternate chirp RZ transmitter with two modulators block diagram is shown in Figure 2-10.

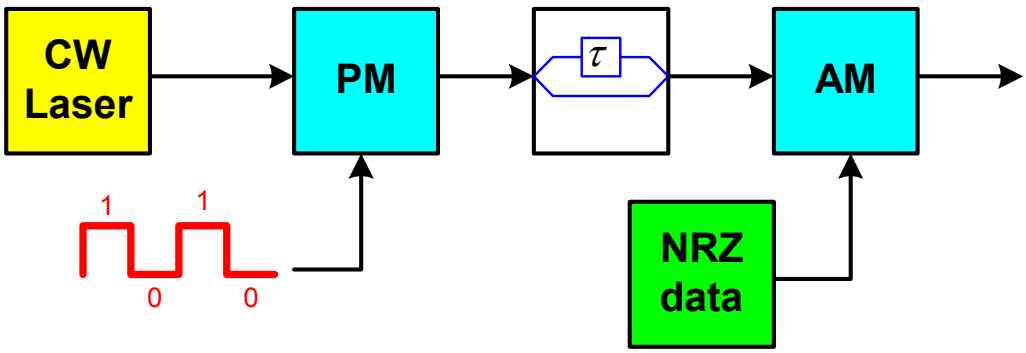

Figure 2-10 Alternate chirp RZ transmitter with two modulators block diagram

The mathematical model can be analyzed for this transmitter in order to prove that the generated pulses are of the RZ type and they have chirp unlike the chirp-free RZ pulses.

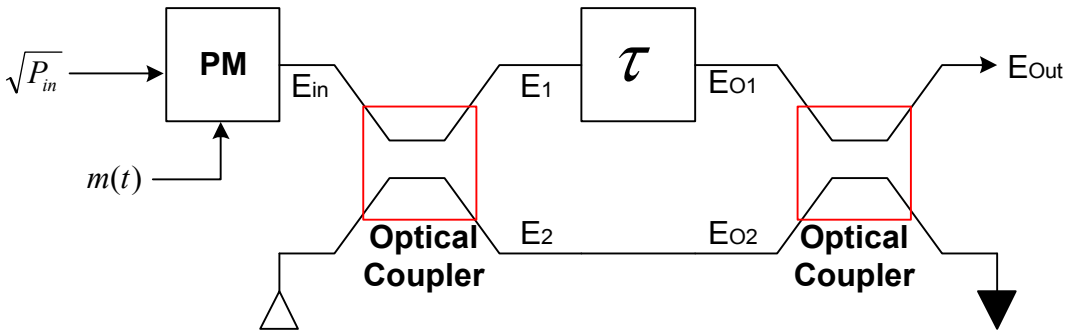

Figure 2-11 Schematic diagram to show the relation between input/output electrical field to/from an optical delay (interferometer)

Figure 2-11 shows the relation between the input electrical field (E_{in}) and the output electrical field pulses (E_{out}). The quantities E_{in}, E_1, E_2, E_{o1}, E_{o2}, and E_{out} can be calculated as following:

$E_{in} = \sqrt{P_{in}} e^{j\phi m(t)}$, where $\phi = \pi$ is the phase modulator index and $m(t)$ is an alternate NRZ encoded pulses (1's and 0's) with rise time of approximately 25% of the bit time.

$E_1 = \sqrt{1-\alpha} E_{in} = \sqrt{\frac{P_{in}}{2}} e^{j\phi m(t)}$, where $\alpha = ½$ is the coupling factor.

$$E_2 = j\sqrt{\alpha} E_{in} = j\sqrt{\frac{P_{in}}{2}} e^{j\phi m(t)}$$

$$E_{o1} = E_1(t-\tau) = \sqrt{\frac{P_{in}}{2}} e^{j\phi m(t-\tau)}$$

$$E_{o2} = j\sqrt{\alpha} E_{in} = j\sqrt{\frac{P_{in}}{2}} e^{j\phi m(t)}$$

$$E_{out} = \sqrt{1-\alpha} E_{o1} + j\sqrt{\alpha} E_{o2} = \frac{\sqrt{P_{in}}}{2}\left[e^{j\phi m(t-\tau)} - e^{j\phi m(t)}\right] \quad \textbf{(2-7)}$$

The output power can be found from equation (2-7) to be $P_{out} = |E_{out}|^2$.

A sample of the output power and chirp is shown in Figure 2-12 where the peak power is set to 1 mW. It is clear that the output signal has an alternate chirp. The presence of this alternate chirp in the signal has a good effect to tolerate nonlinearity effects by reducing the intrachannel four-wave mixing effect [26] and this will prove that

the alternate chirp RZ transmitter is better than the chirp-free RZ and the NRZ transmitters for 10 Gb/s transmission system.

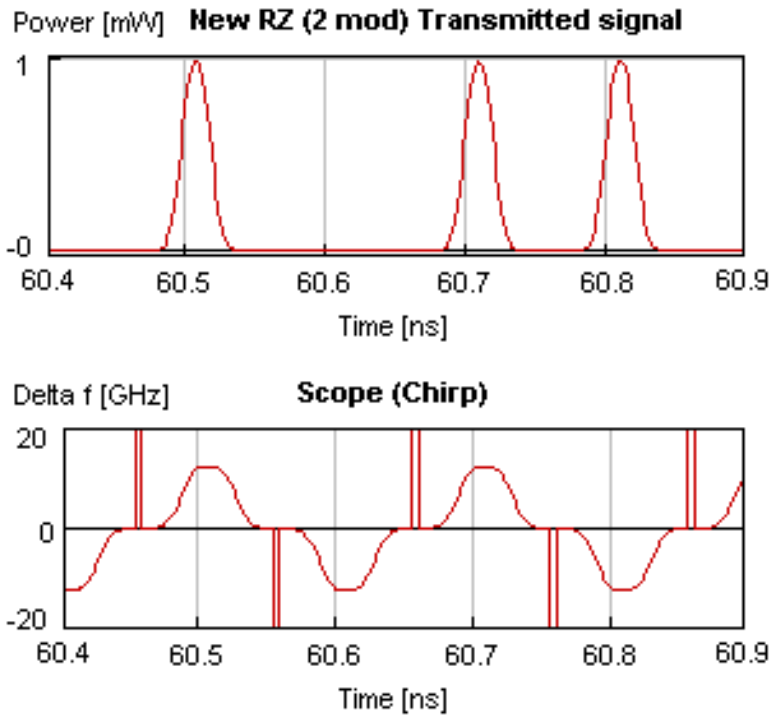

Figure 2-12 Sample of the output power and chirp of the alternate chirp RZ with two modulators transmitter

2.4.2 Alternate Chirp RZ Transmitter with One Modulator

The alternate chirp RZ transmitter with one modulator is similar to the transmitter described in section 2.4.1. The only difference is that instead of using two modulators, one for RZ pulse generation and the second for data modulation, one modulator will be used for both RZ pulse generation and data modulation [22]-[23].

The alternate chirp RZ transmitter with one modulator consists of a CW laser source which is passed through a phase modulator that is driven by a differentially

encoded NRZ data signal as shown in Figure 2-13. A differential encoder can be built using a one bit delay feedback and an exclusive OR (XOR) gate [23]. A sample of the output power and chirp is shown in Figure 2-14 where the peak power is set to 1 mW.

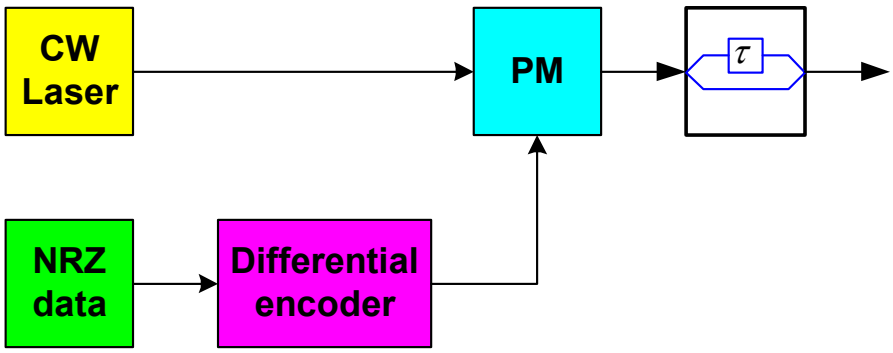

Figure 2-13 Alternate chirp RZ transmitter with one modulator block diagram

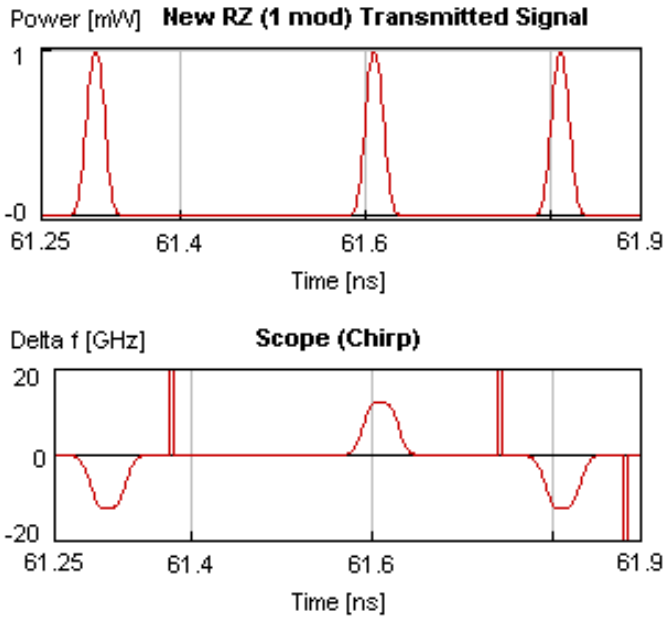

Figure 2-14 Sample of the output power and chirp of the alternate chirp RZ with one modulator transmitter

Both alternate chirp RZ transmitters give the same output. Therefore, in our work we will consider only the alternate chirp RZ transmitter with two modulators which is commercially available [23] and is less expensive than the alternate chirp RZ transmitter with one modulator.

2.5 Performance Evaluation of Alternate Chirp RZ for Different Values of Time Delay and Residual Phase Shift

We use computer simulation to generate output power and chirp for different values of delay time (τ) and residual phase different between the interferometer arms (φ) which is also related to the laser drift. A laser drift of 4 GHz (from 193.1 THz) corresponds to almost 25^{o} if $\tau = 20$ ps [22].

The simulated block diagram of an alternate chirp RZ transmitter including a residual phase shift is shown in Figure 2-15. The simulation has been carried out for τ = 10 ps, τ = 20 ps, and τ = 40 ps for $\varphi = 0^{o}$ and $\varphi = 25^{o}$ for each τ. The output power and chirp at points (A) and (B) are shown in Figure 2-16.

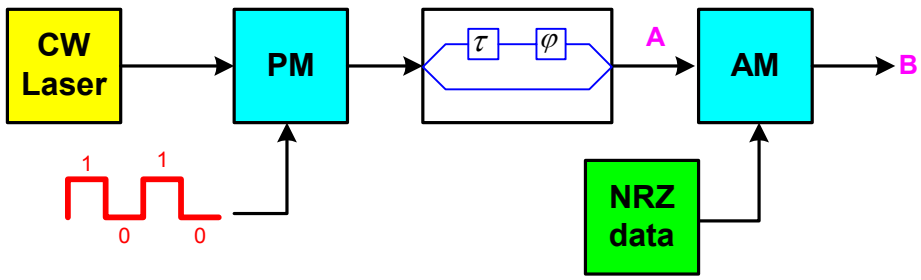

Figure 2-15 Alternate chirp RZ transmitter with interferometer and residual phase shift

Output power & chirp of point (A)

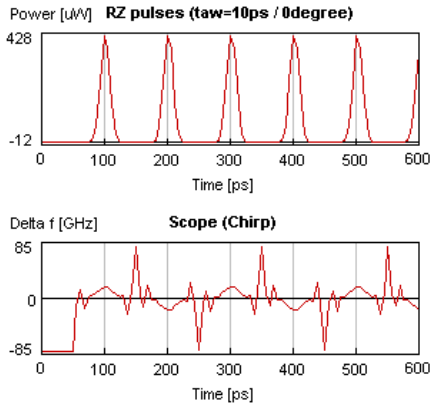

Output power & chirp of point (B)

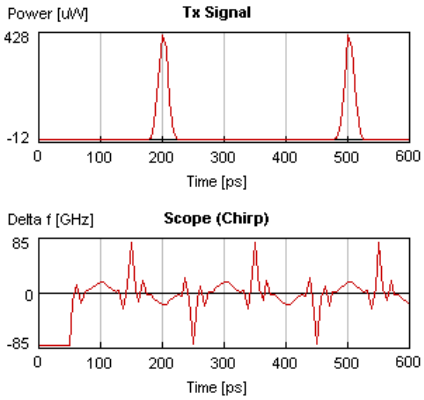

τ = 10 ps and φ = 0°

Output power & chirp of point (A)

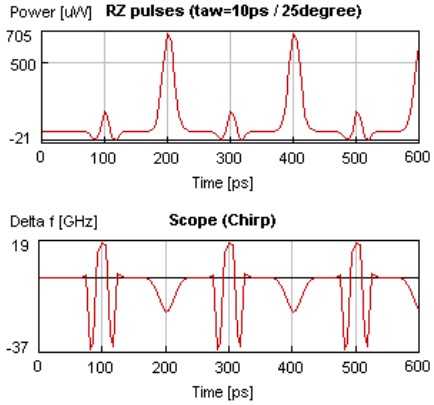

Output power & chirp of point (B)

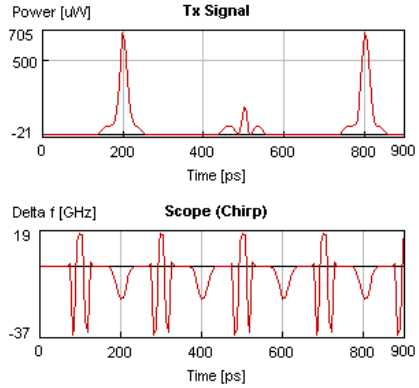

τ = 10 ps and φ = 25°

Output power & chirp of point (A)

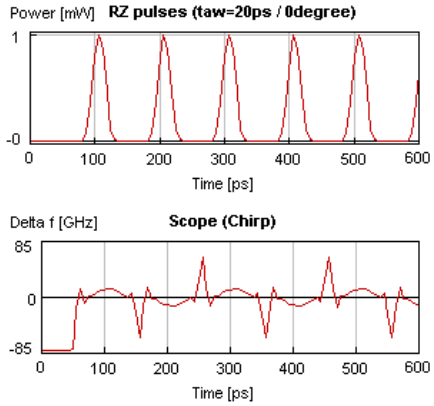

Output power & chirp of point (B)

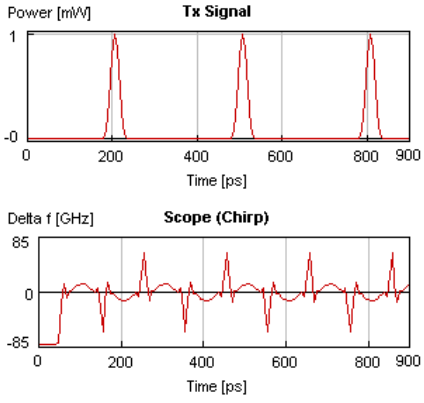

τ = 20 ps and φ = 0°

Output power & chirp of point (A)

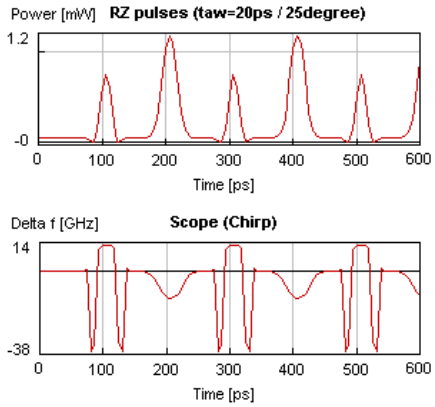

Output power & chirp of point (B)

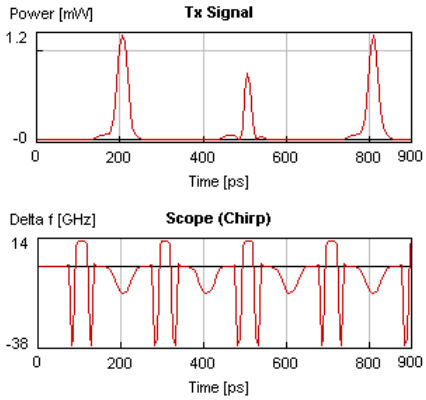

τ = 20 ps and $\varphi = 25^{o}$

Output power & chirp of point (A)

Output power & chirp of point (B)

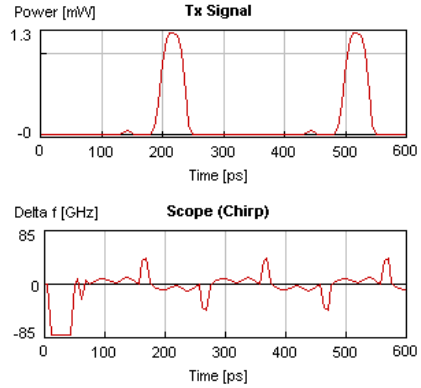

τ = 40 ps and $\varphi = 0^{o}$

Output power & chirp of point (A)

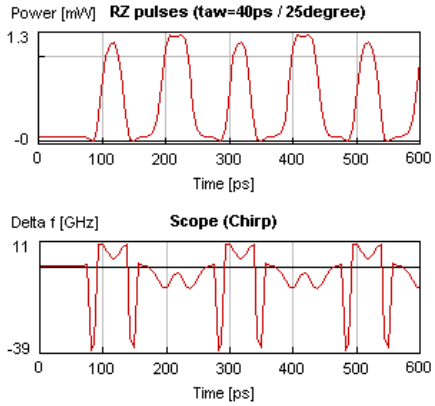

Output power & chirp of point (B)

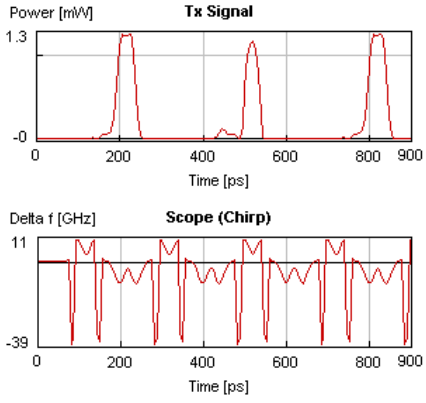

τ = 40 ps and $\varphi = 25^{o}$

Figure 2-16 The output power and chirp of the alternate chirp RZ transmitter with interferometer and phase shift for different τ's and φ's values

It is clear that the pulse amplitude will not be uniform as a result of a residual phase shift. Also the pulse width increases with τ. In this thesis we use 20 ps delay interferometer because of its commercial availability since it is the first stage of 25 GHz to 50 GHz optical interleaver [22]. Products with τ = 10 ps or τ = 40 ps may also be available in future optical components [22].

CHAPTER 3
SYSTEM MODEL

In this thesis, we consider the DWDM system shown in Figure 3-1 in our analysis. It consists of *n* number of transmitters, DWDM multiplexers and demultiplexers, fiber optic links, optical switches, and *n* number of receivers. It is sufficient to model only the propagation of three immediate neighbour channels to the channel of interest [27]. Therefore the number of transmitters and receivers (*n*) in our case has been chosen to equal 7 where the channel no. 4 is the channel of interest. The transmitters could be NRZ, chirp-free RZ-50% duty cycle, chirp-free RZ-33% duty cycle, or alternate chirp RZ with two modulators. The details of these transmitters have already been provided in CHAPTER 2. In this chapter we will focus on modelling the fiber optic link that led to the Nonlinear Schrödinger equation and its numerical solution, describing different nonlinearity effects, design of the fiber optic link, and the use of MEMS in fabricating optical switches.

3.1 Nonlinear Schrödinger (NLS) Equation

The propagation of light pulses in an optical fiber link can be represented as shown in Figure 3-2.

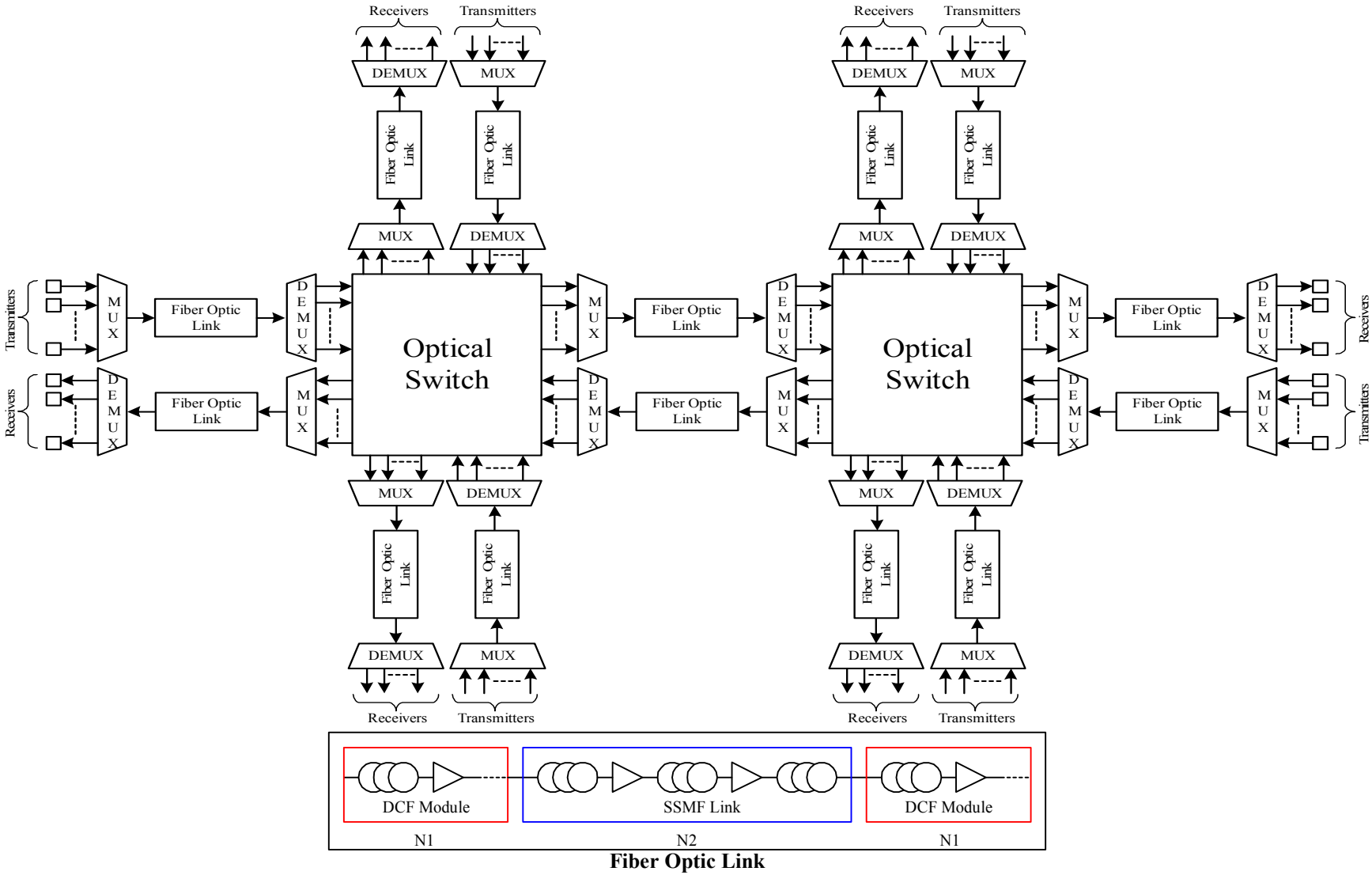

Figure 3-1 System block diagram

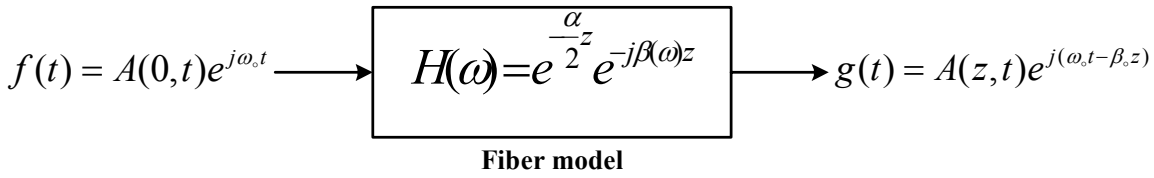

Figure 3-2 Model of fiber optic link

$A(0,t)$ is the input signal to the fiber link at distance $z = 0$, and $\omega_\circ$ is the center frequency which equal to 193.12 THz. For a DWDM of seven channels, $A(0,t) = \sum_{n=-3}^{3} d_n(t)e^{j(2\pi n\Delta f)t}$, where $d_n(t)$ is the input data and $\Delta f = 50\,\text{GHz}$ is the channel spacing.

$$f(t) = A(0,t)e^{j\omega_\circ t} \quad \leftrightarrow \quad F(\omega) = A(0, \omega - \omega_\circ)$$

$$g(t) = A(z,t)e^{j(\omega_\circ t - \beta_\circ z)} \quad \leftrightarrow \quad G(\omega) = A(z, \omega - \omega_\circ)e^{-j\beta_\circ z}$$

Since $G(\omega) = F(\omega) \bullet H(\omega)$, then:

$$A(z, \omega - \omega_\circ)e^{j\beta_\circ z} = A(0, \omega - \omega_\circ)e^{-\frac{\alpha}{2}z} e^{-j\beta(\omega)z}$$

$$A(z, \omega - \omega_\circ) = A(0, \omega - \omega_\circ)e^{-\frac{\alpha}{2}z} e^{-j\beta(\omega)z} e^{j\beta_\circ z} \qquad \textbf{(3-1)}$$

Take the partial derivative of equation (3-1) with respect to (z):

$$\frac{\partial A(z, \omega - \omega_\circ)}{\partial z} = \left[-\frac{\alpha}{2} - j\beta(\omega) + j\beta_\circ \right] A(z, \omega - \omega_\circ) \qquad \textbf{(3-2)}$$

where $A(z,\omega-\omega_\circ) = A(0,\omega-\omega_\circ)e^{-\frac{\alpha}{2}z}e^{-j\beta(\omega)}e^{j\beta_\circ}$.

$\beta(\omega)$ is a function of wavelength. It can be expanded using Taylor series [28]:

$$\beta(\omega) \approx \beta_\circ + \beta_1(\omega-\omega_\circ) + \frac{\beta_2}{2}(\omega-\omega_\circ)^2 + \frac{\beta_3}{6}(\omega-\omega_\circ)^3 + \gamma\left|A(z,t)\right|^2 \qquad \textbf{(3-3)}$$

where $\gamma = \frac{\omega_\circ n_2}{cA_{eff}}$ is the nonlinear parameter, n_2 is the nonlinear index coefficient and is expressed in units of m^2/W, $c = 3\times10^8$ m/s is the speed of light, and A_{eff} is the effective core area of the fiber. Substitute the value of $\beta(\omega)$ into equation (3-2):

$$\frac{\partial A(z,\omega-\omega_\circ)}{\partial z} = \left[-\frac{\alpha}{2} - j\left\{\beta_\circ + \beta_1(\omega-\omega_\circ) + \frac{\beta_2}{2}(\omega-\omega_\circ)^2 + \frac{\beta_3}{6}(\omega-\omega_\circ)^3 + \gamma\left|A(z,t)\right|^2\right\} + j\beta_\circ\right]A(z,\omega-\omega_\circ)$$

$$\frac{\partial A(z,\omega-\omega_\circ)}{\partial z} = \left[\begin{array}{l} -\frac{\alpha}{2} - j\beta_1(\omega-\omega_\circ) - j\frac{\beta_2}{2}(\omega-\omega_\circ)^2 - \\ j\frac{\beta_3}{6}(\omega-\omega_\circ)^3 - j\gamma\left|A(z,t)\right|^2 \end{array}\right]A(z,\omega-\omega_\circ) \qquad \textbf{(3-4)}$$

Equation (3-4) can be expressed in time domain where $\omega-\omega_\circ$ is replaced by the differential operator $-j\frac{\partial}{\partial t}$:

$$\frac{\partial A(z,t)}{\partial z} = \left[-\frac{\alpha}{2} - \beta_1\frac{\partial}{\partial t} + j\frac{\beta_2}{2}\frac{\partial^2}{\partial t^2} + \frac{\beta_3}{6}\frac{\partial^3}{\partial t^3} - j\gamma\left|A(z,t)\right|^2\right]A(z,t) \qquad \textbf{(3-5)}$$

For simplicity, let $A = A(z,t)$, then:

$$\frac{\partial A}{\partial z}+\frac{\alpha}{2}A+\beta_1\frac{\partial A}{\partial t}-j\frac{\beta_2}{2}\frac{\partial^2 A}{\partial t^2}-\frac{\beta_3}{6}\frac{\partial^3 A}{\partial t^3}=-j\gamma|A|^2A \qquad \textbf{(3-6)}$$

where α is the loss coefficient in the fiber, β_1 is the delay coefficient and usually it has very small value so that it can be neglected, β_2 is the dispersion coefficient, and β_3 is the dispersion slope coefficient. If both sides of equation (3-6) are multiplied by (j), then:

$$j\frac{\partial A}{\partial z}+j\frac{\alpha}{2}A+\frac{\beta_2}{2}\frac{\partial^2 A}{\partial t^2}-j\frac{\beta_3}{6}\frac{\partial^3 A}{\partial t^3}-\gamma|A|^2A=0 \qquad \textbf{(3-7)}$$

Equation (3-7) is valid for most of DWDM systems and is known as the Nonlinear Schrödinger (NLS) equation [28].

It can be seen that equation (3-7) is a nonlinear partial differential equation which is difficult to be solved analytically. A numerical solution is highly required to understand the nonlinear effects in fiber optics and to enable the simulation of fiber optic links. One of the famous numerical techniques that is extensively used to solve the NLS equation is the Split-Step Fourier Method (SSFM).

3.1.1 Split-Step Fourier Method (SSFM)

SSFM assumes that in a short propagation distance (h), dispersive and nonlinear effects can be pretended to act independently [28]. Therefore, a long length of fiber can be divided into many small pieces as shown in Figure 3-3 where only dispersion or nonlinearity can exist [25].

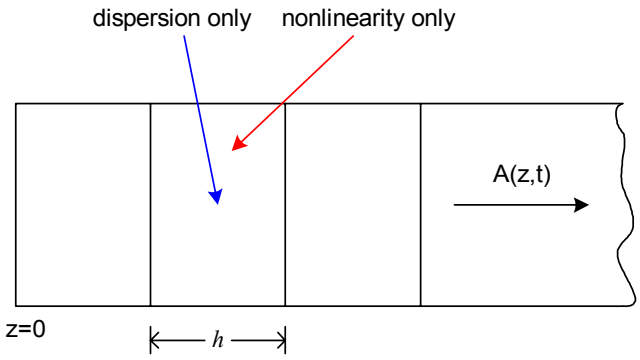

Figure 3-3 Illustration of the split-step Fourier method

Equation (3-7) can be further arranged and written as:

$$\frac{\partial A}{\partial z} = \left(\hat{D} + \hat{N}\right)A \qquad \textbf{(3-8)}$$

where: $\hat{D} = j\frac{\beta_2}{2}\frac{\partial^2}{\partial t^2} + \frac{\beta_3}{6}\frac{\partial^3}{\partial t^3} - \frac{\alpha}{2}$ represents the dispersion, dispersion slope and loss in fiber in a linear medium, and $\hat{N} = -j\gamma|A|^2$ is a nonlinear operator that governs the effect of fiber nonlinearities on pulse propagation [28].

If we assumed that the term $(\hat{D} + \hat{N})$ in equation (3-8) is constant and equal to K, then the solution for equation (3-9) can be found as mentioned below:

$$\frac{\partial A}{\partial z} = KA \quad \rightarrow \quad \frac{\partial A}{\partial z} - KA = 0$$

$$A(z) = Ce^{Kz}$$

$$A(z) = Ce^{(\hat{D}+\hat{N})z} \tag{3-9}$$

where C is a constant and it can be found from the initial condition A(0).

We can expect that the solution of equation (3-7) should be of an exponential form as the one shown in equation (3-9). Let us go back to equation (3-8) and transfer it to the frequency domain by replacing each partial derivative with $j\omega$, and we'll ignore the delay:

$$\frac{\partial A(z,t)}{\partial z} = \left[-\frac{\alpha}{2} + j\frac{\beta_2}{2}\frac{\partial^2}{\partial t^2} + \frac{\beta_3}{6}\frac{\partial^3}{\partial t^3} - j\gamma\left|A(z,t)\right|^2 \right] A(z,t)$$

$$\frac{\partial A(z,\omega)}{\partial z} = \left[-\frac{\alpha}{2} - j\frac{\beta_2}{2}\omega^2 - j\frac{\beta_3}{6}\omega^3 - j\gamma\left|A(z,t)\right|^2 \right] A(z,\omega) \tag{3-10}$$

Equation (3-10) can be solved easily for a small length of fiber (h):

$$A(z+h,\omega) \approx \exp\left(\left[-\frac{\alpha}{2} - j\frac{\beta_2}{2}\omega^2 - j\frac{\beta_3}{6}\omega^3 - j\gamma\left|A(z,t)\right|^2 \right] h \right) A(z,\omega)$$

$$A(z+h,\omega) \approx \exp\left(\left[-\frac{\alpha}{2} - j\frac{\beta_2}{2}\omega^2 - j\frac{\beta_3}{6}\omega^3 \right] h \right) \exp\left(\left[- j\gamma\left|A(z,t)\right|^2 \right] h \right) A(z,\omega) \tag{3-11}$$

Equation (3-11) can be transferred back to the time domain:

$$A(z+h,t) \approx \exp\left(\hat{D}h\right)\exp\left(\hat{N}h\right)A(z,t) \tag{3-12}$$

Equation (3-12) is the approximate numerical solution of the NLS equation.

The exponential operator $\exp\left(\hat{D}h\right)$ is evaluated in the frequency domain using Fast Fourier Transform (FFT). The use of the FFT algorithm makes numerical evaluation of equation (3-12) relatively fast and this is why SSFM is extensively used in solving the NLS equation [28].

The evaluation of the NLS equation can be improved by adopting the symmetrized split-step Fourier method to propagate the optical pulse over a distance of (h). This method depends on evaluating the dispersive operator ($\hat{D}$) over half of the distance ($h/2$), then evaluate the nonlinear operator ($\hat{N}$) over the whole distance (h), and finally evaluate the dispersive operator over the remaining half of the distance as shown in Figure 3-4 [28].

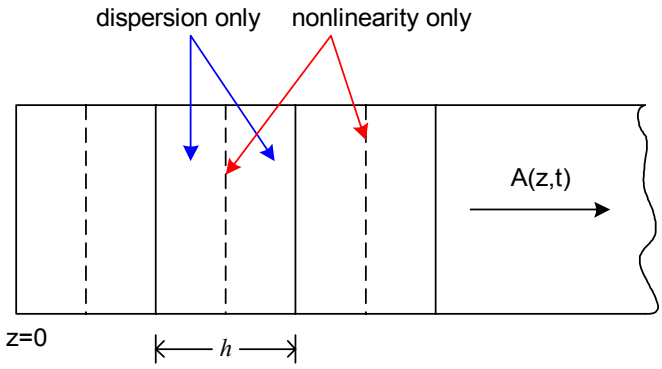

Figure 3-4 Illustration of the symmetrized split-step Fourier method

The approximate solution of equation (3-8) using the symmetrized split-step Fourier method will be:

$$A(z+h,t) \approx \exp\left(\frac{h}{2}\hat{D}\right)\exp\left(h\hat{N}\right)\exp\left(\frac{h}{2}\hat{D}\right)A(z,t) \quad \textbf{(3-13)}$$

By now we have described the problems associated with transmitting optical pulses over long-haul terrestrial optical links. Therefore the design of the fiber optic transmission link should overcome these problems by proper solving of the NLS equation.

3.2 Fiber Nonlinearity Effects

Nonlinearity effects arose as optical fiber data rates, transmission lengths, number of wavelengths, and optical power levels increased. It actually represents the fundamental limiting mechanisms to the amount of data that can be transmitted on a fiber optic link. It has been experimentally proven that RZ signals can resist the fiber nonlinearity effect more than the NRZ ones [4] & [29]. Nonlinearity has different effects on fiber such as four-wave mixing, self-phase modulation, and cross-phase modulation.

3.2.1 Four-Wave Mixing (FWM)

FWM is usually exhibited in systems that carry a number of simultaneous wavelengths such as DWDM. It is classified as a third-order distortion phenomenon. Third-order distortion mechanism generates third-order harmonics in systems with one channel. For example, if three optical signals with carrier frequencies ω_1, ω_2, and ω_3 co-propagate inside the fiber simultaneously, the third-order distortion mechanism generates

a fourth signal whose wavelength is ω_4 which is related to other wavelengths by the relation $\omega_4 = \omega_1 \pm \omega_2 \pm \omega_3$ [7].

The values of ω_4 cause the most problems since they often fall near or on top of the desired signals. If they fall on top of the desired signal, then they will be mixed with it and they cannot be removed by any means. The number of interfering products increases as $\frac{1}{2}\left(N^3 - N^2\right)$ where N is the number of channels [30].

Intrachannel four-wave mixing (IFWM) is similar to the FWM, however, the distortion of the signal will be caused by the nonlinearity effect within the channel itself.

3.2.2 Self-Phase Modulation (SPM)

SPM occurs due to the power dependency of the refractive index of the fiber core. As an optical pulse travels down the fiber, the leading edge of the pulse causes the refractive index of the fiber to rise, resulting in a blue shift (increase in frequency). The falling edge of the pulse decreases the refractive index of the fiber causing a red shift (decrease in frequency). These red and blue shifts introduce a frequency chirp on each edge which interacts with the fiber dispersion to broaden the pulse [30].

3.2.3 Cross-Phase Modulation (XPM)

XPM involves two pulses of light instead of one pulse as in case of SPM. Two pulses travel down the fiber, each changing the refractive index as the optical power varies. If these two pulses happen to overlap, they will introduce distortion into the other pulses through XPM. Unlike SPM, fiber dispersion has little impact on XPM [30].

3.3 Upgrading of Existing 2.5 Gb/s Fiber Links to 10 Gb/s

An example of existing 2.5 Gb/s NRZ systems is shown in Figure 3-5. The maximum fiber length due to chromatic dispersion is equal to 640 km [31]. After this distance, the signal has to be regenerated by an optical/electrical/optical (OEO) regenerator.

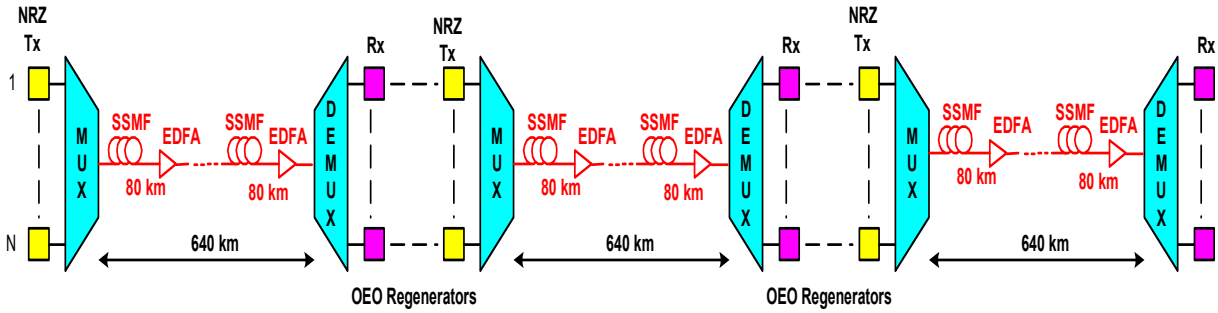

Figure 3-5 Present 2.5 Gb/s NRZ systems

The chromatic dispersion penalty depends on B^2L [31], where B is the bit rate and L is the fiber length. If this relation is being applied to 10 Gb/s bit rate systems, then the maximum fiber length that the signal can cross is only 40 km due to the chromatic

dispersion problem. Therefore, it is very essential to add DCF modules for all 10 Gb/s systems.

Upgrading the present 2.5 Gb/s NRZ systems to 10 Gb/s systems requires replacing of all 2.5 Gb/s NRZ transmitters in all sites (including the OEO regenerator sites) with 10 Gb/s NRZ transmitters. In addition to that, DCF modules with their EDFA optical amplifiers have to be inserted after each SSMF. Such system is shown in Figure 3-6. It's obvious that this is a costly solution.

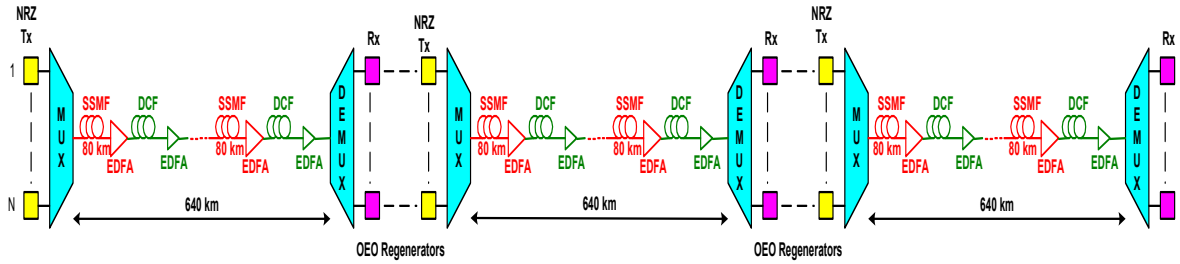

Figure 3-6 Upgrading of 2.5 Gb/s NRZ systems to 10 Gb/s NRZ systems

One solution to overcome the high cost of upgrading 2.5 Gb/s NRZ systems to 10 Gb/s systems is to replace the 2.5 Gb/s NRZ transmitters at the transmitter sites with 10 Gb/s RZ transmitters as shown in Figure 3-7. In this case, there is no need any more for an OEO regeneration of the signal every 640 km. However, the dispersion problem has to be solved by adding the DCF modules with their EDFA optical amplifiers after each SSMF (periodic compensation). This solution has defiantly reduces the cost if compared with the previous one.

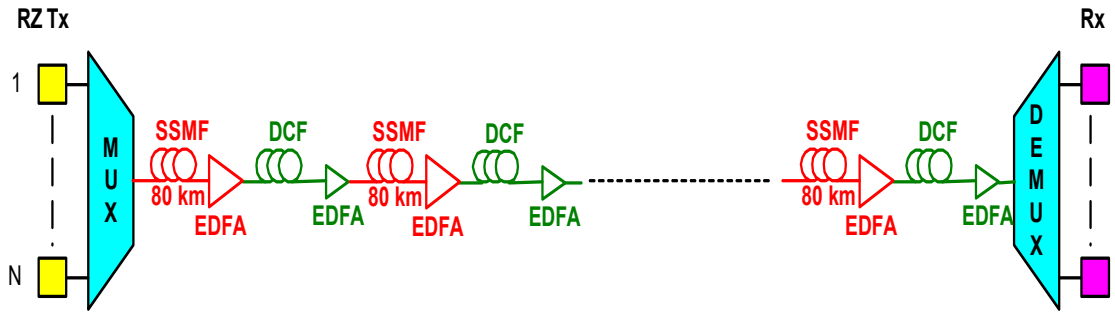

Figure 3-7 10 Gb/s RZ systems with periodic compensation

The second solution is shown in Figure 3-8. The 2.5 Gb/s NRZ transmitters are replaced with 10 Gb/s RZ transmitters. The dispersion in this case is compensated only at the transmitter and the receiver sites and therefore there is no need to visit each SSMF site. This is the first cost effective solution that we are proposing in this thesis.

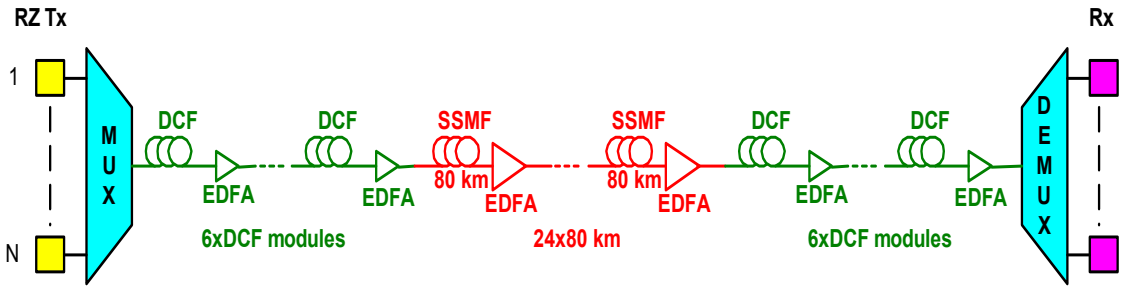

Figure 3-8 10 Gb/s RZ systems with end-to-end compensation

The second cost effective solution (shown in Figure 3-9) that we are proposing in this thesis is to compensate the dispersion at the transmitter, receiver, optical add/drop multiplexers, and optical switches sites which are normally located at 640 km (super span).

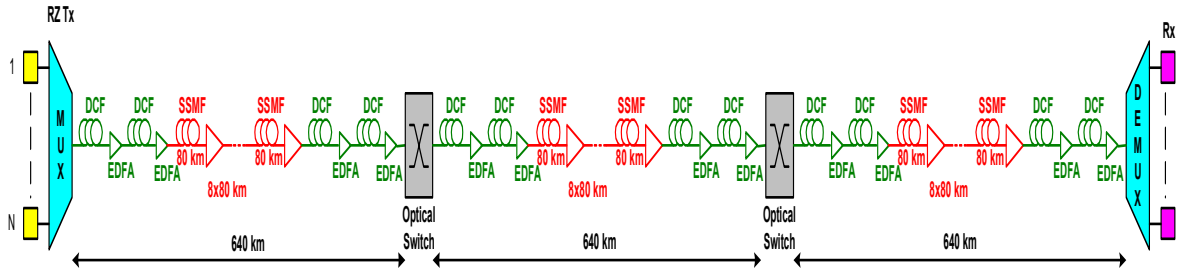

Figure 3-9 10 Gb/s RZ systems with compensation at optical switches sites

CHAPTER 4

PERFORMANCE EVALUATION OF 10 Gb/s LONG-HAUL DWDM SYSTEMS FOR DIFFERENT RZ SOURCES USING COMPUTER SIMULATION

Many next generation optical transmission systems at 10 Gb/s will be utilizing RZ line coding to mitigate fiber dispersion and nonlinear effects for extending the reach of fiber links to a few thousand kilometers without electronic regeneration [32]. Transmission systems utilizing chirp-free RZ transmitters typically require two modulators for pulse generation and data encoding as described in CHAPTER 2. RZ coding with 50% duty cycle requires two modulators for a chirp-free output. A chirp-free RZ coding with 33% duty cycle requires also two modulators but the electric drive signal used is 6 dB higher than the drive signal used for the 50% duty cycle case. A new scheme for generating RZ signal using NRZ driven phase modulator followed by an optical filter interferometer has been described in CHAPTER 2. This scheme is capable of using one modulator only if differential encoder is employed [22] & [23].

In this chapter, we will use computer simulation using VPItransmissionMaker^{TM}WDM simulation tool to demonstrate the advantages of alternate chirp RZ transmitter with two modulators relative to 33% and 50% duty cycle chirp-free RZ, and NRZ transmitters if end-to-end dispersion compensation at transmitter and receiver sites is used instead of periodic compensation [29]. We aim to provide telecom carriers with a low cost solution for upgrading existing 2.5 Gb/s fiber links to 10

Gb/s without re-inserting dispersion compensating fiber (DCF) modules at all EDFA sites in the link, but using only DCF modules at the transmitter and receiver sites.

4.1 System Description

A DWDM system of 7 channels modulated at 10 Gb/s is simulated, with channel spacing of 50 GHz. The optical filters in the MUX/DEMUX are 3rd order Bessel with 3-dB bandwidth 25 GHz [33]. The electrical received signal is obtained by a fast PIN photodiode followed by an electrical Bessel filter of the 3rd order, 3-dB bandwidth 7 GHz. 2048 PRBS[6] (pseudorandom binary sequence) bits with sampling rate of 64 samples per bit is being used as data source.

The transmission line consists of N_1×(32 km DCF + 16 dB EDFA) + N_2×(80 km SSMF + 20 dB EDFA) + N_1×(32 km DCF + 16 dB EDFA), where N_1 is the number of DCF circulations and N_2 is the number of SSMF circulations. The SSMF has loss of 0.25 dB/km, dispersion of 16 ps/nm/km, core area of 80 μm^2, and the DCF has loss of 0.5 dB/km, dispersion of –80 ps/nm/km, core area of 25 μm^2. All EDFAs have the same noise figure of 7 dB and all fibers have the same nonlinear index of 2.6×10^{-20} m^2/W. The ASE noise generated by all EDFAs is included in the simulation. The simulated system was shown in Figure 3-8.

[6] Pseudorandom means that the generated combination or sequence of ones and zeros will eventually repeat but randomly [17].

Two sets of tests are simulated. In the first one, the fiber length is 960 km, this means that $N_1 = 3$ and $N_2 = 12$. The fiber length is 1920 km in the second test and therefore $N_1 = 6$ and $N_2 = 24$. The Q-factor value is normalized at 8 when fiber nonlinearity is zero and EDFAs noise is included at fiber length of 1920 km. The peak output power at the fiber input is set to 13 mW, 4.7 mW, 3.6 mW, and 1.9 mW for the alternate chirp RZ with two modulators, chirp-free RZ-33% duty cycle, chirp-free RZ-50% duty cycle, and NRZ transmitters respectively. The optical fields of all channels are co-polarized, which represents the worst case of inter-channel interference. Because of the rapid broadening of pulses in the quasi-linear transmission, the intra-channel four-wave mixing (IFWM) due to the overlap of pulses within one channel becomes the major manifestation of fiber nonlinearity [34].

4.2 Results

4.2.1 First Test Results

The simulation results for the received central channel signals after 960 km transmission are shown in Figure 4-1. The fiber nonlinearity degrades the eyes dramatically in the case of NRZ transmitter, and the RZ transmitters (alternate chirp RZ, chirp-free RZ-33%, and chirp-free RZ-50%) show more tolerance to the nonlinearity. It is shown that the intrachannel nonlinear impairments have been reduced [35] for the case of the RZ transmitters.

4.2.2 Second Test Results

The simulation results for the received central channel signals after 1920 km transmission are shown in Figure 4-2. Note that the nonlinear penalty grows as the transmission distance increases. The fiber nonlinearity completely closes the eye of the received NRZ signal as shown in Figure 4-2 (d), and it almost closes the eyes of the chirp-free RZ with 33% duty cycle and 50% duty cycle signals as shown in Figure 4-2 (b) and (c). By contrast, the eye remains well open when the alternate chirp RZ transmitter is used as shown in Figure 4-2 (a).

4.2.3 Q-factor, BER & BER ISI Results

The BER, BER ISI, and Q-factor results are shown in APEENDIX B and they are summarized in Table 4-1. BER results indicate that after 1920 kilometers the NRZ received signal is completely distorted. On other hand, the chirp-free RZ with 33% duty cycle, chirp-free RZ with 50% duty cycle, and alternate chirp RZ signals can go for longer distance. However, alternate chirp RZ signal has better chance to reach longer distance than the chirp-free RZ with 33% duty cycle and chirp-free RZ with 50% duty cycle signals.

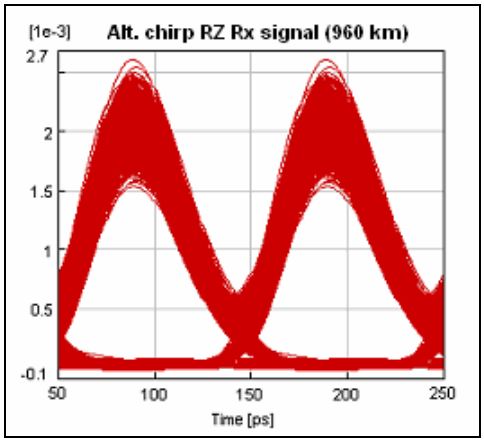

(a)

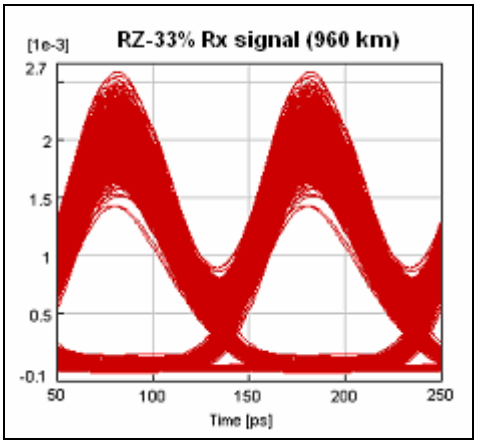

(b)

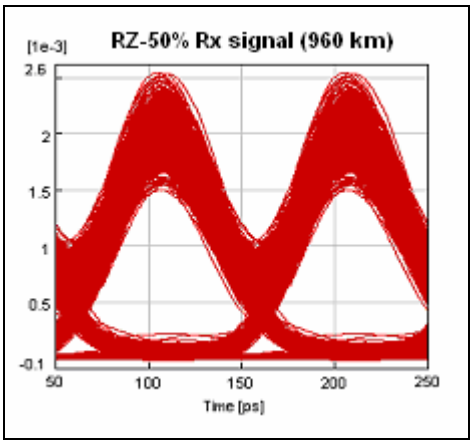

(c)

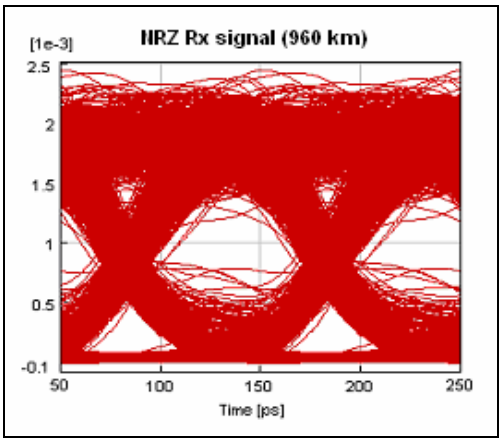

(d)

Figure 4-1 Received signals eye diagrams for the (a) alternate chirp RZ, (b) chirp-free RZ-33%, (c) chirp-free RZ-50%, and (d) NRZ transmitters after 960 km

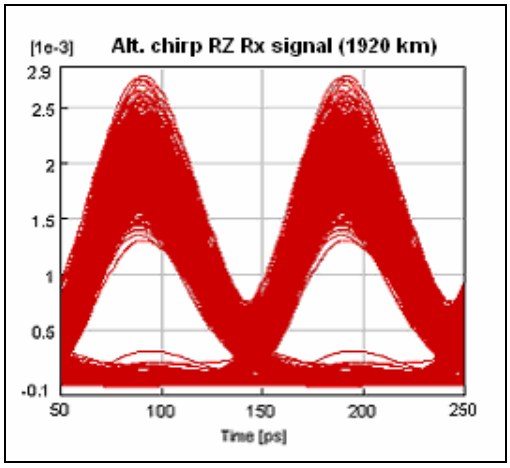

(a)

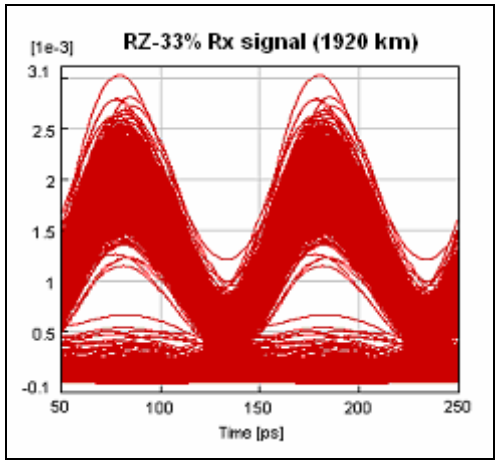

(b)

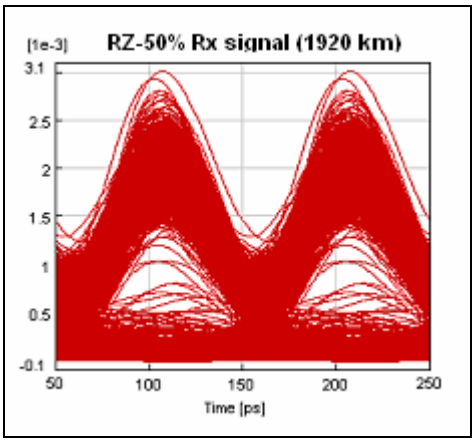

(c)

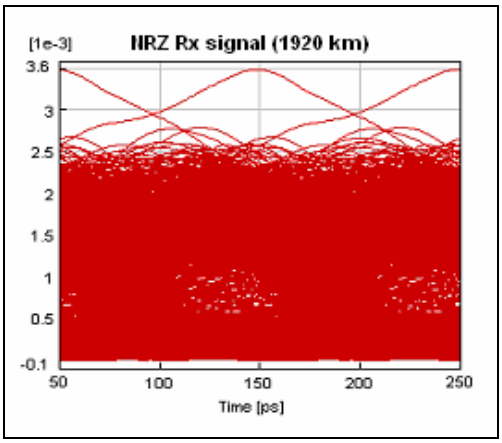

(d)

Figure 4-2 Received signals eye diagrams for the (1) alternate chirp RZ, (b) chirp-free RZ-33%, (c) chirp-free RZ-50%, and (d) NRZ transmitters after 1920 km

Table 4-1 The Q, BER, and BER ISI values of the received central channel signals for the alternate chirp RZ, chirp-free RZ-33%, chirp-free RZ-50%, and NRZ transmitters using end-to-end compensation

Transmitter type	Distance (km)	Q	BER	BER ISI
Alternate chirp RZ	960	10.5	1.0×10^{-25}	1.0×10^{-20}
	1920	7.3	1.0×10^{-12}	1.0×10^{-11}
RZ-33%	960	10.4	1.0×10^{-24}	1.0×10^{-20}
	1920	5.9	5.0×10^{-9}	5.0×10^{-7}
RZ-50%	960	10.2	1.0×10^{-23}	1.0×10^{-19}
	1920	5.4	1.0×10^{-7}	7.5×10^{-6}
NRZ	960	6.2	1.0×10^{-9}	5.0×10^{-7}
	1920	2.26	1.0×10^{-2}	4.0×10^{-2}

CHAPTER 5

PERFORMANCE EVALUATION OF 10 Gb/s LONG-HAUL DWDM SYSTEMS WITH DIFFERENT SUPER SPANS USING COMPUTER SIMULATION

Computer simulation is used again to demonstrate the advantages of alternate chirp RZ transmitter to the chirp-free RZ with 33% and 50% duty cycle and NRZ transmitters with four super spans (2560 km). This provides telecommunication carriers also with a low cost solution for upgrading existing 2.5 Gb/s fiber links to 10 Gb/s without re-inserting dispersion compensating fiber (DCF) modules at all EDFA sites in the link but using only DCF modules at receiver, transmitter, OADM, or optical switches sites.

5.1 System Description

A DWDM system of 7 channels modulated at 10 Gb/s is simulated, with channel spacing of 50 GHz. The optical filters in the MUX/DEMUX are 3rd order Bessel with 3-dB bandwidth 25 GHz [33]. The electrical received signal is obtained by a fast PIN photodiode followed by an electrical Bessel filter of the 3rd order, 3-dB bandwidth 7 GHz. 2048 PRBS (pseudo random binary sequence) bits with sampling rate of 64 samples per bit is being used as data source.

The transmission line consists of N×[2×(32 km DCF + 16 dB EDFA) + 8×(80 km SSMF + 20 dB EDFA) + 2×(32 km DCF + 16 dB EDFA)], where N is the number of super spans. The SMF has loss of 0.25 dB/km, dispersion of 16 ps/nm/km, core area of 80 μm^2, and the DCF has loss of 0.5 dB/km, dispersion of –80 ps/nm/km, core area of 25 μm^2. All EDFAs have the same noise figure of 7 dB and all fibers have the same nonlinear index of 2.6×10^{-20} m^2/W. The ASE noise generated by all EDFAs is included in the simulation. The simulated system was shown in Figure 3-9.

Four sets of tests will be simulated in which the number of super spans (N) will be changeable. In the first one, N will be set to one and therefore the fiber length will be 640 kilometers. Secondly, N will be set to two so that the fiber length will be 1280 kilometers. Thirdly, N will be set to three so that the fiber length will be 1920 kilometers. And finally, N will be set to four to have a fiber length of 2560 kilometers. The Q-factor value is normalized at 8 when fiber nonlinearity is zero, and EDFAs noise is included at super spans is four. The peak output power at the fiber input is set to 16 mW, 6.1 mW, 3.8 mW, and 2.6 mW for the alternate chirp RZ, chirp-free RZ-33% duty cycle, chirp-free RZ-50% duty cycle, and NRZ transmitters respectively. The optical fields of all channels are co-polarized, which represents the worst case of interchannel interference.

5.2 Results

The simulation results for the received central channel signals after one super span (640 km) are shown in Figure 5-1. It's clear that all transmitters were able to efficiently

tolerate the nonlinearity effects and transmit their signals successfully. However, RZ transmitted signals were showing more tolerance than the NRZ transmitted signal.

After two super spans (1280 km), the NRZ transmitted signal got seriously affected by the nonlinearity effects as shown in Figure 5-2 (d) and it won't be able to resist the nonlinearity effects any further. Whereas all RZ transmitted signals were still able to tolerate the nonlinearity effects as shown in Figure 5-2 (a), (b) & (c).

The results of the transmitted signals after three super spans (1920 km) are shown in Figure 5-3. The NRZ signal eye is completely closed as expected. Chirp-free RZ-33% and RZ-50% signals started to get affected by the nonlinearity. On the other hand, alternate chirp RZ signal eye is still well opened and can tolerate nonlinearity for longer spans.

After four super spans (2560 km), the alternate chirp RZ signal is still perfectly able to tolerate the nonlinearity effects as shown in Figure 5-4 (a). The chirp-free RZ-33% and RZ-50% signals eyes started to close as shown in Figure 5-4 (b) and (c), which is an indication that they won't be able to tolerate the nonlinearity effects for longer spans.

Four super spans is our aim from this test. However, it is good to check the performance of the RZ transmitters for higher number of super spans. After five super spans (3200 km), chirp-free RZ signals gave up and they won't be able to tolerate the

nonlinearity effects any more as shown in Figure 5-5 (b) and (c). However, alternate chirp RZ signal can go for one more super span as indicated by its eye diagram shown in Figure 5-5 (a).

The final test has been performed on the alternate chirp RZ transmitter only, since it is the only transmitter which shows good resistivity to nonlinearity effects till now. Alternate chirp RZ eye signal after six super spans is shown in Figure 5-6 and the eye diagram indicates that this type of signal cannot tolerate the nonlinearity effects any further. Therefore the maximum distance that alternate chirp RZ can cover without any electronic regeneration of the signal is 3840 km.

The BER, BER ISI, and Q-factor results are shown in APEENDIX C and they are summarized in Table 5-1. The BER ISI for the NRZ transmitted signal after two super spans is 2.5×10^{-3}, which is less than the maximum acceptable bit error rate (1.0×10^{-3}) if forward error correction (FEC)[7] is not being used, with FEC this figure can be minimized to be less than 1.0×10^{-15} [36]. This means that NRZ signal can go far up to 640 km only. Chirp-free RZ-50% transmitted signal is much better than the NRZ signal. It can tolerate the nonlinearity effects up to 2560 km.

[7] FEC requires that data first be encoded. For *k* information bits, the encoding process results in *n* coded bits where n>k. All *n* bits are transmitted. At the receiver, channel measurements are made and estimates of the transmitted *n* bits are generated. An FEC decoder utilizes these *n* bit estimates, along with knowledge of how all *n* bits were created, to generate estimates of the *k* information bits. The decoding process effectively detects and corrects errors in the *n*-channel bit estimates while recovering the original *k* information bits. This process is known as forward error correction because the receiver never requests retransmission of the information so the flow of data is always moving forward.

Chirp-free RZ-33% transmitted signal is not better than the chirp-free RZ-50% signal. It can go up to 2560 km with nonlinearity effects tolerated. However, alternate chirp free RZ is far better than all other transmitters. It was perfectly able to tolerate the nonlinearity effects and transmission of up to 3840 km was possible with bit error rate of 1.0×10^{-3}.

It has been observed that as the fiber length increases, the nonlinearity penalty increases too. The reason for that is as the fiber length increases, more number of optical amplifiers will be added and hence the signal power will increase which will accordingly increase the nonlinearity effects.

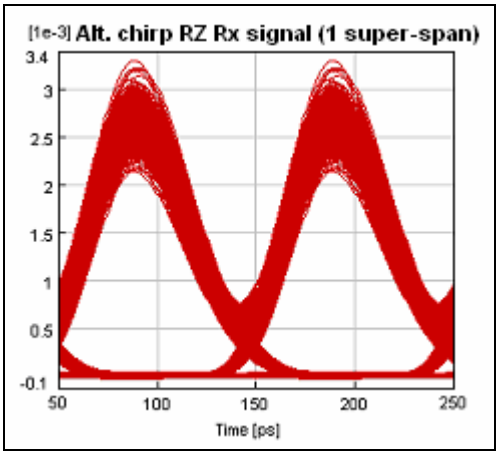

(a)

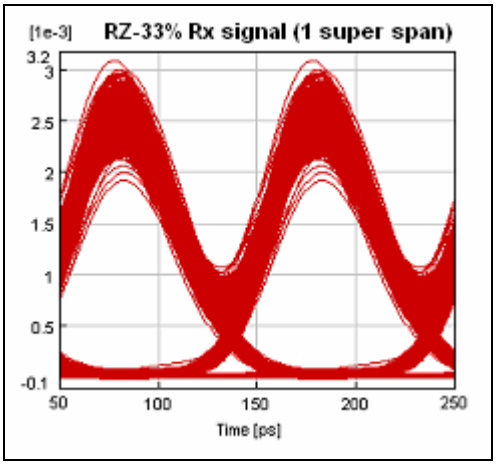

(b)

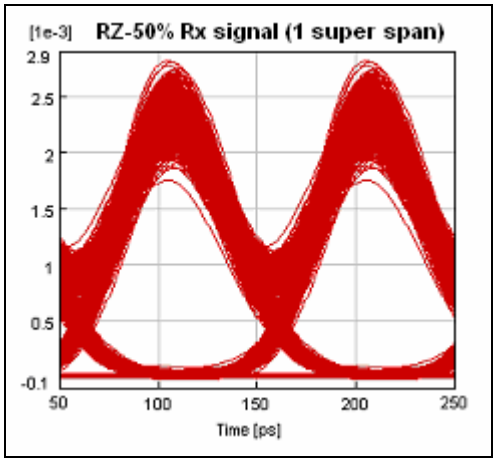

(c)

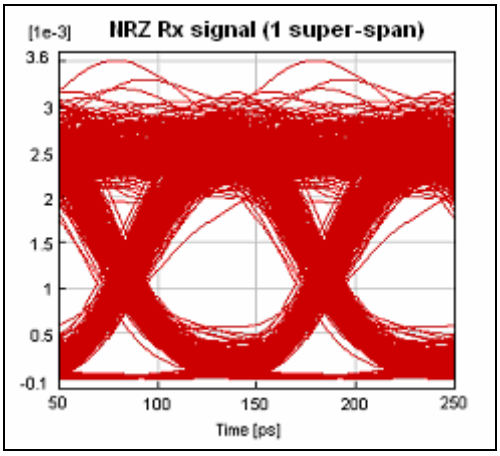

(d)

Figure 5-1 Received signals eye diagrams for the (a) alternate chirp RZ, (b) chirp-free RZ-33%, (c) chirp-free RZ-50%, and (d) NRZ transmitters after one super span

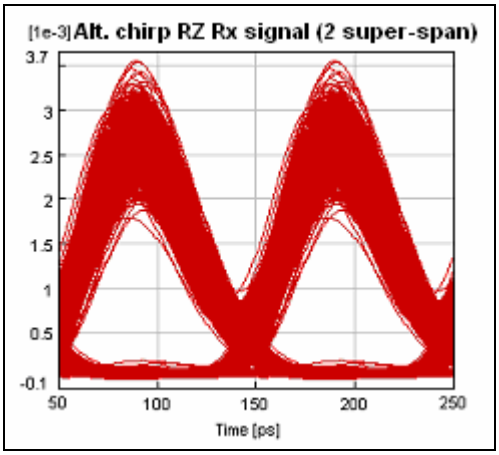

(a)

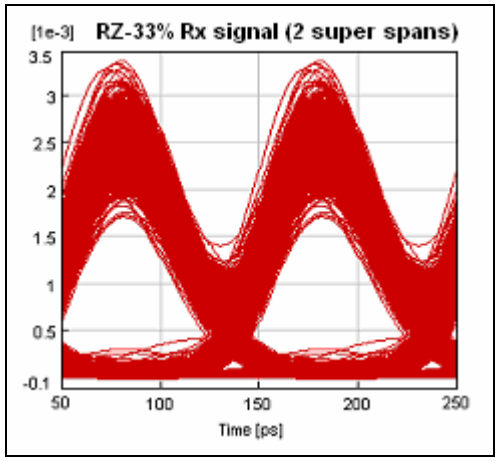

(b)

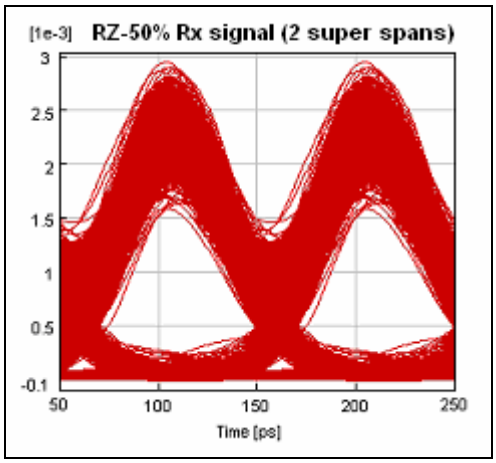

(c)

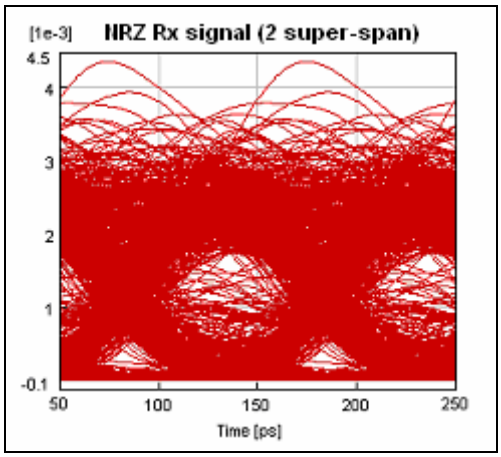

(d)

Figure 5-2 Received signals eye diagrams for the (a) alternate chirp RZ, (b) chirp-free RZ-33%, (c) chirp-free RZ-50%, and (d) NRZ transmitters after two super spans

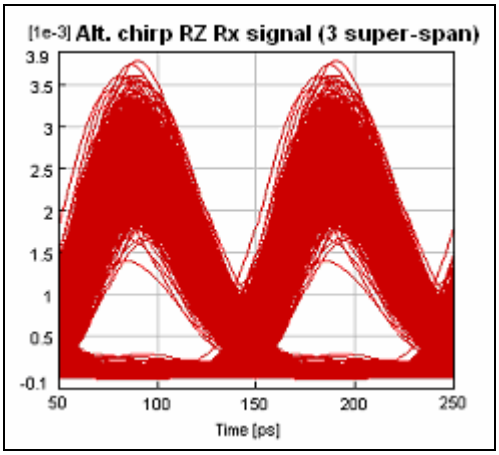

(a)

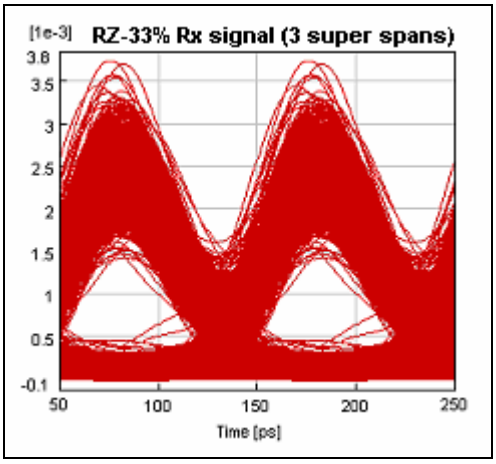

(b)

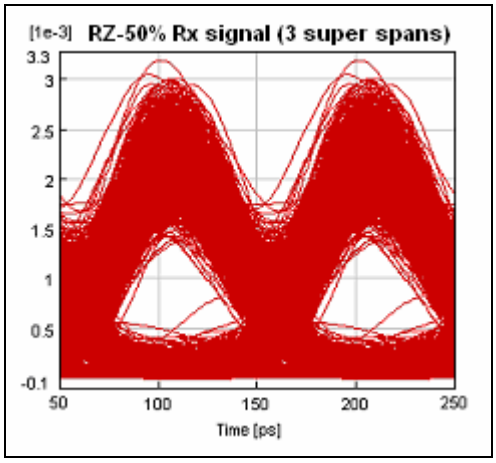

(c)

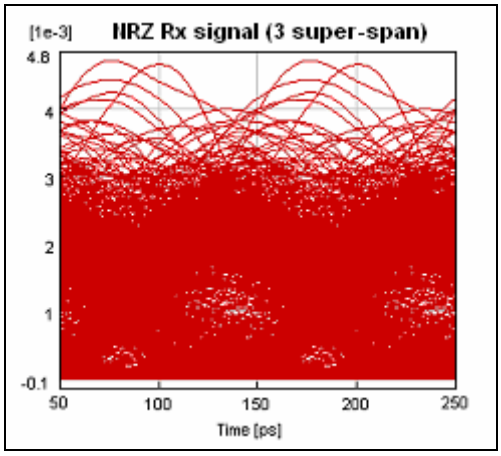

(d)

Figure 5-3 Received signals eye diagrams for the (a) alternate chirp RZ, (b) chirp-free RZ-33%, (c) chirp-free RZ-50%, and (d) NRZ transmitters after three super spans

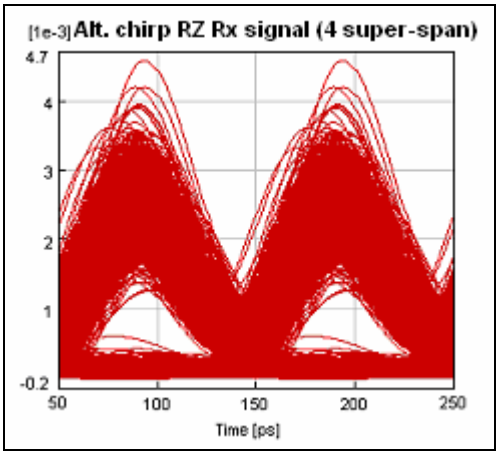

(a)

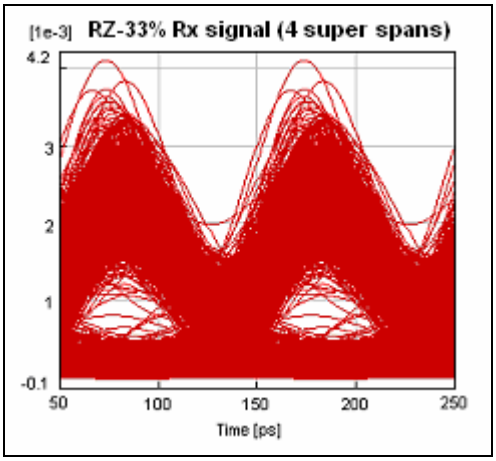

(b)

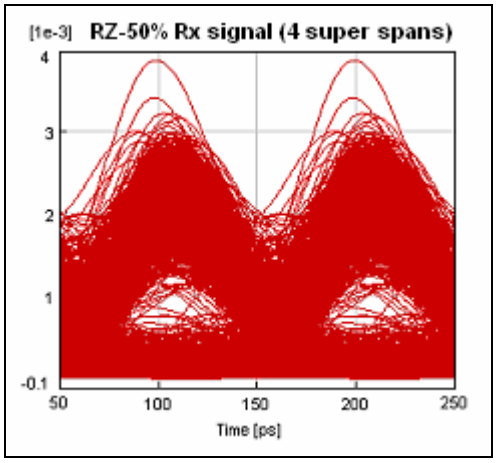

(c)

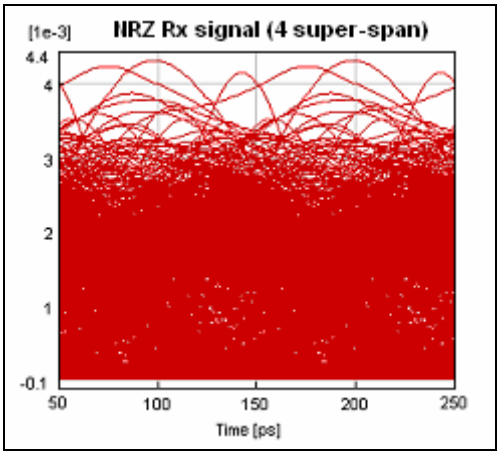

(d)

Figure 5-4 Received signals eye diagrams for the (a) alternate chirp RZ, (b) chirp-free RZ-33%, (c) chirp-free RZ-50%, and (d) NRZ transmitters after four super spans

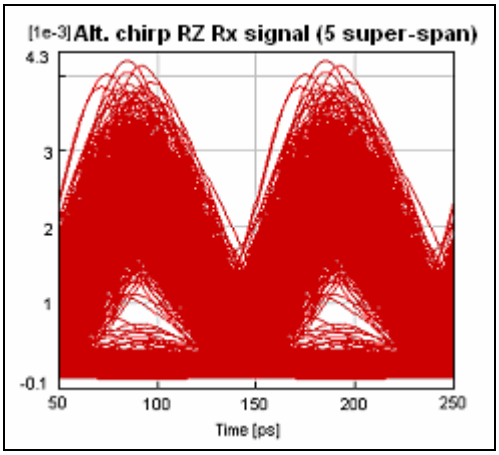

(a)

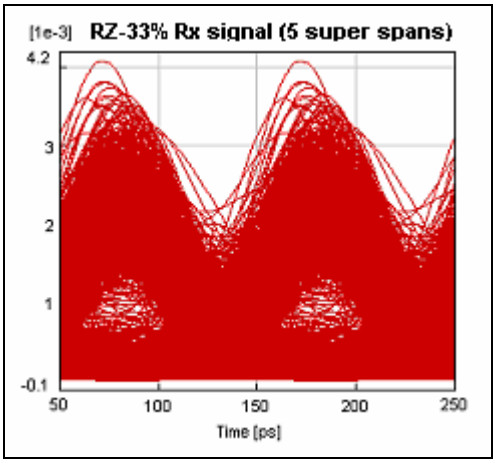

(b)

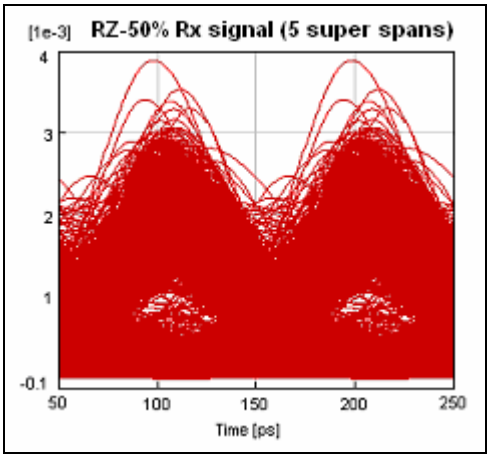

(c)

Figure 5-5 Received signals eye diagrams for the (a) alternate chirp RZ, (b) chirp-free RZ-33%, and (c) chirp-free RZ-50% transmitters after five super spans

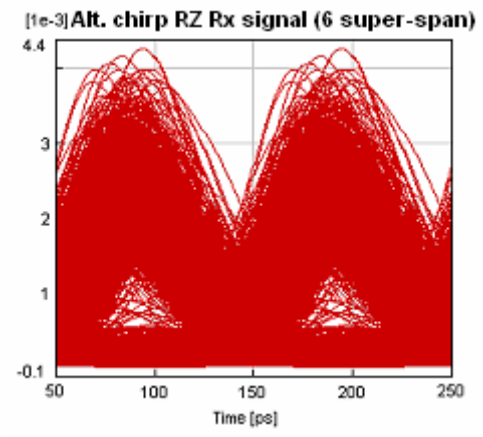

Figure 5-6 Received signal eye diagram for the alternate chirp RZ transmitter after six super spans

Table 5-1 The Q, BER, and BER ISI values of the received central channel signals for the alternate chirp RZ, chirp-free RZ-33%, chirp-free RZ-50%, and NRZ transmitters using super span

Transmitter type	No. of super-span	Q	BER	BER ISI
Alternate chirp RZ	1	13.3	1.0×10^{-39}	1.0×10^{-30}
	2	8.9	1.0×10^{-18}	1.0×10^{-15}
	3	6.5	1.0×10^{-10}	1.0×10^{-8}
	4	4.9	1.0×10^{-6}	5.0×10^{-6}
	5	4.0	5.0×10^{-5}	1.0×10^{-4}
	6	3.3	7.5×10^{-4}	1.0×10^{-3}
RZ-33%	1	14.7	1.0×10^{-47}	1.0×10^{-40}
	2	8.6	1.0×10^{-17}	1.0×10^{-13}
	3	5.8	5.0×10^{-9}	5.0×10^{-5}
	4	4.2	1.0×10^{-5}	1.0×10^{-4}
	5	3.2	7.5×10^{-4}	2.5×10^{-3}
RZ-50%	1	14.2	1.0×10^{-44}	1.0×10^{-40}
	2	8.4	1.0×10^{-16}	1.0×10^{-13}
	3	5.7	1.0×10^{-8}	1.0×10^{-6}
	4	4.1	2.5×10^{-5}	5.0×10^{-4}
	5	3.1	1.0×10^{-3}	5.0×10^{-3}
NRZ	1	8.8	1.0×10^{-18}	1.0×10^{-13}
	2	3.7	2.5×10^{-4}	2.5×10^{-3}
	3	2.03	2.0×10^{-2}	5.0×10^{-2}
	4	1.27	1.0×10^{-1}	1.0×10^{-1}

CHAPTER 6
CONCLUSION

6.1 Summary

We have demonstrated through out this thesis that by using the alternate chirp RZ transmitter and by compensating the chromatic dispersion using end-to-end compensating or every 640 km, telecommunication carriers can easily upgrade their existing 2.5 Gb/s fiber links to 10 Gb/s.

The performance of four types of optical transmitters (alternate chirp RZ, chirp-free RZ transmitter with 33% duty cycle, chirp-free RZ transmitter with 50% duty cycle, and NRZ transmitter) has been evaluated using DWDM system with 7 channels at 10 Gb/s with two types of compensating schemes.

The first compensating scheme was to insert the DCF modules at the transmitter and receiver sites and to compensate the chromatic dispersion after 960 km or 1920 km. Computer simulation results indicated that transmission up to almost 2000 km is possible with the RZ sources but not possible with NRZ source. However, the performance of the low cost alternate chirp RZ source was much better than other chirp-free RZ sources.

Similar results were achieved by using the second compensating scheme which we called it super span. In super span, the DCF modules were inserted at transmitter, receiver, OADM, or optical switches sites. Computer simulation results indicated that transmission up to almost 4000 km is possible with the low cost alternate chirp RZ source but not possible with the chirp-free RZ sources or NRZ source.

Modeling of the propagation of light in an optical fiber link using the Nonlinear Schrödinger equation was also demonstrated and a numerical solution using the Split-Step Fourier method was presented.

MEMS technology is playing a key rule in the development of optical components such as optical switches. 2D MEMS mirrors and 3D MEMS mirrors are becoming the core technologies for fabricating optical switches. An overview of MEMS in optical switches was presented in this thesis too.

6.2 Future Work

It has been shown that transmission of 10 Gb/s over almost 4000 km is possible using the alternate chirp RZ transmitter. Similar trial has to be repeated for a DWDM system with 7 channels at 40 Gb/s to evaluate the alternate chirp RZ transmitter performance. In addition to the optical transmitters used in this thesis, an RZ DPSK (RZ Differential Phase Shift Keying) optical transmitter performance has to be evaluated and compared with other optical transmitters.

REFERENCES

[1] Simon Haykin, "Communication systems", 3rd ed.. New York: John Wiley & Sons, Inc., 1994, pp.2.

[2] Martin S. Roden, "Analog and digital communication systems", 3rd ed.. New Jersey: Prentice Hall, 1991, pp.390-391.

[3] K. S. Cheng, and Jan Conradi, “Reduction of pulse-to-pulse interaction using alternative RZ formats in 40-Gb/s systems,” IEEE Photonics Technology Letters, Vol. 14, No. 1, pp. 98-100, January 2002.

[4] M. I. Hayee, and A. E. Willner, “NRZ versus RZ in 10-40 Gb/s dispersion-managed WDM transmission systems,” IEEE Photonics Technology Letters, Vol. 11, No. 8, pp. 991-993, August 1999.

[5] A. H. Gnauck, X. Liu, X. Wei, D. M. Gill, and E. C. Burrows, "Comparison of modulation formats for 42.7-Gb/s single-channel transmission through 1980 km of SSMF," IEEE Photonics Technology Letters, Vol. 16, No. 3, pp. 909-911, March 2004.

[6] "Chromatic dispersion and polarization mode dispersion," Begineers' Guides, August 01, 2001. Available: http://www.lightreading.com/

[7] Govind P. Agrawal, "Fiber-optic communication systems," 3rd ed.. New York: Wiley-Interscience, 2002.

[8] John Powers, “An introduction to fiber optic systems,” 2nd ed.. Chicago: Irwin, 1997.

[9] "Introduction to DWDM for Metropolitan Networks", Cisco Systems, Inc., Chapter 2, pp. 2-1 – 2-22. Available: http://www.cisco.com/

[10] Gerd Keiser, "Optical communications essentials." New York: McGraw-Hill, 2003.

[11] "Distributed feedback (DFB) lasers," Begineers' Guides, August 01, 2001. Available: http://www.lightreading.com/

[12] Rajiv Ramaswami and Kumar Sivarajan, "Optical networks: a practical perspective," 2nd ed.. Morgan Kaufmann, 2002.

[13] Armand Neukermans and Rajiv Ramaswami, "MEMS technology for optical networking applications," IEEE Communications Magazine, pp. 62-69, January 2001.

[14] C. J. Anderson, J. A. Lyle, “Technique for evaluating system performance using Q in numerical simulations exhibiting intersymbol interference,” Electronics Letters, Vol. 30, No. 1, pp.71–72, 1994.

[15] "Illustrated fiber optic glossary." Available: www.fiber-optics.info.

[16] "VPItransmissionMaker^{TM}WDM: WDM user's manual." NJ: VPIphotonics, 2003.

[17] Gerd Keiser, "Optical fiber communications," 3rd ed.. Boston: McGraw-Hill, 2000.

[18] R. März, "Integrated optics: design and modeling," Boston: Artech House, 1994, p. 183.

[19] MATTHEW DRU and ANGUS LAI, Vitesse Semiconductor, DAVID HUFF and JIAMING ZHANG, T-Networks, "Lowering the cost and size of RZ," Lightwave Web Exclusive, April 02, 2004. Available: http://lw.pennnet.com/

[20] Yi Dong, Zhihong Li, Jinyu Mo, Yixin Wang, Chao Lu, and Tee Hiang Cheng, "Pulse width-tunable CS-RZ signal format with better tolerance to dispersion and nonlinear degradation in optical transmission system," IEEE Photonics Technology Letters, Vol. 16, No. 5, pp 1409-1411, May 2004.

[21] Y. Miyamoto, A. Hirano, K. Yonenaga, A. Sano, H. Toba, K. Murata, and O. Mitomi, "320 Gbit/s (8x40 Gbits/s) WDM transmission over 367 km with 120 km repeater spacing using carrier-suppressed return-to-zero format," Electronics Letter, Vol. 35, pp. 2041-2042, 1999.

[22] Haiqing Wei, Aly F. Elrefaie, Xin Xue, and Shih-Yuan Wang, "Generation of optical signals with return-to-zero format," Patent no.: US 2002/0196508 A1, December 26, 2002.

[23] Peter J. Winzer and Juerg Leuthold, "Return-to-zero modulator using a single NRZ drive signal and an optical delay interferometer," IEEE Photonics Technology Letters, Vol. 13, No. 12, pp. 1298-1300, December 2001.

[24] R. Ohhira, D. Ogasahara, and T. Ono, "Novel RZ signal format with alternate-chirp for suppression of nonlinear degradation in 40 Gb/s based WDM," in Proc. OFC 2001, paper WM2.

[25] Oleg V. Sinkin, Ronald Holzlöhner, John Zwech, and Curtis R. Menyuk, "Optimization of the split-step Fourier method in modling optical-fiber communications systems," Journal of Lightwave Technology, Vol. 21, No. 1, pp 61-68, January 2003.

[26] John Zwech and Curtis R. Menyuk, "Reduction of intrachannel four-wave mixing using subchannel multiplexing," IEEE Photonics Technology Letters, Vol. 15, No. 2, pp. 323-325, February 2003.

[27] Arthur Lowery, Olaf Lenzmann, Igor Koltchavov, Rudi Moosburger, Ronald Freund, Adre Richter, Stefan Georgi, Dirk Breuer, and Harald Hamster, "Multiple signal representation simulation of photonic devices, systems, and networks," IEEE Journal of Selected Topics in Quantum Electronics, Vol. 6, No. 2, pp 282-296, March/April 2000.

[28] Govind P. Agrawal, "Nonlinear fiber optics," 3rd ed.. San Diego: Academic Press, 2001.

[29] Sang-Gyu Park, A. H. Gnauck, J. M. Wiesenfeld, and L. D. Garrett, "40-Gb/s transmission over multiple 120-km spans of conventional single-mode fiber using highly dispersed pulses," IEEE Photonics Technology Letters, Vol. 12, No. 8, pp. 1085-1087, August 2000.

[30] "Fiber nonlinearities." Availabe: http://www.fiber-optics.info/

[31] A. F. Elrefaie, R. E. Wagner, D. A. Atlas, and D. G. Daut, “Chromatic dispersion limitations in coherent lightwave transmission systems,” Journal of Lightwave Technology, Vol. 6, No. 5, pp 704-709, May 1988.

[32] C. Caspar, H. M. Foisel, A. Gladisch, N. Hanik, F. Küppers, R. Ludwig, A. Mattheus, W. Pieper, B. Strebel, and H. G. Weber, "RZ versus NRZ modulation format for dispersion compensated SMF-based 10-Gb/s transmission with more than 100-km amplifier spacing," IEEE Photonics Technology Letters, Vol. 11, No. 4, pp. 481-483, April 1999.

[33] N. N. Khrais, A. F. Elrefaie, R. E. Wagner, and S. Ahmed, “Performance of cascaded misaligned optical demultiplexers in multiwavelength optical networks,” IEEE Photonics Technology Letters, Vol. 8, No. 8, pp 1073-1075, August 1996.

[34] A. Mecozzi, C. B. Clausen, M. Shtaif, S. Park, and A. H. Gnauck, “Cancellation of timing and amplitude jitter in symmetric links using highly dispersed pulses,” IEEE Photonics Technology Letters, Vol. 13, No. 5, pp 445-448, May 2001.

[35] Zweck J., Menyuk C.R, "Reduction of intrachannel four wave mixing using subchannel multiplexing," IEEE Photonics Technology Letters, Vol. 15, No.2, pp. 323-325, February 2003.

[36] Douglas M. Gill, Xiang Liu, Xing Wei, Sonali Banerjee, and Yikai Su, “π/2 Alternate-phase on-off keyed 40-Gb/s transmission on standard single-mode fiber,” IEEE Photonics Technology Letters, Vol. 15, No. 12, pp 1776-1778, December 2003.

[37] VPItransmissionMaker^{TM}WDM web site. Available: http://www.vpiphotonics.com/

APPENDIX A

"VPItransmissionMaker^{TM}WDM"

SIMULATION TOOL

VPItransmissionMaker^{TM}WDM is a photonic simulation tool which has been developed by "VPIphotonics" company for modelling all types of photonic systems and networks. It focuses on WDM systems, as these offer the most severe technical challenges, and potentially the most rewards. It provides an automated formal design process for WDM systems, aided at every stage by accurate and efficient numerical techniques [16].

VPItransmissionMaker™WDM accelerates the design of new photonic systems. Over 250 design templates are provided with regular updates on the Optical Systems Forum. An unrivaled range of photonic and electronic modules supports almost every system concept. The graphical interface allows almost any topology to be built and simulated using sample and block modes, both in unidirectional and bidirectional simulations [37].

VPItransmissionMaker™ offers [16]:

1. **Design-assistants** capture common simulation tasks and provide automated synthesis and verification tools. They are written in a simple scripting language,

mimicking keyboard and mouse interactions with the simulator, so enabling the user to incorporate his own design rules and test specifications. Design Assistants can be used to capture company know-how, and electronically distribute it between design teams, or to provide interactive applications notes for customers. Design Assistants improve efficiency and repeatability, impose company-wide standards, and allow new ideas in design to be captured and distributed almost instantaneously.

2. **Vertically-integrated design process** with layered simulation technologies that enable concurrent analysis across network levels.

3. **Co-simulation capability** so designers can integrate third party tools and their own models alongside a comprehensive library of component and system models.

4. **Tailored GUI** with easy to use optimizers, parameter and module sweep capabilities. Extensive library of photonic modules covering the latest photonic technologies over several levels of abstraction, from detailed physical models, to Black-Box, measured, and Data Sheet Models.

APPENDIX B

BER, BER ISI, AND Q-FACTOR MEASUREMENTS OF THE END-TO-END COMPENSATION

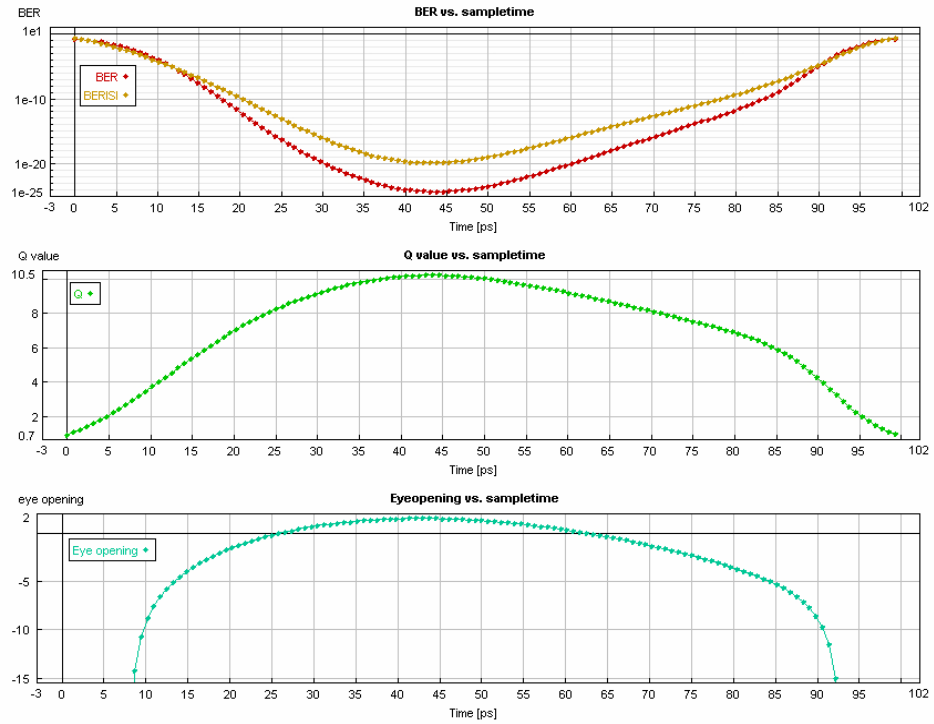

Figure B–1 BER, BER ISI, and Q-factor measurements of the received alternate chirp RZ signal after 960 km

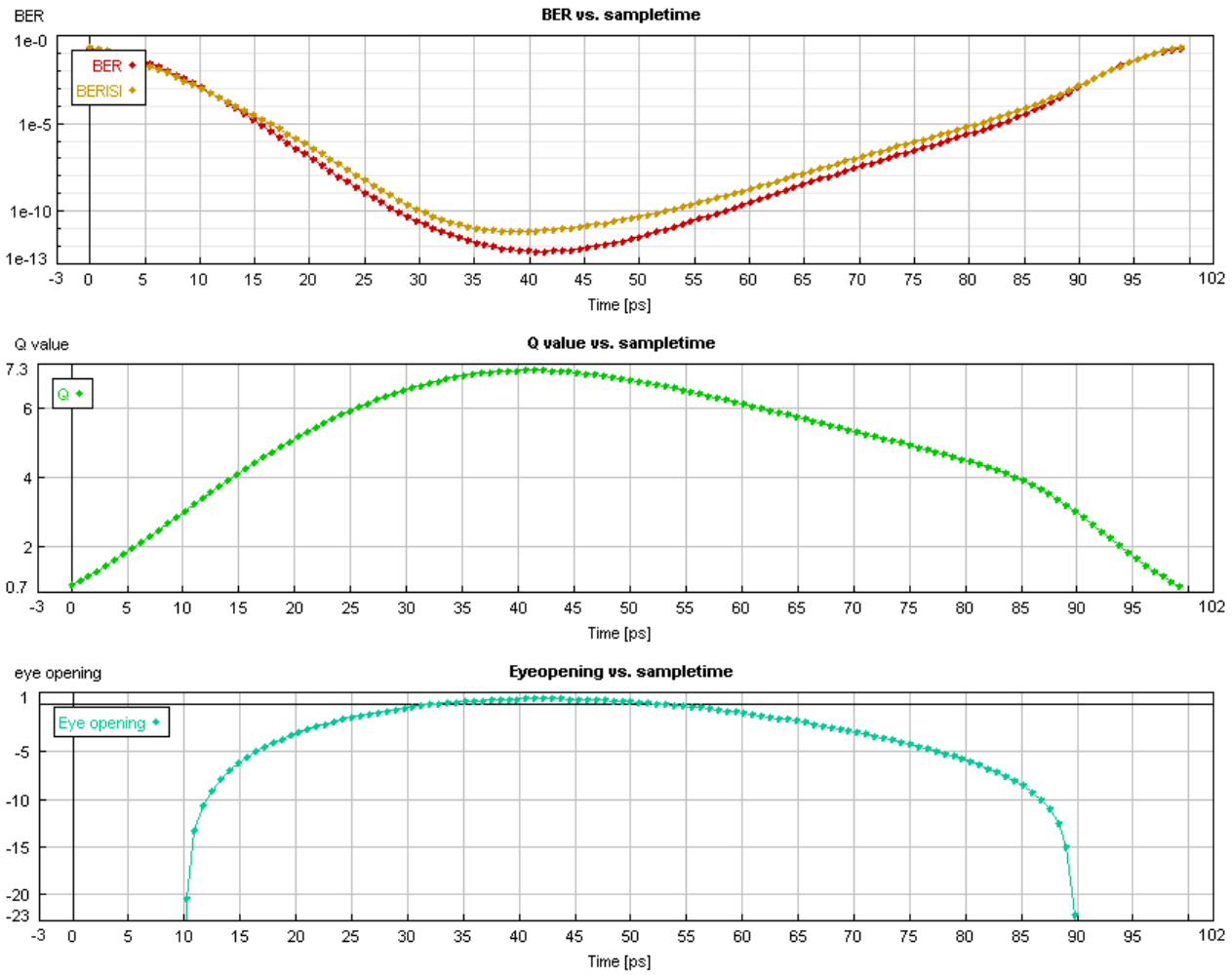

Figure B–2 BER, BER ISI, and Q-factor measurements of the received alternate chirp RZ signal after 1920 km

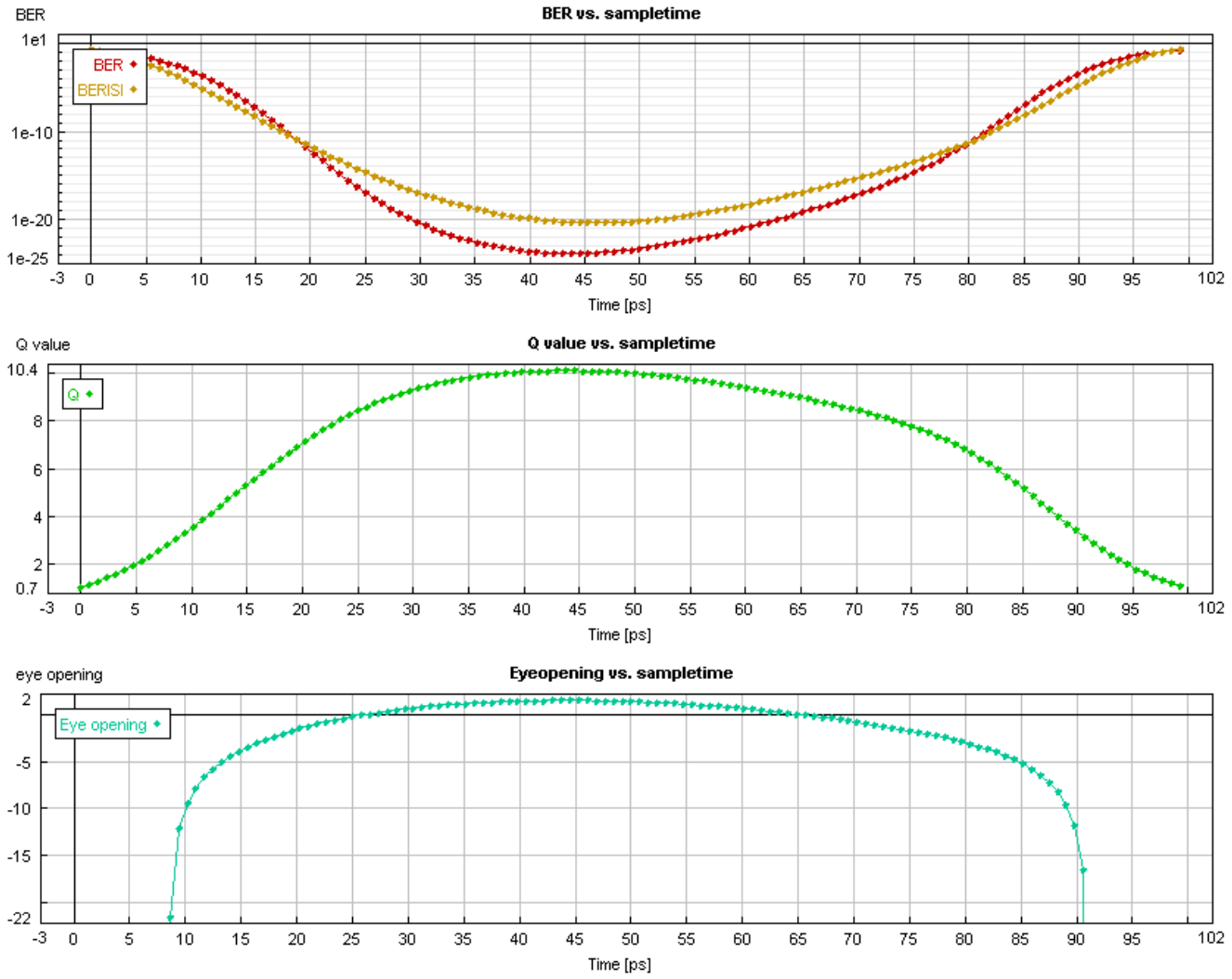

Figure B–3 BER, BER ISI, and Q-factor measurements of the received chirp-free RZ-33% signal after 960 km

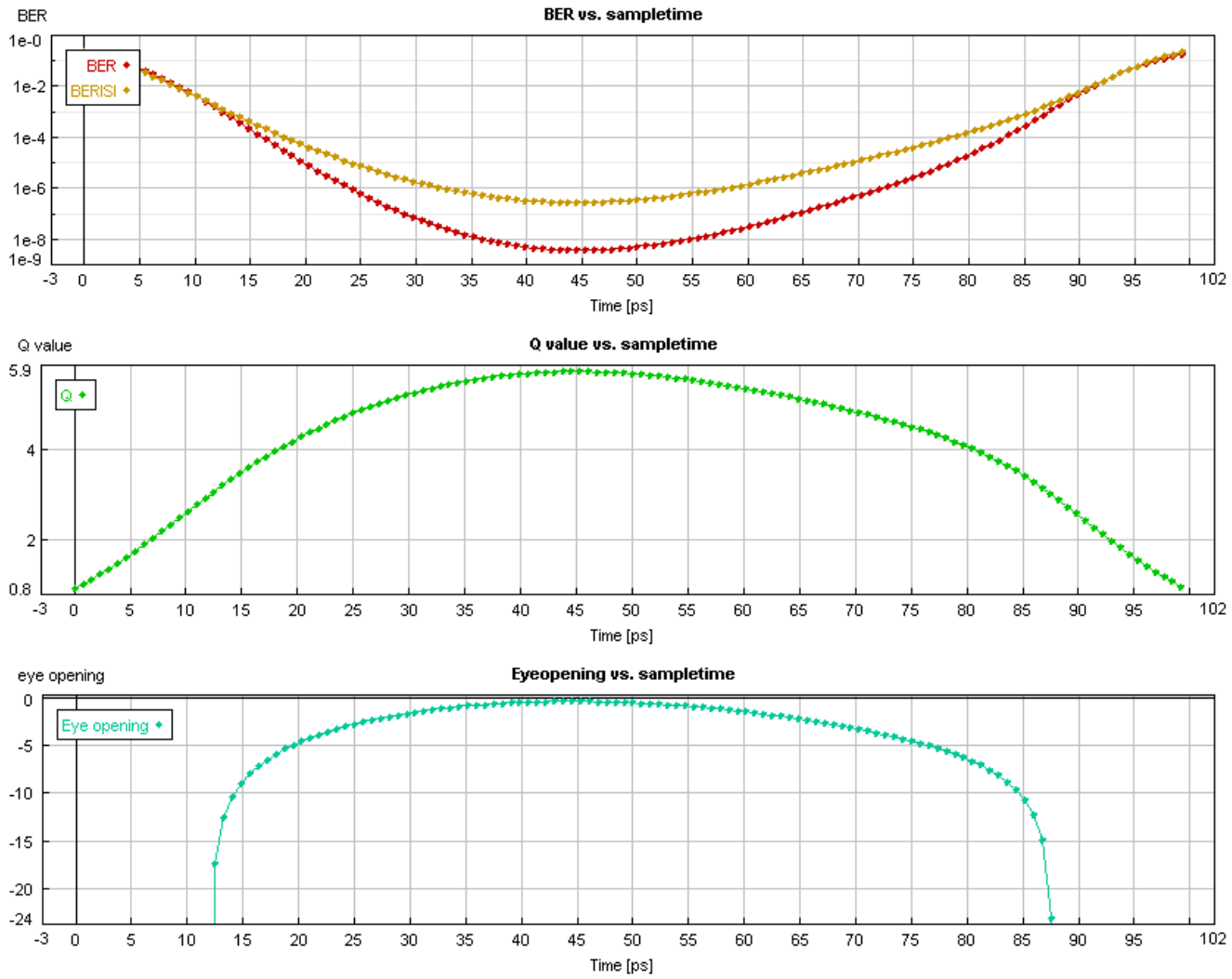

Figure B–4 BER, BER ISI, and Q-factor measurements of the received chirp-free RZ-33% signal after 1920 km

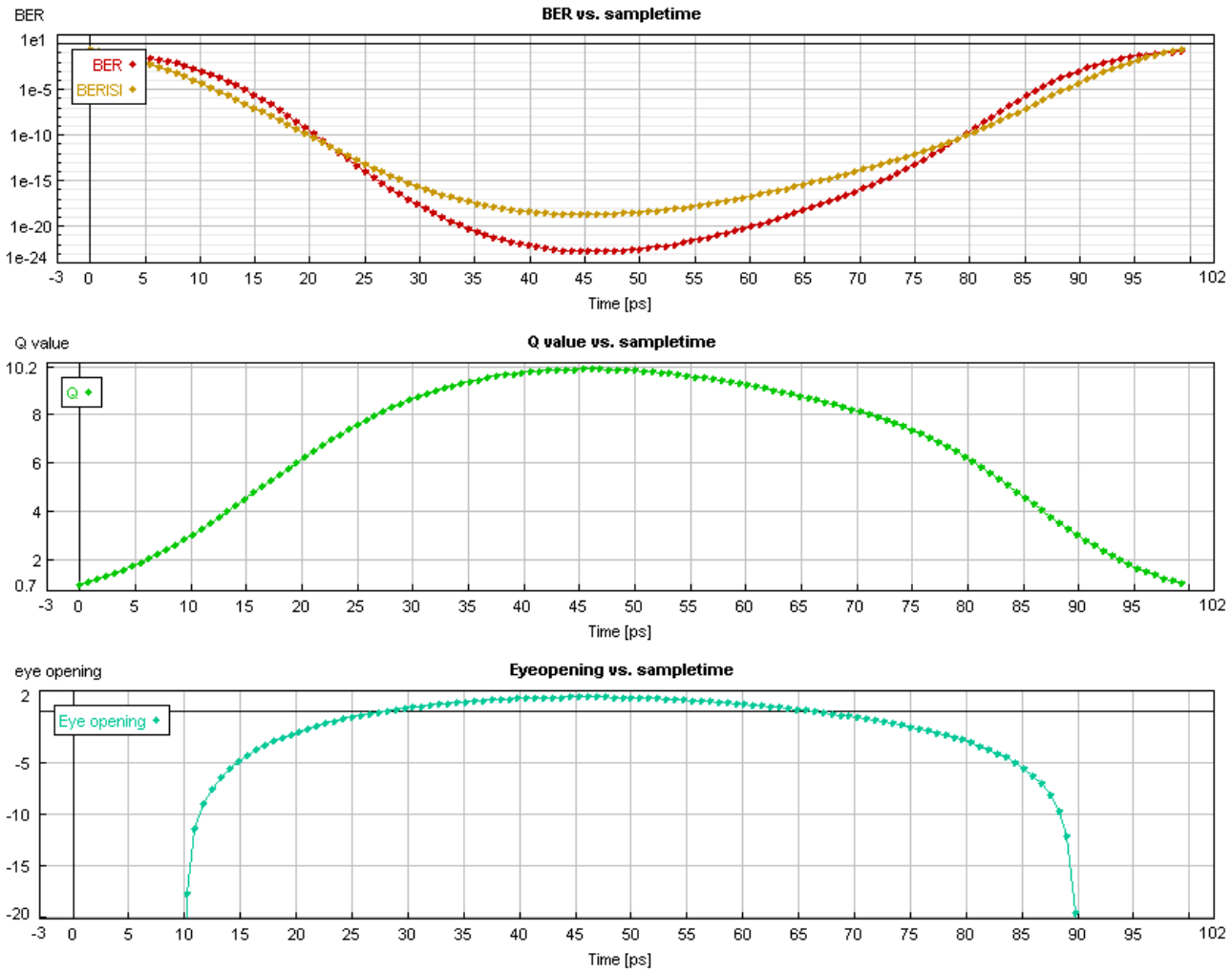

Figure B–5 BER, BER ISI, and Q-factor measurements of the received chirp-free RZ-50% signal after 960 km

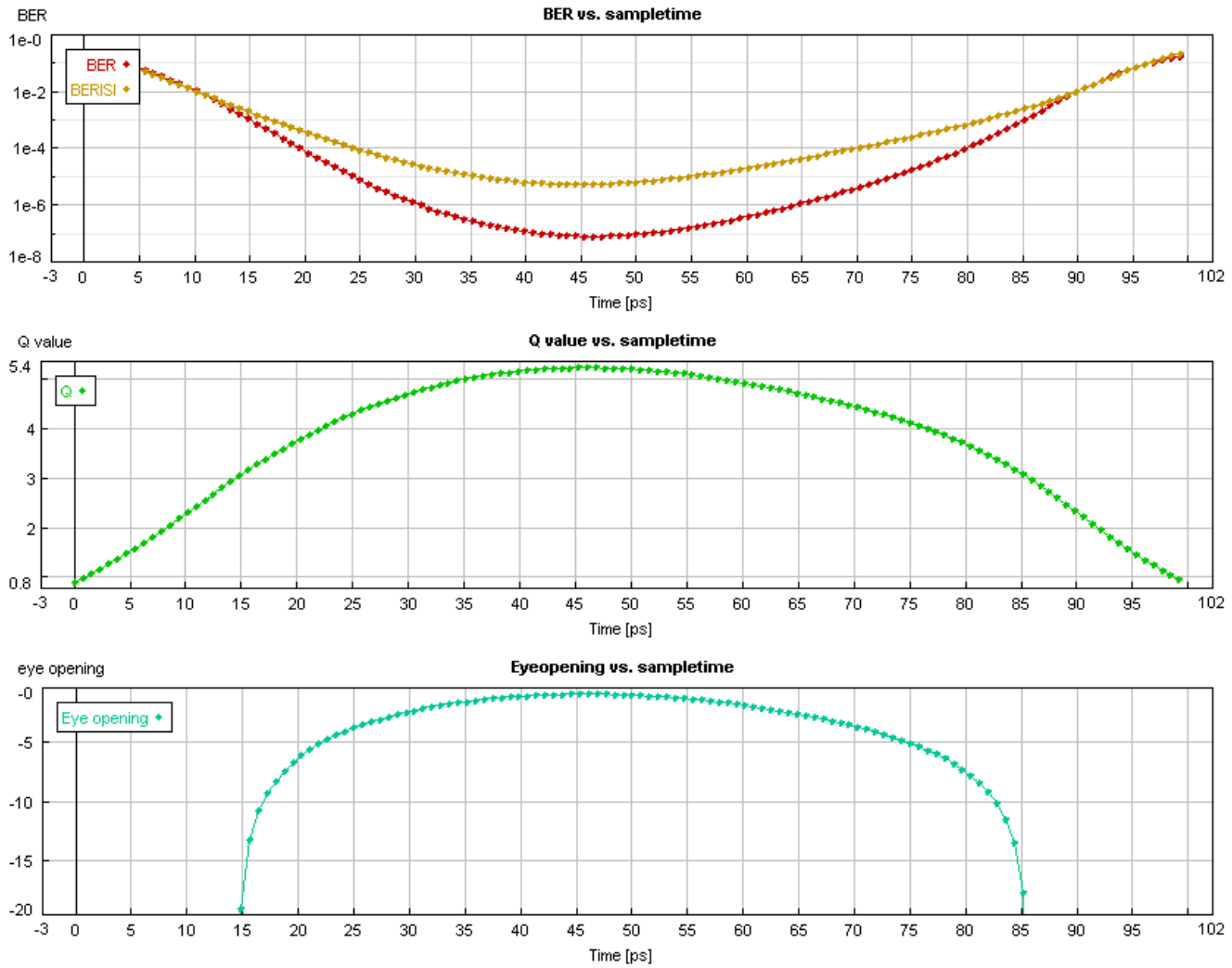

Figure B–6 BER, BER ISI, and Q-factor measurements of the received chirp-free RZ signal after 1920 km

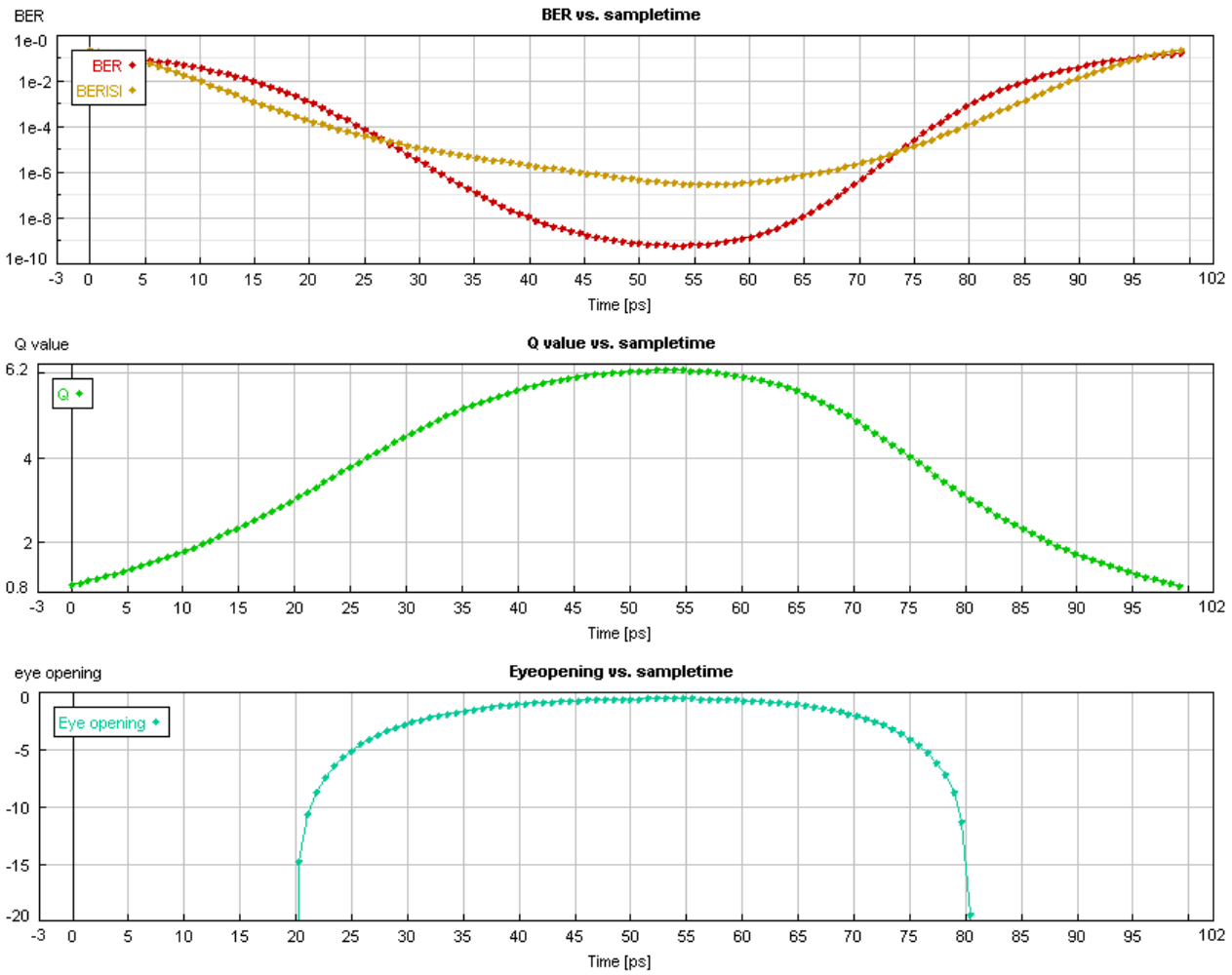

Figure B–7 BER, BER ISI, and Q-factor measurements of the received NRZ signal after 960 km

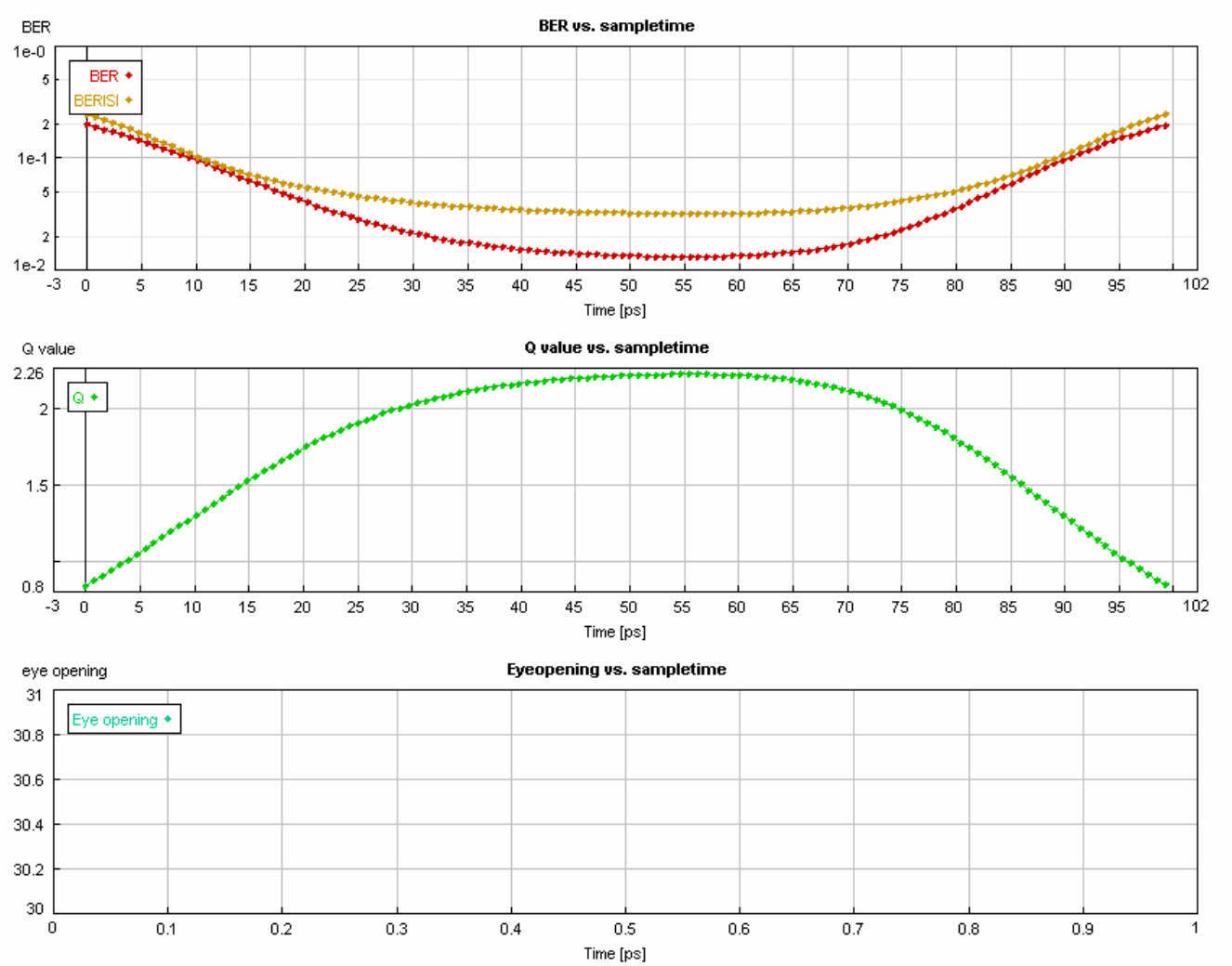

Figure B–8 BER, BER ISI, and Q-factor measurements of the received NRZ signal after 1920 km

APPENDIX C

BER, BER ISI, AND Q-FACTOR MEASUREMENTS USING SUPER SPAN

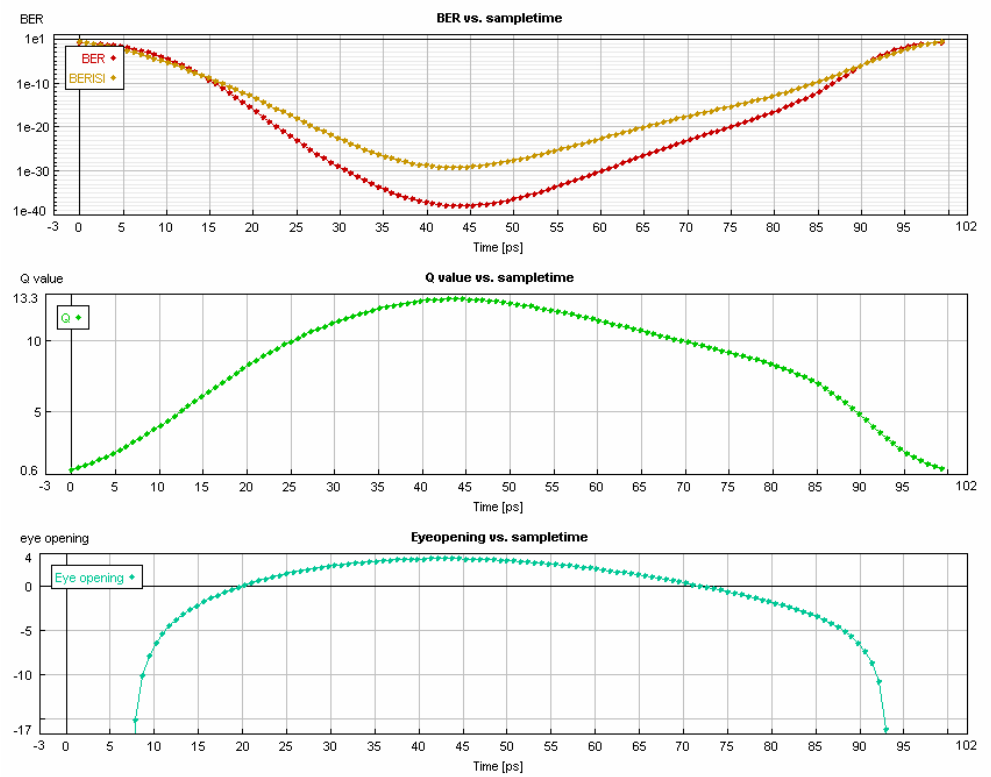

Figure C–1 BER, BER ISI, and Q-factor measurements of the received alternate chirp RZ signal after 1 super span

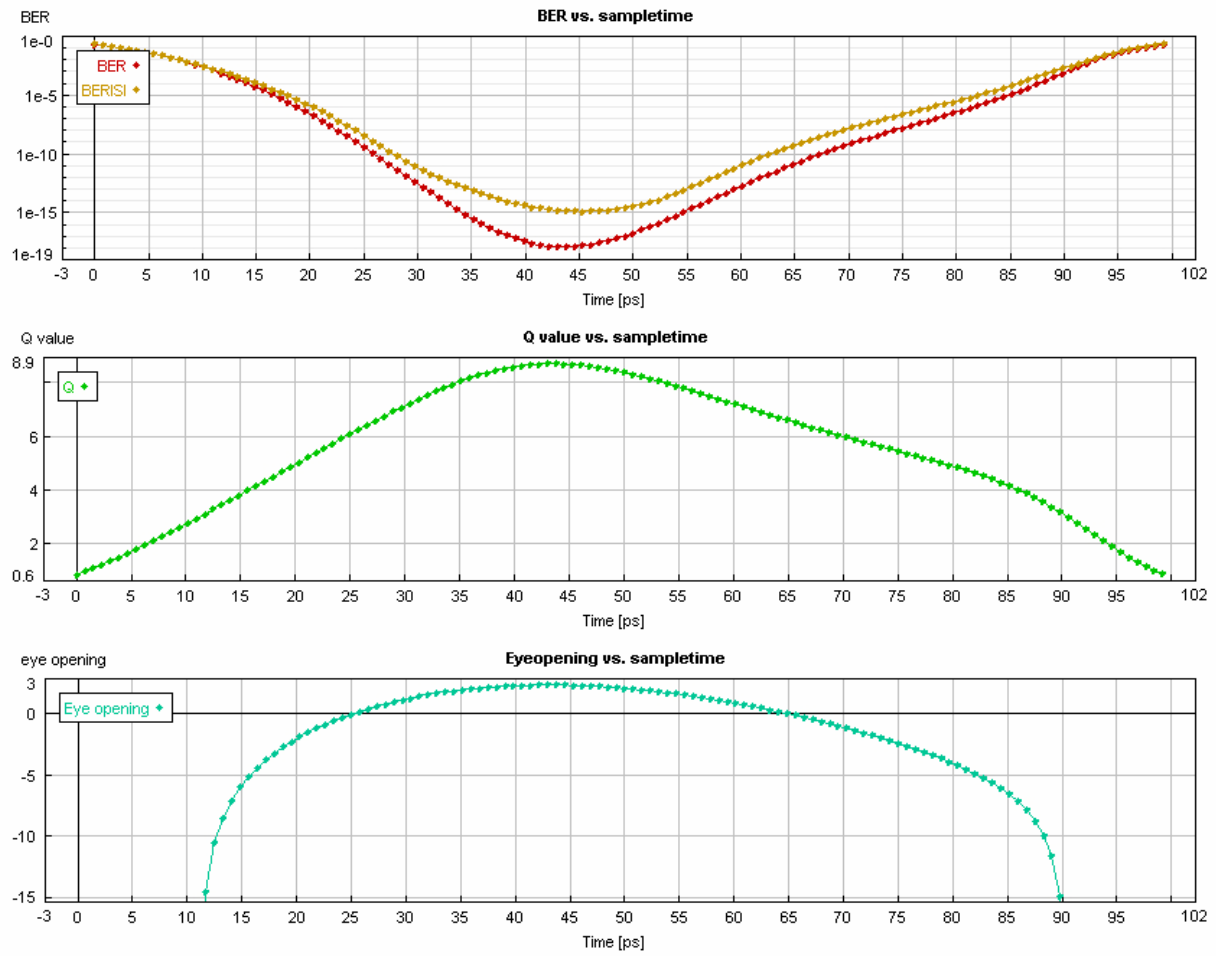

Figure C-2 BER, BER ISI, and Q-factor measurements of the received alternate chirp RZ signal after 2 super spans

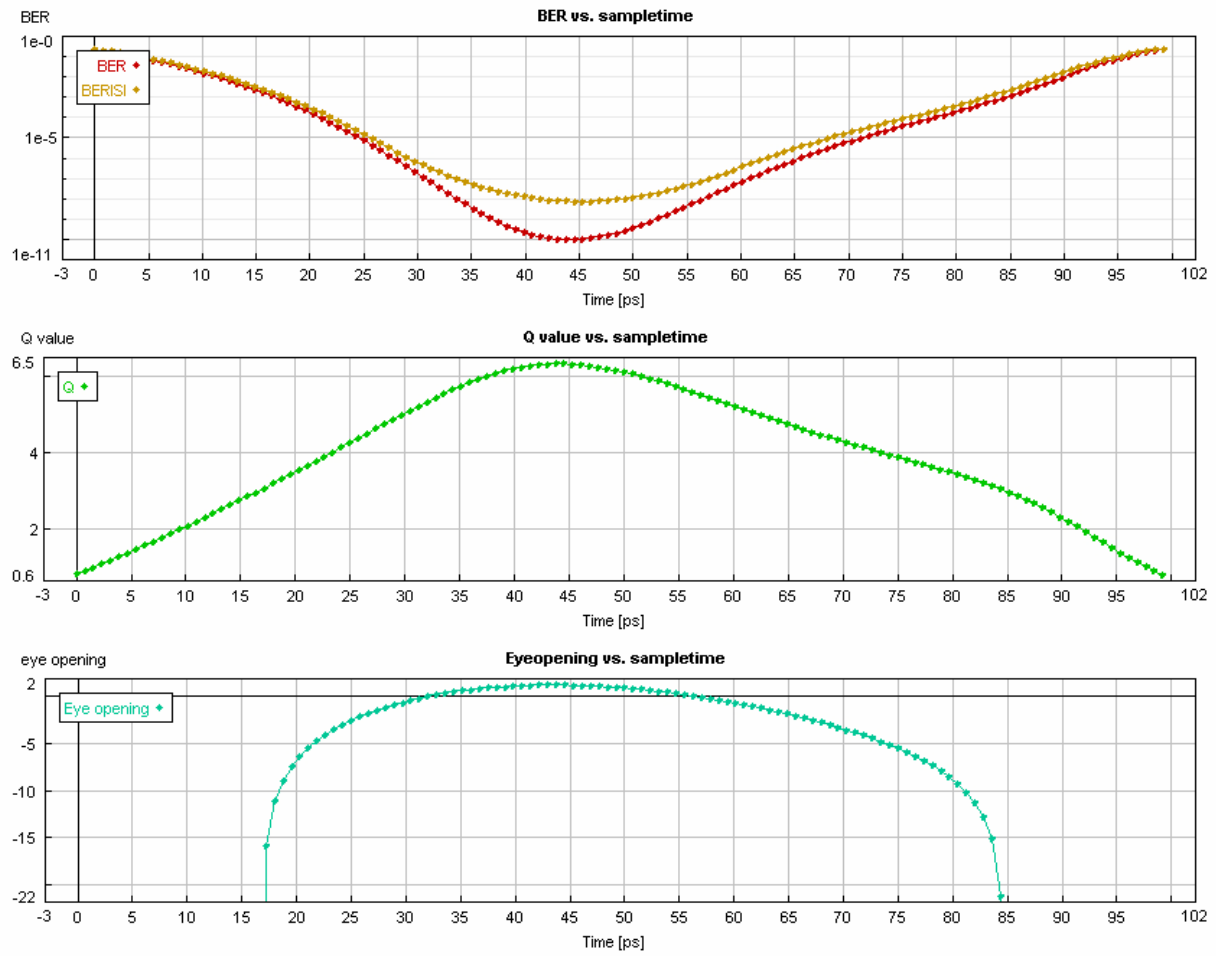

Figure C–3 BER, BER ISI, and Q-factor measurements of the received alternate chirp RZ signal after 3 super spans

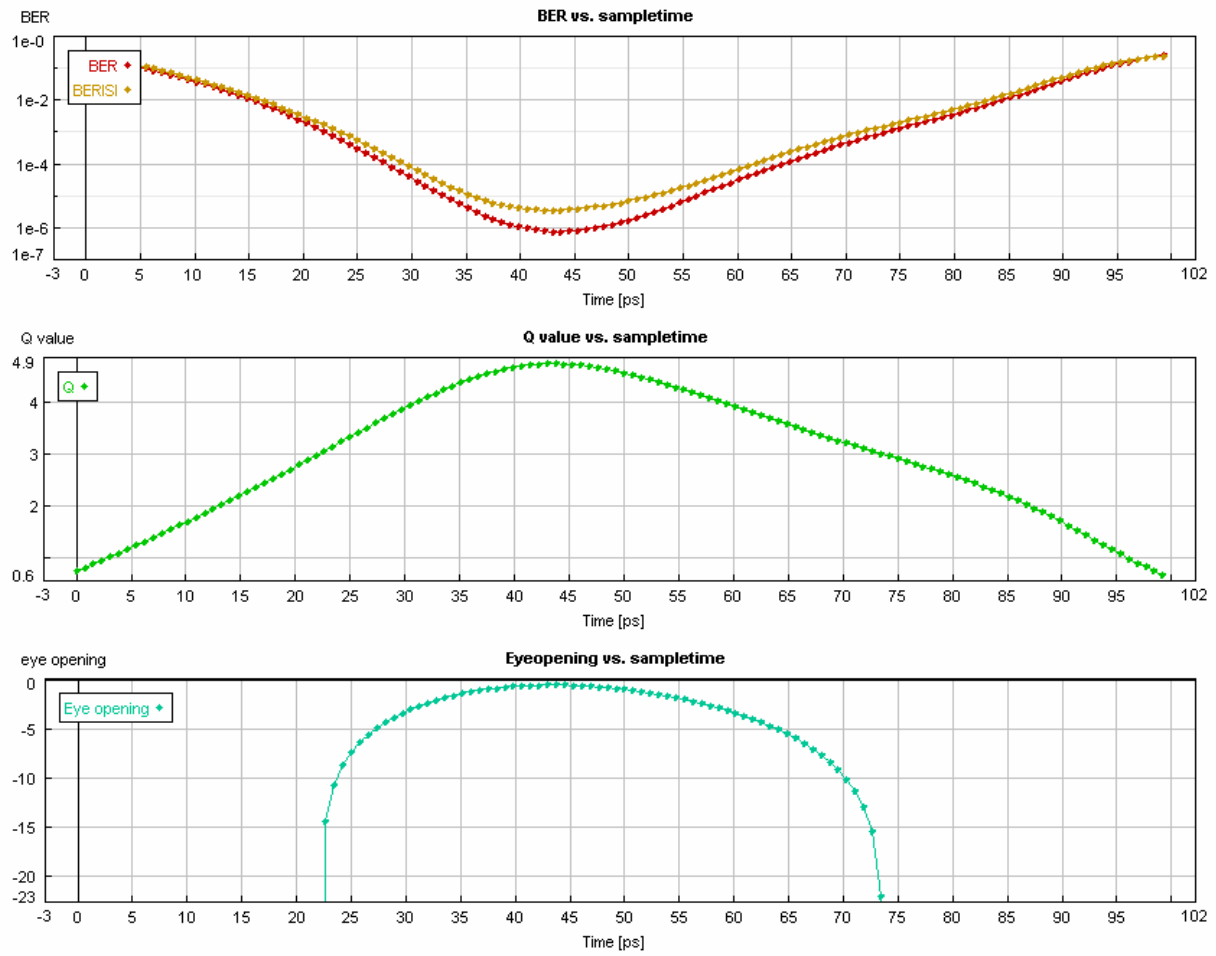

Figure C-4 BER, BER ISI, and Q-factor measurements of the received alternate chirp RZ signal after 4 super spans

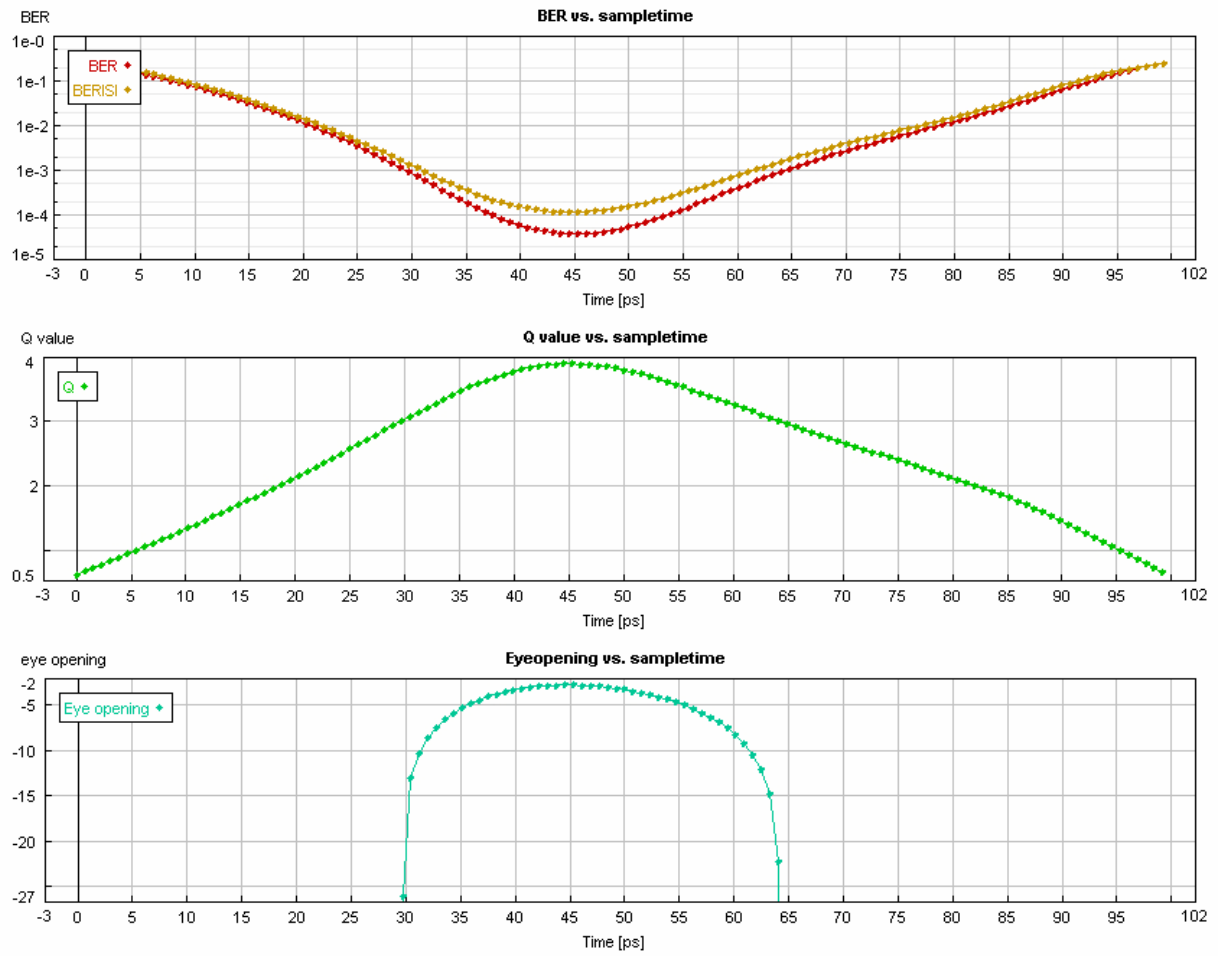

Figure C-5 BER, BER ISI, and Q-factor measurements of the received alternate chirp RZ signal after 5 super spans

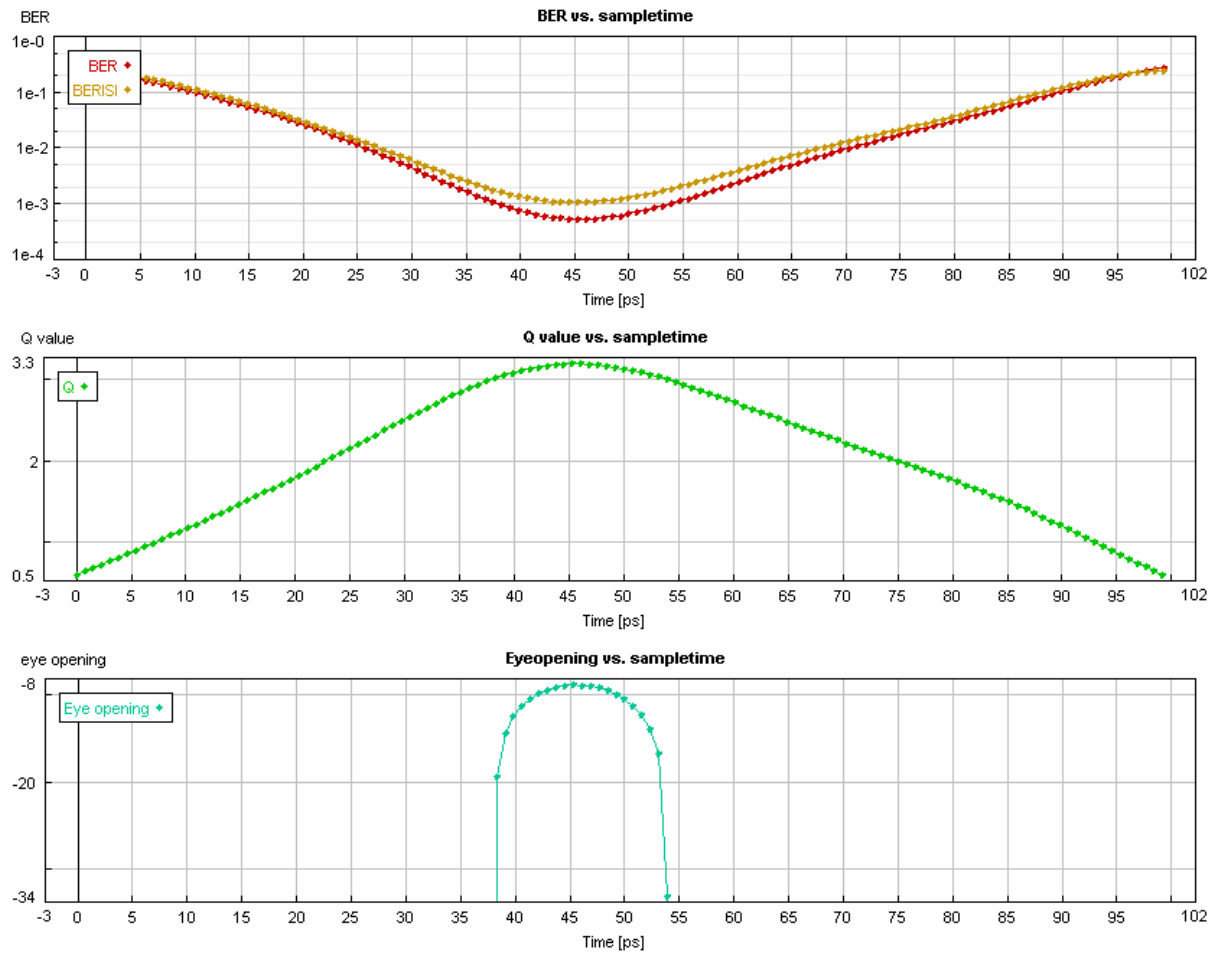

Figure C-6 BER, BER ISI, and Q-factor measurements of the received alternate chirp RZ signal after 6 super spans

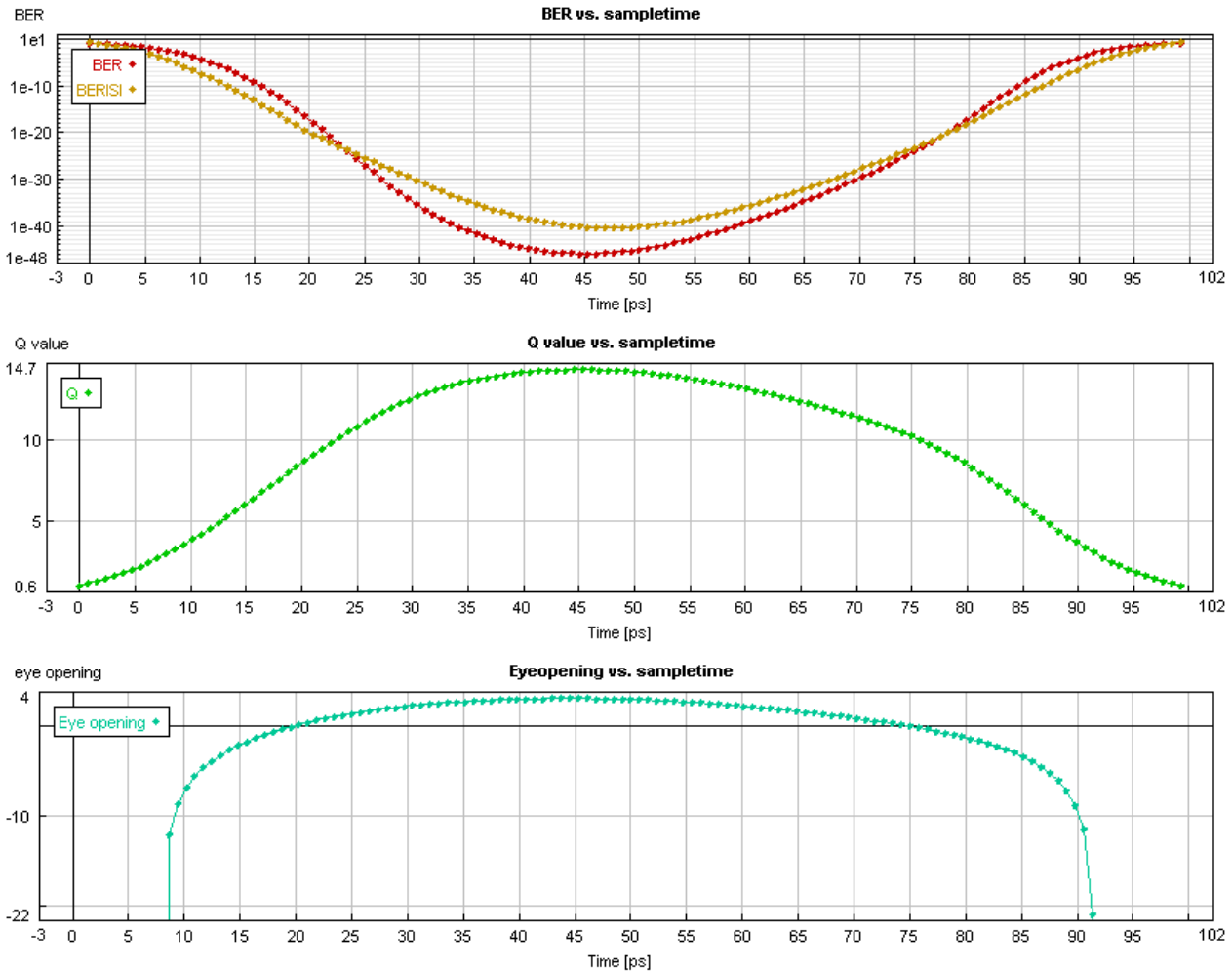

Figure C-7 BER, BER ISI, and Q-factor measurements of the received chirp-free RZ-33% signal after 1 super span

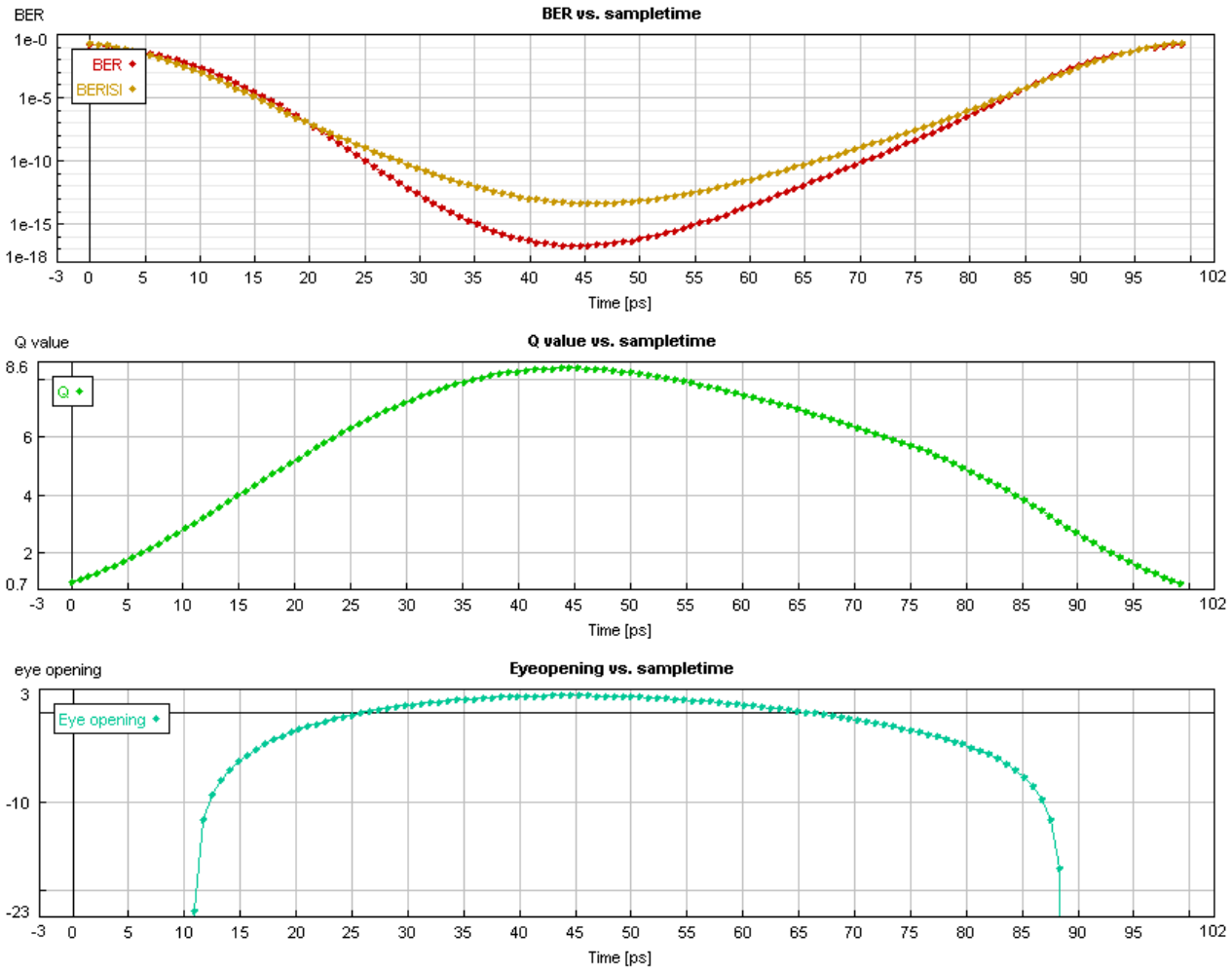

Figure C-8 BER, BER ISI, and Q-factor measurements of the received chirp-free RZ-33% signal after 2 super spans

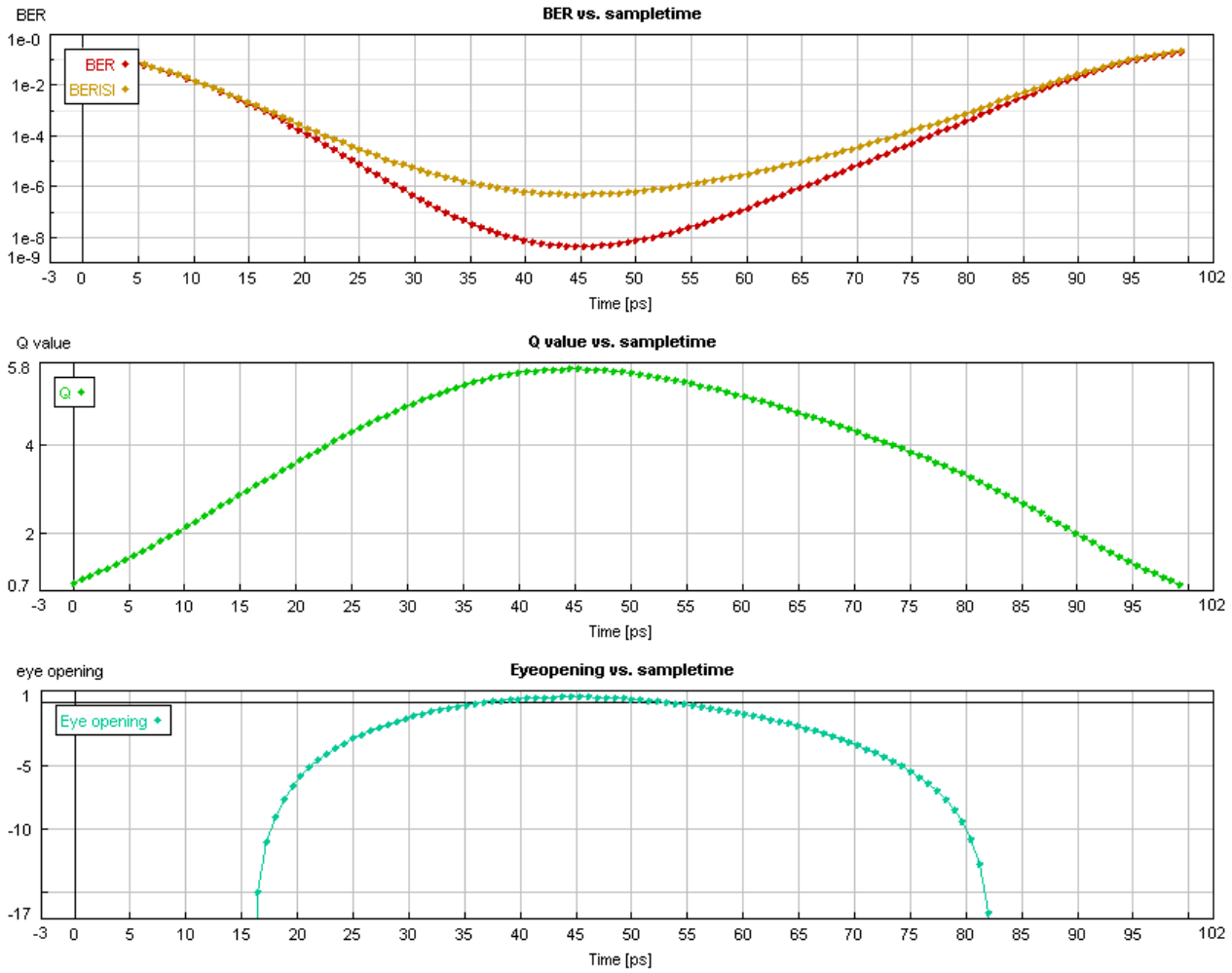

Figure C-9 BER, BER ISI, and Q-factor measurements of the received chirp-free RZ-33% signal after 3 super spans

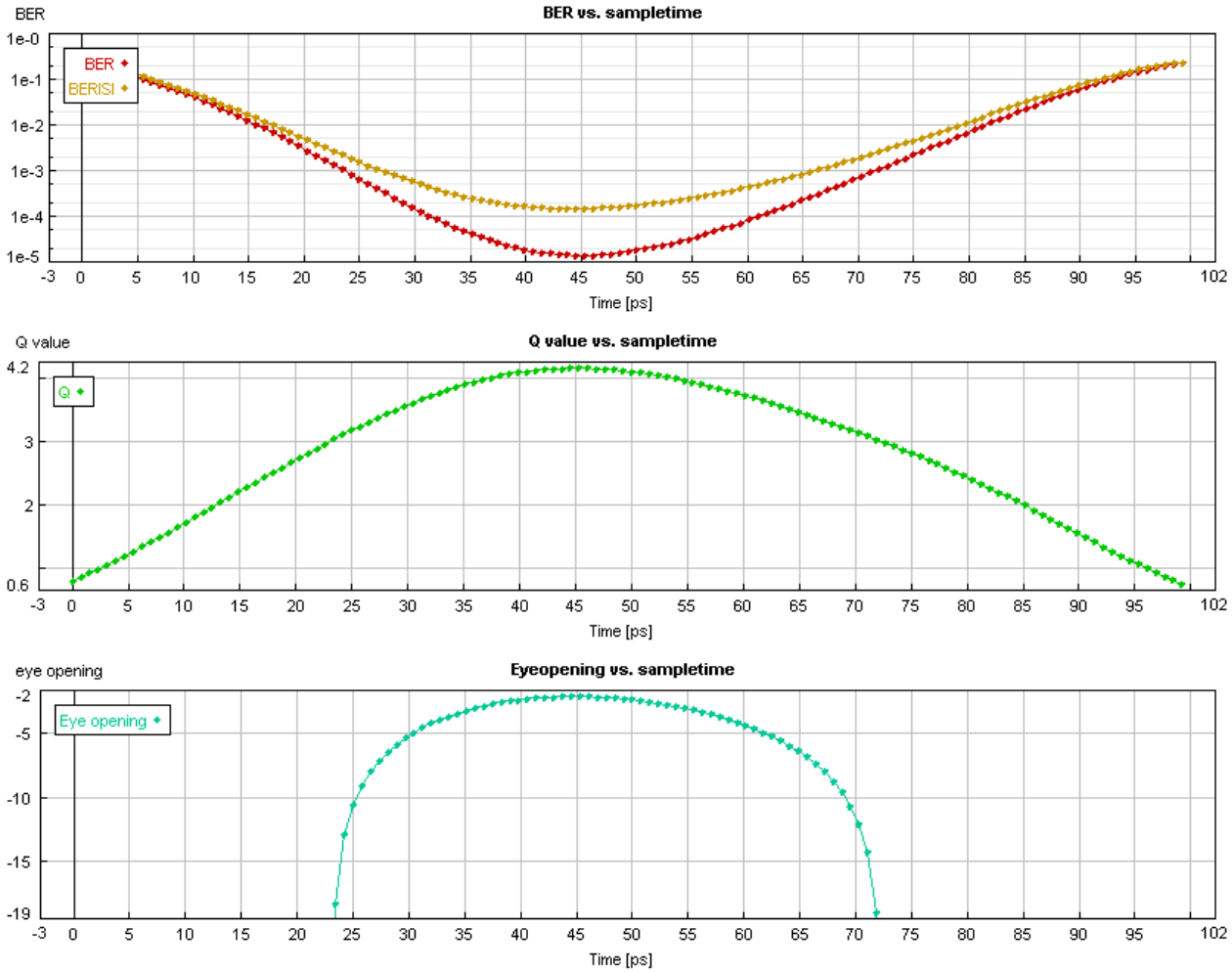

Figure C-10 BER, BER ISI, and Q-factor measurements of the received chirp-free RZ-33% signal after 4 super spans

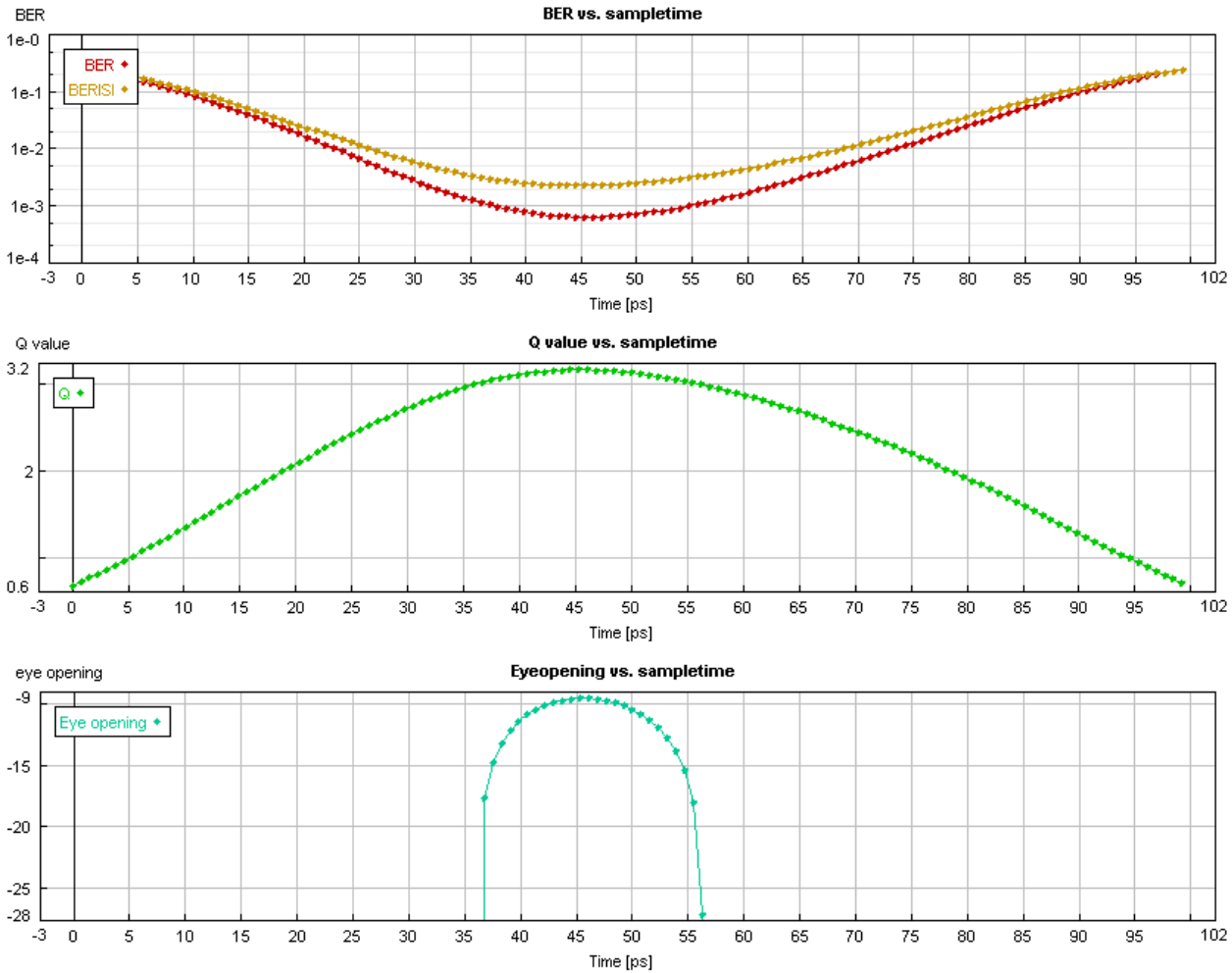

Figure C-11 BER, BER ISI, and Q-factor measurements of the received chirp-free RZ-33% signal after 5 super spans

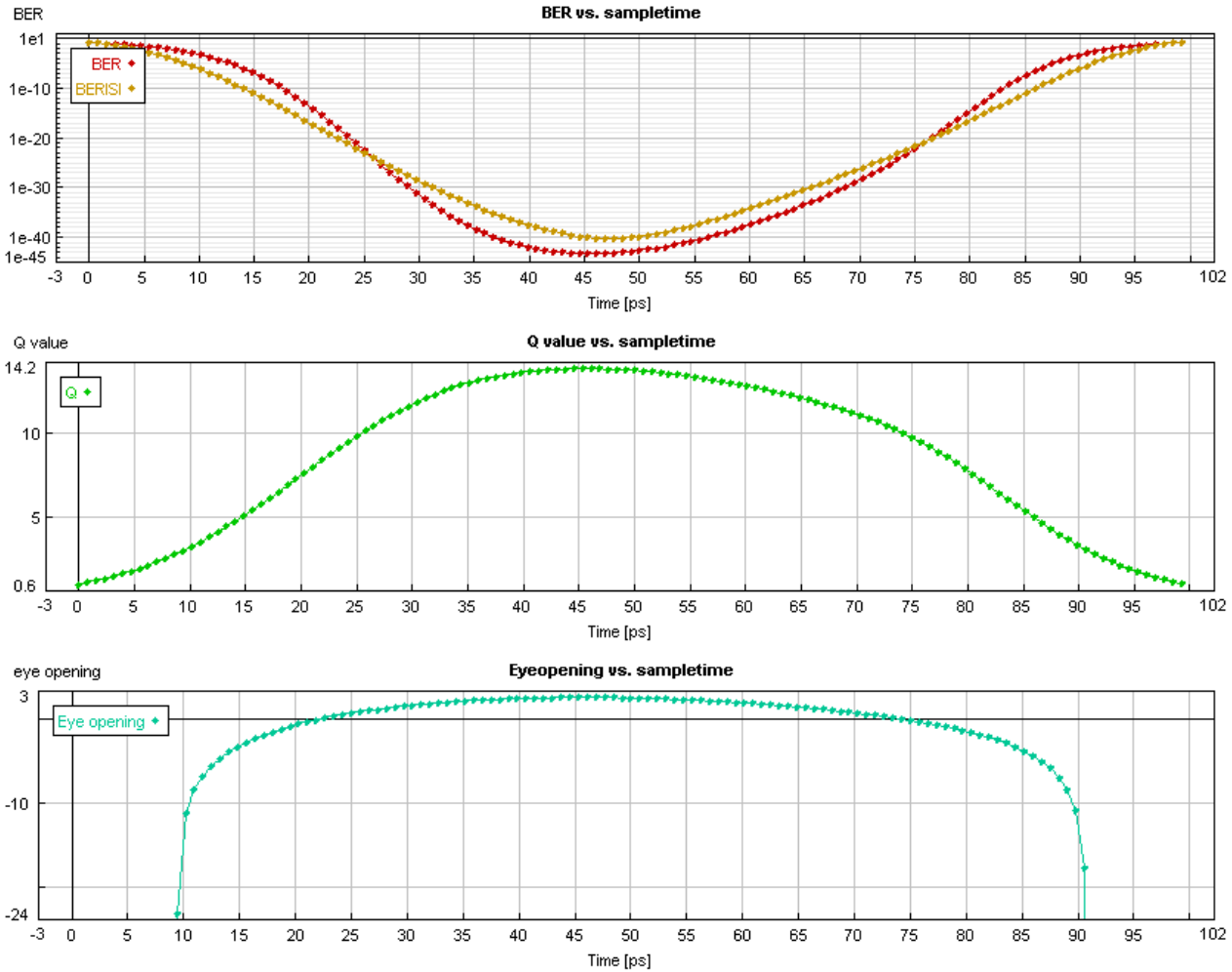

Figure C-12 BER, BER ISI, and Q-factor measurements of the received chirp-free RZ-50% signal after 1 super span

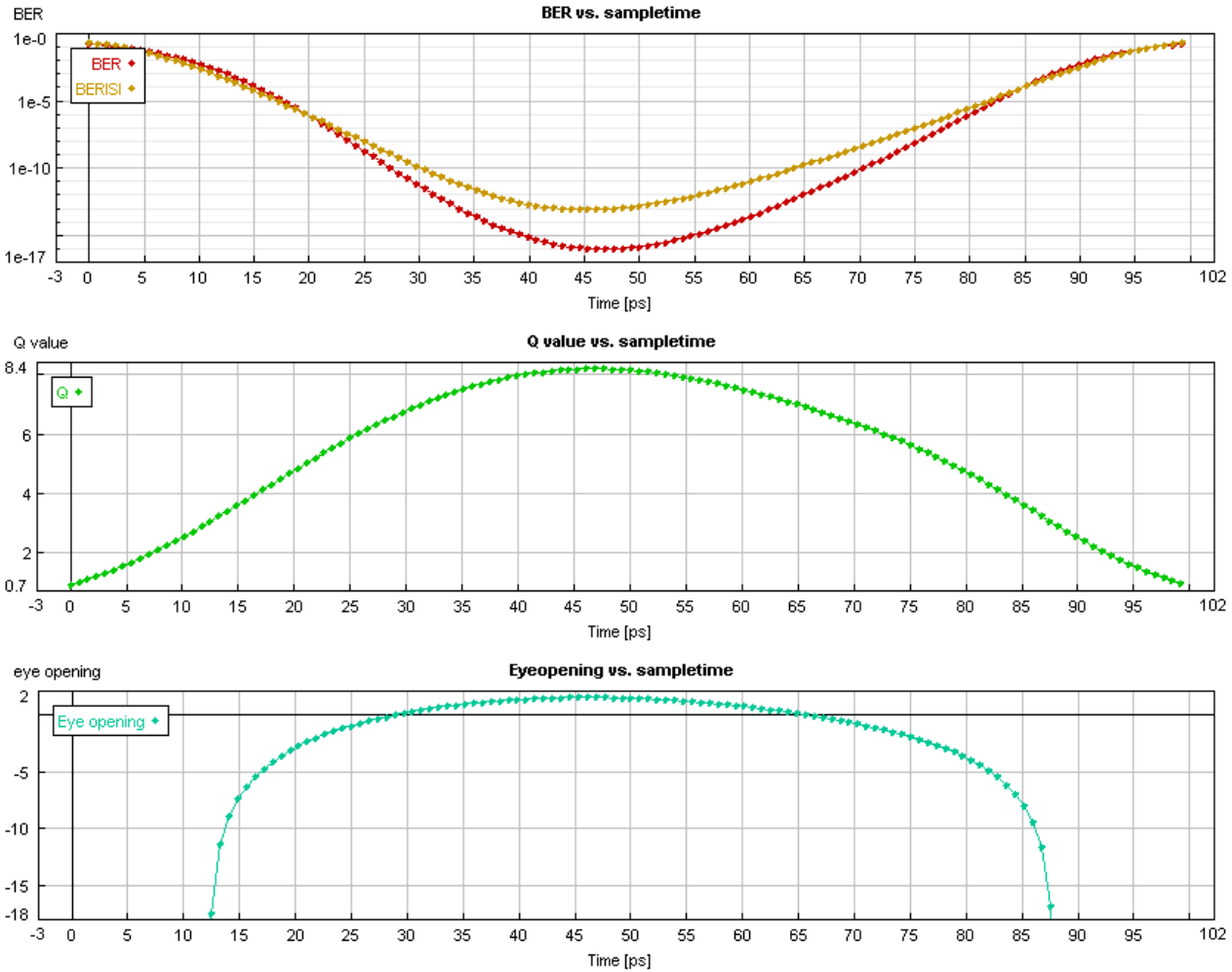

Figure C-13 BER, BER ISI, and Q-factor measurements of the received chirp-free RZ-50% signal after 2 super spans

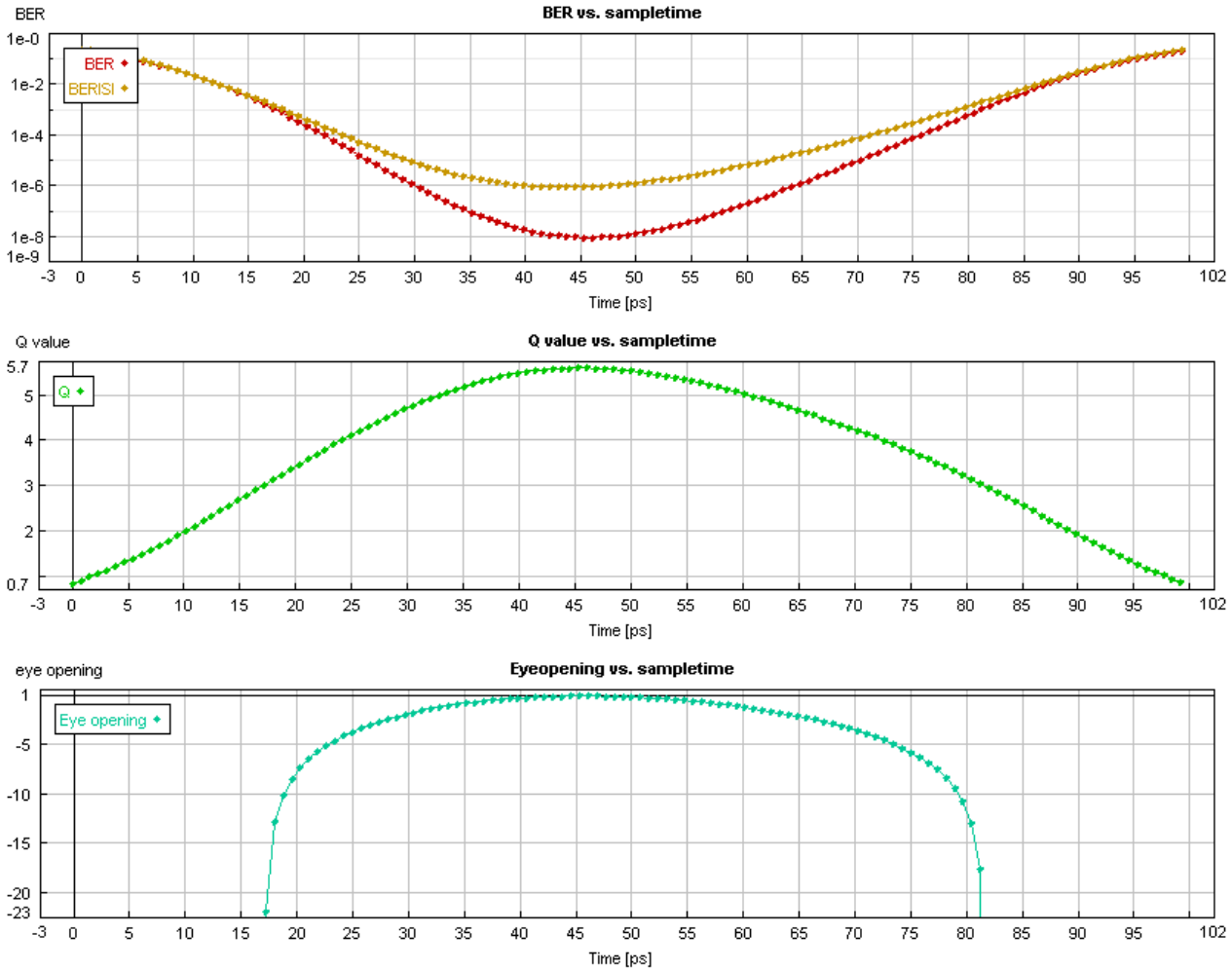

Figure C-14 BER, BER ISI, and Q-factor measurements of the received chirp-free RZ-50% signal after 3 super spans

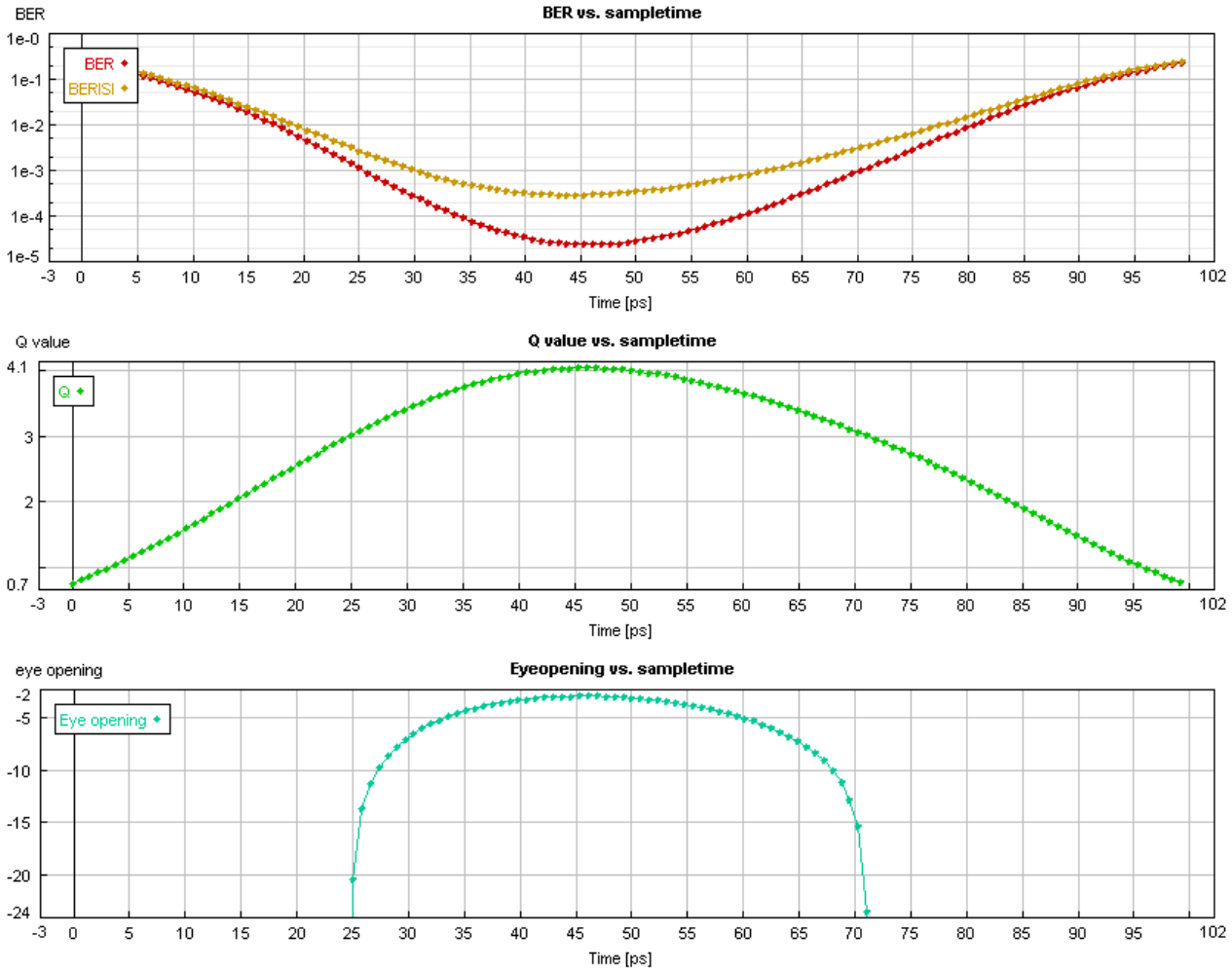

Figure C-15 BER, BER ISI, and Q-factor measurements of the received chirp-free RZ-50% signal after 4 super spans

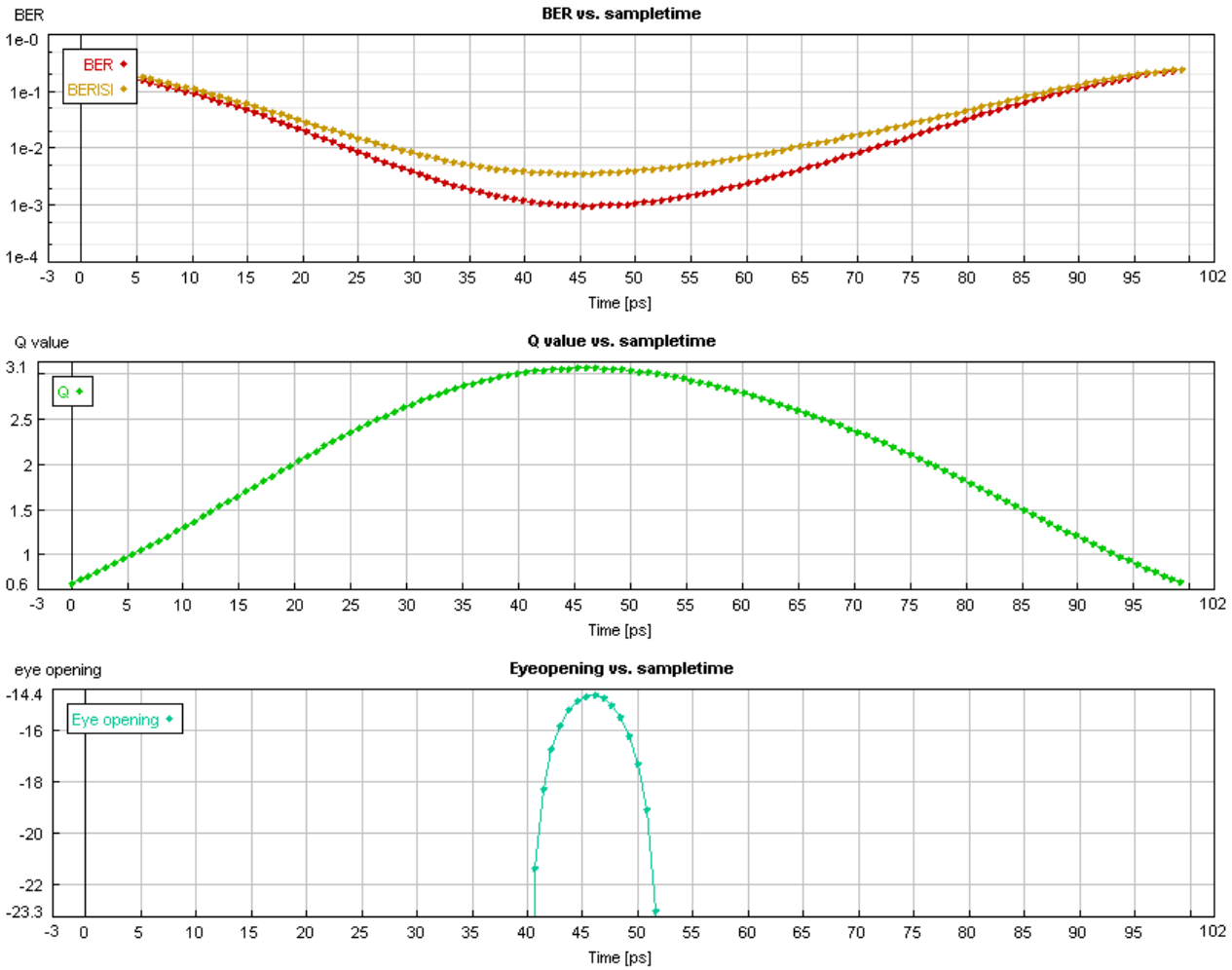

Figure C-16 BER, BER ISI, and Q-factor measurements of the received chirp-free RZ-50% signal after 5 super spans

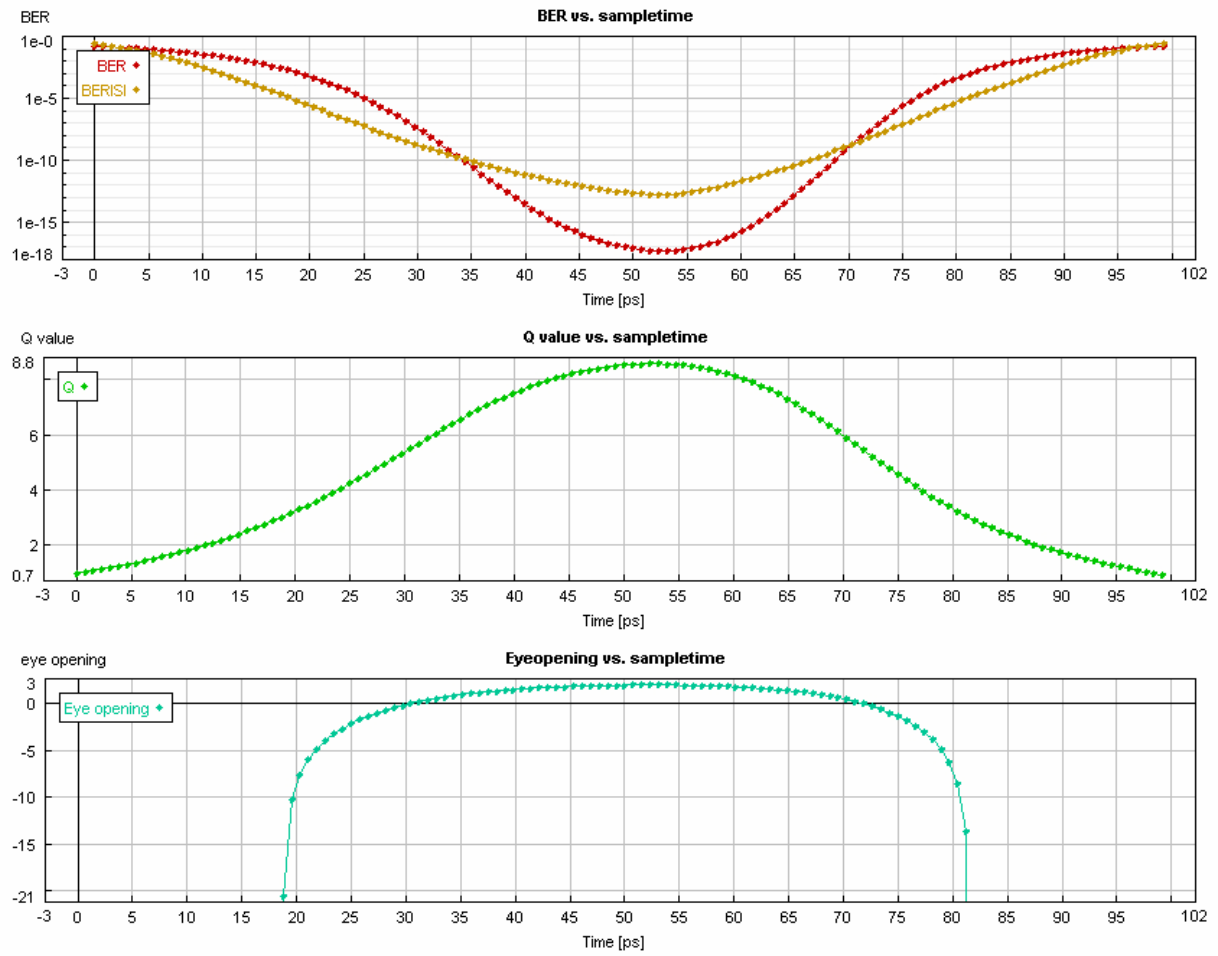

Figure C-17 BER, BER ISI, and Q-factor measurements of the received NRZ signal after 1 super span

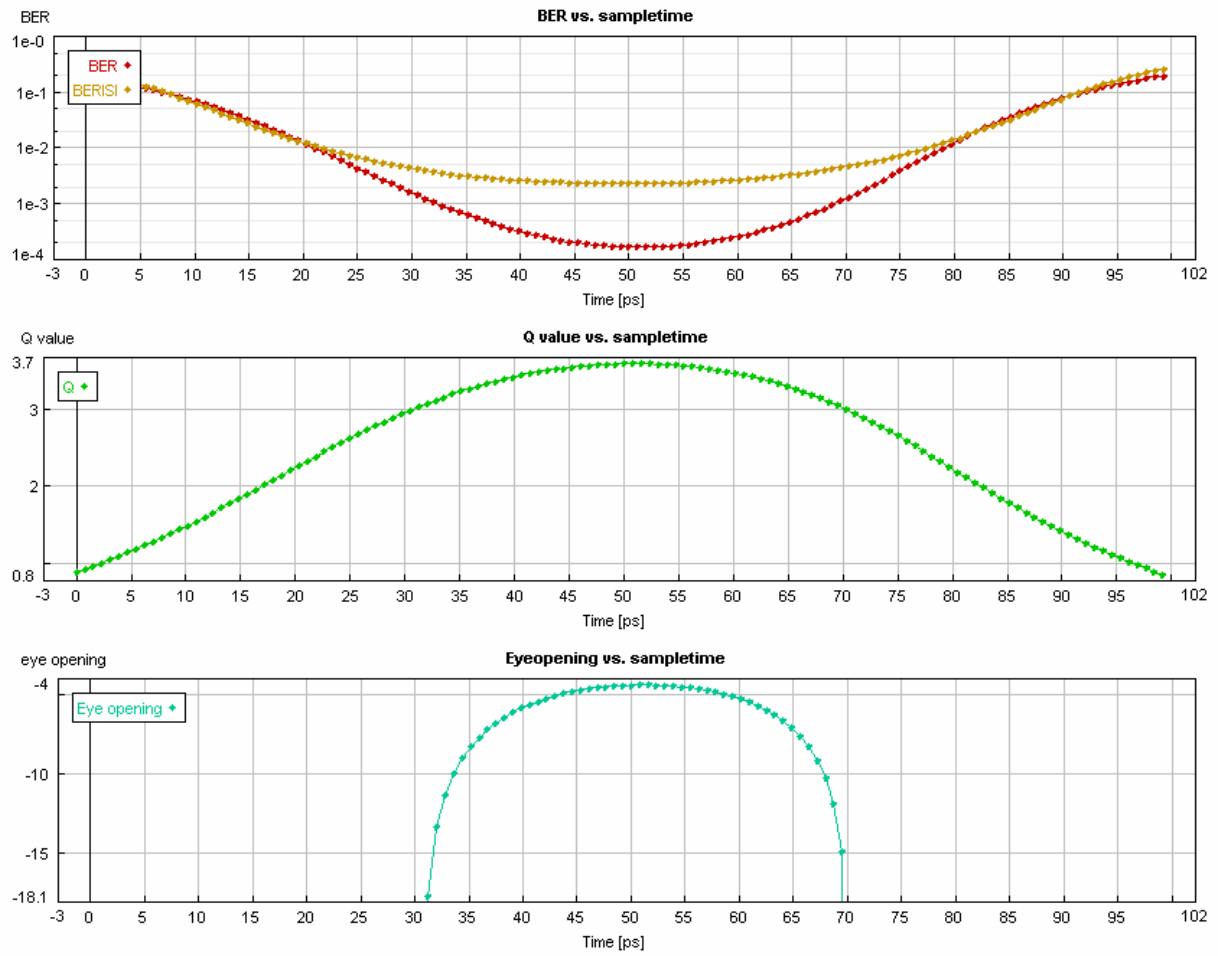

Figure C-18 BER, BER ISI, and Q-factor measurements of the received NRZ signal after 2 super spans

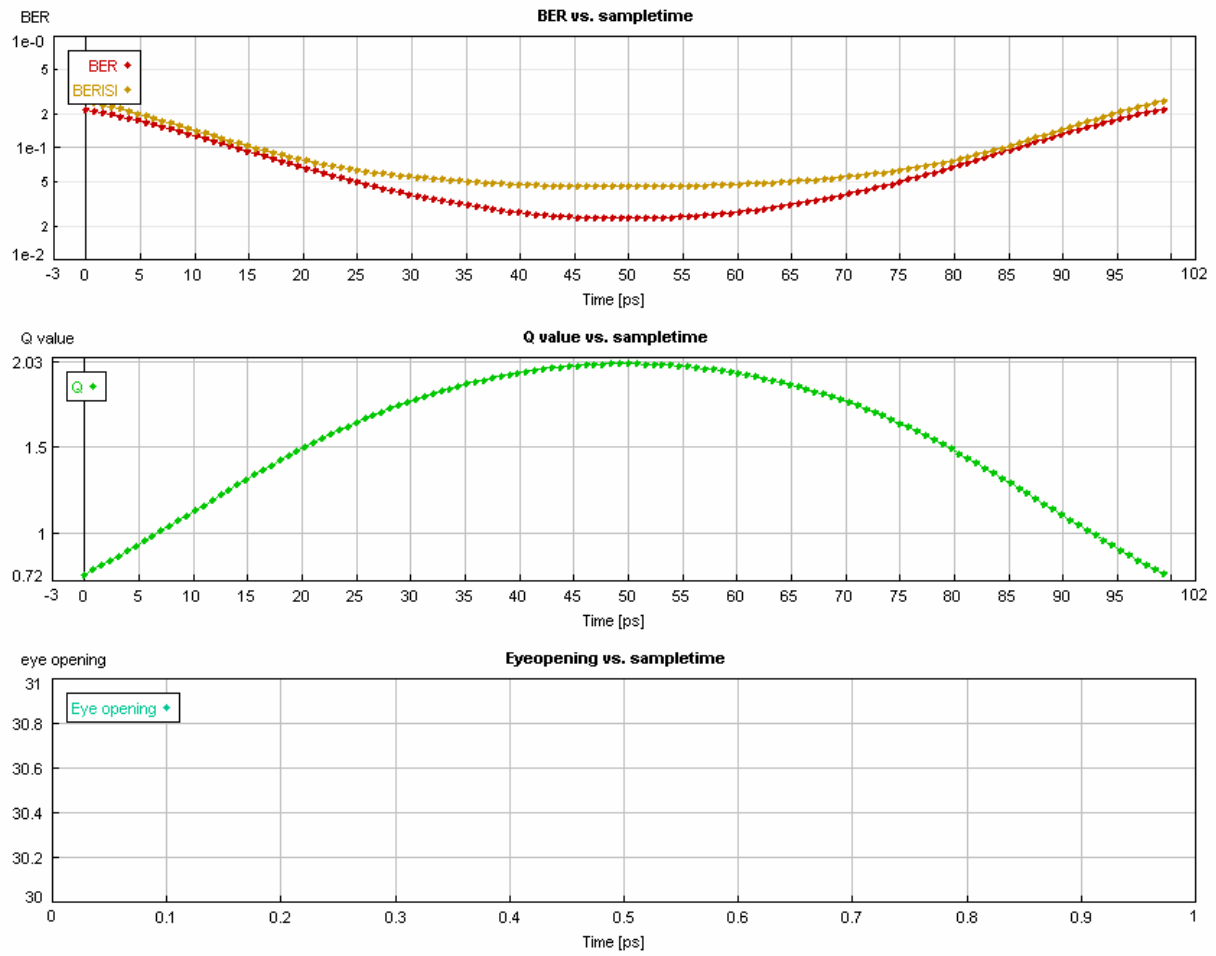

Figure C-19 BER, BER ISI, and Q-factor measurements of the received NRZ signal after 3 super spans

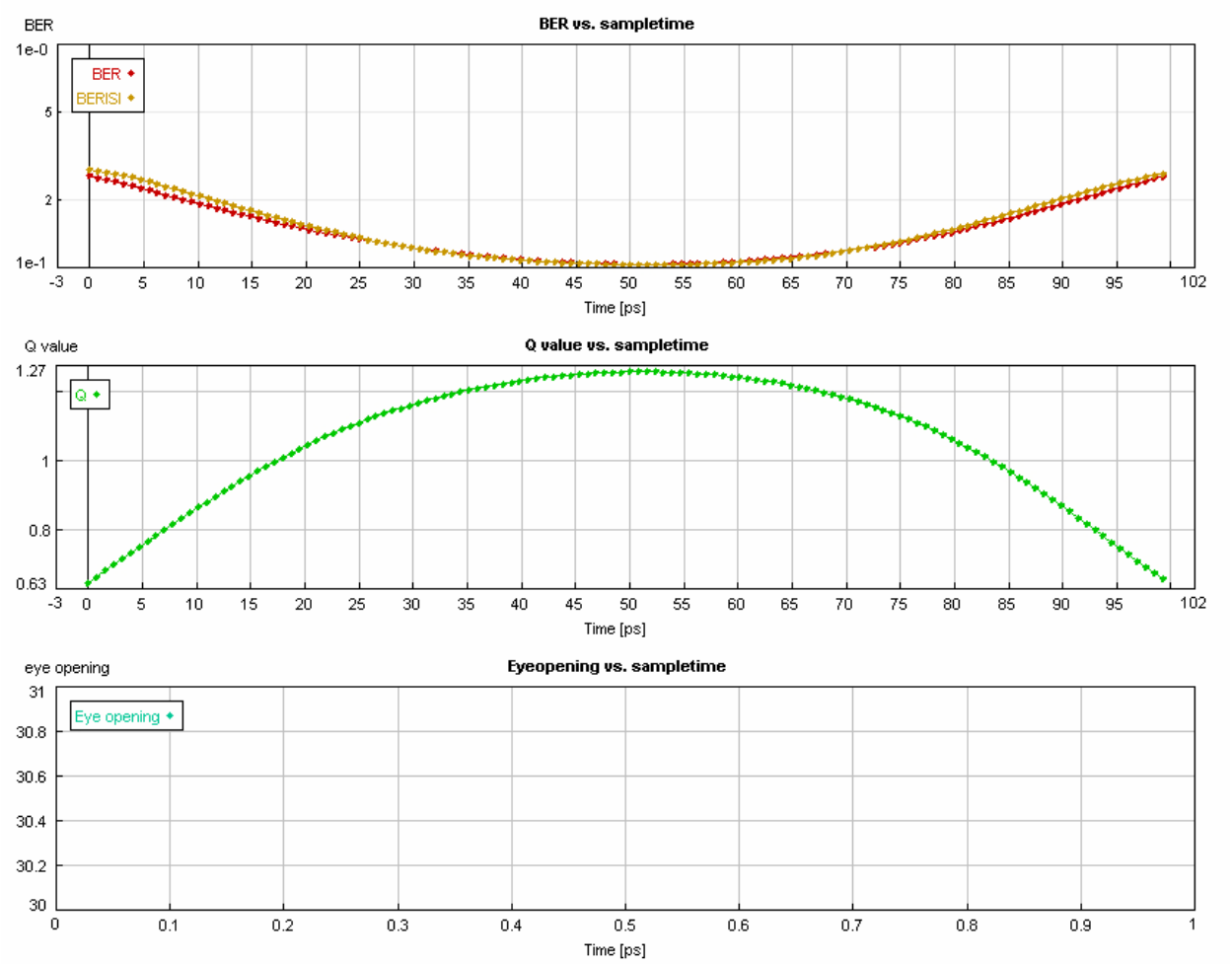

Figure C-20 BER, BER ISI, and Q-factor measurements of the received NRZ signal after 4 super spans